DELIVERY OF BMP-2 FOR BONE TISSUE ENGINEERING APPLICATIONS

A Dissertation
Presented to
The Academic Faculty

by

Mela R. Johnson

In Partial Fulfillment
of the Requirements for the Degree
Doctorate of Philosophy in Bioengineering

Georgia Institute of Technology
May 2010

DELIVERY OF BMP-2 FOR BONE TISSUE ENGINEERING APPLICATIONS

Approved by:

Dr. Robert Guldberg, Advisor
School of Mechanical Engineering
Georgia Institute of Technology

Dr. Mark Prausnitz
School of Chemical & Biomolecular Engineering
Georgia Institute of Technology

Dr. Johnna Temenoff
School of Biomedical Engineering
Georgia Institute of Technology

Dr. Simon Cool
Institute of Medical Biology
*A*STAR, Singapore*

Dr. Ravi Bellamkonda
School of Biomedical Engineering
Georgia Institute of Technology

Date Approved: December 17, 2009

To my parents, for giving me strength and endless support

ACKNOWLEDGEMENTS

There aren't enough words or sentiments that can fully thank those that have helped me grow and learn through this process.

Many thanks to my advisor, Dr. Robert Guldberg, for believing in my abilities from the beginning and accepting me into this lab. I sincerely appreciate that you always encouraged me to be an independent researcher and challenge me to go beyond my own expectations.

Thank you to my committee Dr. Johnna Temenoff, Dr. Mark Prausnitz, Dr. Ravi Bellamkonda, and Dr. Simon Cool for your input and guidance in this project. I greatly appreciate your enthusiasm for my project and constructive feedback to help me become a better scientist.

Guldberg and Garcia labs, you all have made this experience so much fun! I could not have asked for a better group of people to work with and I will miss you all. Angela Lin, you've been a great office-mate these past few years, thanks for always putting up with my loud laughter while I watched the Daily Show during lunch. Hazel Stevens, you have been a huge help these past few years and I thank you for always being patient with me and making sure I always had what I needed. Dr. Alex Peister, you taught me everything I know about cell culture and I would have never been able to tackle this project without your guidance. You've been a great mentor and friend, thank you for always being willing to listen. Dr. Yash Kolambkar, I have truly admired your hard work and dedication, you are a fantastic researcher and I know you will do great things. Ken Dupont and Joel Boerckel, I am forever indebted to you both for your

countless hours of help with surgeries and analysis in the midst of your own hectic projects. Brent Uhrig, its been fun being able to give you a hard time this past year, just stop being so hard on yourself all the time. To the rest of the Guldberg lab, past and present, you've been a great bunch to work with and I'll never find another group quite so dynamic. Dave Dumbauld and Sean Coyer, my partners in crime, your ridiculous antics have kept me laughing even on the worst days. I don't know who else you'll find to distract you all the time. Dr. Abbey Wojtowizc, thank you for always laughing with me and reminding me to go home everyday.

Many many many thanks to my BGSA folks. Ashley Johnson/cuzzo, thank you for being a great friend and neighbor, you will always be my cuzzo. Dr. Tammy McCoy, thank you for always going along with my clowning around and always lending a listening ear. Christianna Taylor, thank you for being my breakfast buddy and thank you for putting a roof over my head. Dimitri Hughes, thank you for all the D and Mela time, I needed those talks more than you know. Dr. Clarence Wardell, thanks for putting up with me. You really helped me stay calm through the end of my dissertation and reminded me that it would all get done somehow. Dr. Roderick Jackson, thank you for being my grad school buddy from the start. Our countless lunches reminded me that I'm not in this alone and it was reassuring to know that I wasn't the only one losing my mind over this degree. Adaora Okwo, thank you for always bringing people together and making my grad school years so much fun. Dr. Keith Reed, Dr. Sekou Remy, Dr. Chris Green, Shara McClendon, and Doug Brooks you have all been a huge support and thank you for all the fun we've had over the years. I will miss you all.

Hannah Cho, I can't even begin to thank you enough. Thank you for always dealing with my tantrums and my lack of ability to plan anything. I would have fallen apart if you weren't always around to remind me to take a break and eat or sleep. You are the most generous person I know and I can't thank you enough for always helping me. You'll always be my mini-Cho and a giant in my eyes.

Marisa Biondi, thank you for sticking by me through this even when I got too busy to keep in touch. Thank you for being the crazy person you are and helping me break out of my shell so long ago.

Meghann Moragne El, thank you for being my eternal cheerleader and finding something to be enthusiastic about for me.

Thank you to my long-time mentor Dr. Akhtar Khan. Your confidence in me always reminded me that I could accomplish this lofty goal.

Thank you to Mr. and Mrs. Meyerhoff for supporting the education of so many students and helping me to succeed.

Thank you to all the women who have come before me. You paved the way to make this a possibility. I can only hope to live up to your legacies.

Lastly, thank you to my family. This would never have been possible without your support and love.

Grandma and grandpa, thank you for teaching me the value of hard work, it does always pay off.

AJ, thank you for being a great big brother. You've reminded me to have fun and not to be so serious all the time. I will always look up to you and try to make you proud.

Dad, thank you for your unconditional support, always worrying about me, and always taking care of me. Thank you for reminding me that I don't have to do everything on my own. Thank you for still treating me like your little girl, sometimes I needed that.

Mom, thank you for always reminding me that it's the journey, not the destination, that's important. Your hippie words really helped me keep things in perspective. Thank you for coming to visit so often, somehow always at the times I needed my mom the most. Its been quite a journey and I'm so glad I could share this doctoral experience with you. I look forward to celebrating your doctorate with you.

TABLE OF CONTENTS

LIST OF TABLES

LIST OF FIGURES

LIST OF SYMBOLS AND ABBREVIATIONS

ALP	Alkalkine phsophatase
BMP	Bone morphogenetic protein
BSP	Bone sialoprotein
CHO	Chinese hamster ovary cells
CV	Coefficient of variance
DBM	Demineralized bone matrix
$DC_{8,9}PC$	1,2-bis(tricosa-10,12-diyonyl)-sn-3-phosphocholine
DMMB	Dimethylmethylene blue
DMMB	Dimethylmethylene blue
ECM	Extracellular matrix
ELISA	Enzyme-linked immunosorbent assay
FBS	Fetal bovine serum
FITC	Fluorescein isothiocyanate
HA	Hydroxyapatite
LMWH	Low molecular weight heparin
Micro-CT, μ-CT	Micro-computed tomography
MSC	Mesenchymal stem cell
OCN	Osteocalcin
PCL	Polycaprolactone
RT-PCR	Reverse transcription polymerase chain reaction
Runx2	Runt-related transcription factor 2
sGAG	Sulfated glycosaminoglycan
VOI	Volume of interest

SUMMARY

Bone defects and fracture non-unions remain a substantial challenge for clinicians due to a high occurrence of delayed union or non-union requiring surgical intervention. The current grafting procedures used to treat these injuries have many limitations and further long-term complications associated with them. This has resulted in research efforts to identify graft substitution therapies that are able to repair and replace tissue function. Many of these tissue engineered products include the use of growth factors to induce cell differentiation, migration, proliferation, and/or matrix production. However, current growth factor delivery methods are limited by poor retention of growth factors upon implantation resulting in low bioactivity. These limiting factors lead to the use of high doses and frequent injections, putting the patients at risk for adverse effects.

The goal of this work was to develop and evaluate the efficacy of BMP-2 delivery systems to improve bone regeneration. We examined two approaches for delivery of BMP-2 in this work. First, we evaluated the use of a self-assembling lipid microtube system for the sustained delivery of BMP-2. We determined that sustained delivery of BMP-2 from the lipid microtube system was able to enhance osteogenic differentiation compared to empty microtubes, however did not demonstrate a significant advantage compared to a bolus BMP-2 dose *in vitro*. Second, we developed and assessed the functionality of an affinity-based system to sequester BMP-2 at the implant site and retain bioactivity by incorporating heparin within a collagen matrix. Incorporation of heparin in the collagen matrix improved BMP-2 retention and bioactivity, thus enhancing cell-mediated mineralized matrix deposition *in vitro*. Lastly, the affinity-based BMP-2

delivery system was evaluated in a challenging *in vivo* bone repair model. Delivery of pre-bound BMP-2 and heparin in a collagen matrix resulted in new bone formation with mechanical properties not significantly different to those of intact bone. Whereas delivery of BMP-2 in collagen or collagen/heparin matrices had similar volumes of regenerated mineralized tissue but resulted in mechanical properties significantly less than intact bone properties.

The work presented in this thesis aimed to address parameters currently preventing optimal performance of protein therapies including stability, duration of exposure, and localization at the treatment site. We were able to demonstrate that sustained delivery of BMP-2 from lipid microtubes was able to induce osteogenic differentiation, although this sustained delivery approach was not significantly advantageous over a bolus dose. Additionally, we demonstrated that the affinity-based system was able to improve BMP-2 retention within the scaffold and *in vitro* activity. However, *in vivo* implantation of this system demonstrated that only delivery of pre-complexed BMP-2 and heparin resulted in regeneration of bone with mechanical properties not significantly different from intact bone. These results indicate that delivery of BMP-2 and heparin may be an advantageous strategy for clinically challenging bone defects.

CHAPTER 1

INTRODUCTION

1.1 Motivation

Bone defects and fracture non-unions remain a substantial challenge for clinicians. Millions of fractures occur each year in the U.S. and 5-10% result in delayed union or non-union requiring some type of surgical intervention [1, 2]. Grafting procedures are presently the most common treatment used to restore function to damaged or degenerated tissue. These procedures, however, are largely limited by the availability of graft material and have resulted in high rates of failure, donor site morbidity, and/or disease transmission [1, 3-5]. Nearly 25% of the graft patients experience re-fracture and/or continued pain at the donor site, often due to poor mechanical and/or biological environments during the repair process [1, 6, 7]. Consequently, there is an immense need for new tissue engineering strategies, which aim to restore, maintain, or remodel damaged or degenerated skeletal tissues [4, 8-10].

The success of tissue engineering therapies depends largely on the interaction and synergy of the scaffolds, cells, and/or growth factors used to restore and remodel the damaged tissue [11]. Few tissue engineering products have gained FDA approval due to complex designs, poor control groups for clinical studies, and high costs [12-14]. Thus, research has focused on determining methods to more effectively deliver cells, growth factors, and other bioactive agents.

One aspect of tissue-engineered strategies includes the delivery of growth factors to induce cell differentiation, migration, proliferation, and/or matrix production. Growth

factor therapies have demonstrated serious potential for tissue engineering because of their highly specific activity and ability to induce a variety of cell functions vital to tissue repair. However, current protein therapies are largely limited by protein stability and localization at the treatment site, resulting in the use of high doses, and often requiring frequent administrations. To address these limitations, delivery systems that are able to maintain protein stability as well as optimally control the rate and location of growth factor release to sustain a therapeutic concentration are being investigated. Existing growth factor delivery systems include lipid-based and polymeric encapsulation vehicles, matrix carriers, and affinity-based systems.

Bone morphogenetic proteins (BMPs) have been used in combination with various carrier materials, such as collagen and demineralized bone matrix (DBM), for bone tissue engineering approaches [6, 15-17]. Presently, collagen is the only FDA approved carrier for BMP-2; however, research has shown that BMP-2 has low affinity for collagen, leading to rapid diffusion from the construct and a significant decrease in the local BMP-2 concentration [15, 18]. Furthermore, soluble or free BMP-2 quickly loses bioactivity due to proteolytic degradation and denaturing caused by physiologic conditions (i.e. pH, temperature, salt concentration). Therefore, recent efforts have focused on either encapsulating the BMP molecule to protect it from degradation or enhancing the binding affinity of BMPs to the carrier material [17, 19-22]. The *overall objective* of this work was to develop and evaluate the efficacy of BMP-2 delivery systems to improve bone regeneration. This objective will be addressed by employing two delivery approaches including a lipid-based microtube vehicle for the sustained delivery of BMP-2 and a heparinized collagen matrix for BMP-2 retention. The *central*

hypothesis for this work is that the controlled delivery of BMP-2 will enhance osteogenic differentiation *in vitro* and bone regeneration *in vivo*.

1.2 Specific Aims

The central hypothesis will be tested through the following three specific aims:

I. Validate lipid microtubes as a sustained delivery system for BMP-2 through *in vitro* bioassays.

Sustained delivery systems have been developed for the use of various growth factors in tissue engineering applications in order to overcome difficulties associated with the short half-life of proteins. However, many of these systems continue to have limitations associated with low loading efficiencies and minimal biological activity after release. In order to address these issues, delivery systems with predictable release kinetics and loading efficiencies are being developed. The work in this thesis evaluates the use of such a system for the delivery of BMP-2.

The *hypothesis* is that encapsulation of BMP-2 in lipid microtubes will provide sustained release of BMP-2, thereby maintaining a consistent concentration of BMP-2, while also protecting the growth factor from degradation, resulting in increased mineralization. The results of Specific Aim I are discussed in Chapter 3.

II. Evaluate heparin as a BMP-2 binding matrix component in an affinity-based delivery system using *in vitro* bioassays.

A major limitation of clinical BMP-2 treatments is the rapid diffusion from the implant site, causing a significant decrease in local concentration, as well as rapid loss of bioactivity in the soluble form. Various affinity-based delivery systems have been developed to sequester and protect the structure of growth factors. Recently, heparin-based systems have been developed to exploit the inherent binding properties

with BMP-2. This work evaluates the incorporation of heparin in a collagen matrix system to improve BMP-2 retention and bioactivity.

The *hypothesis* is that heparin will significantly enhance BMP-2 retention within the collagen matrix and subsequently increase osteogenic differentiation of progenitor cells. The results of Specific Aim II are discussed in Chapter 4.

III. Evaluate the capability of a BMP-2 controlled delivery system to induce bone formation in an *in vivo* critically-sized defect model.

BMPs were originally identified as molecules that could induce ectopic bone formation when implanted in subcutaneous or intramuscular sites, classifying them as osteoinductive proteins. Thus, the in vivo rodent subcutaneous or intramuscular ectopic implantation assay has been established as the standard model to demonstrate BMP-2 activity in initiating and maintaining the bone formation cascade. However, the ectopic assay does not provide a clinically relevant in vivo model for fracture healing. A challenging segmental defect model will be utilized in this study to assess the performance of a BMP-2 controlled delivery system for fracture healing.

The *hypothesis* is that controlled delivery of BMP-2 will enhance bone formation *in vivo*. The results of Specific Aim III are discussed in Chapter 5.

1.3 Significance

Recent advances in biotechnology have led to increased availability of protein therapeutics for tissue engineering applications. These treatments are expected to enhance and accelerate tissue regeneration. However, current protein, or growth factor, therapies are limited by poor stability and rapid transport away from the treatment site, resulting in the need for controlled delivery approaches. This work is *innovative* because it examined the use of two delivery systems in efforts to improve BMP-2 mediated

mineralization. First, self-assembling lipid microtubes were used for the sustained delivery of an osteogenic growth factor, which did not involve the use organic solvents during fabrication and encapsulation processes. Additionally, we examined the use of an affinity-based system to sequester BMP-2 at the implant site and retain the protein structure by utilizing the intrinsic binding properties of heparin and BMP-2 without covalently linking molecules to the carrier. Currently, sustained release of growth factors is achieved by incorporating the protein into a degradable polymeric vehicle [23-25]. However, the fabrication of these polymer vehicles often involves the use of organic solvents and harsh processes that may denature and deactivate the protein. Affinity-based systems have previously been achieved by covalently-linking molecules or growth factors to the carrier material [20, 26-28]. While these approaches have shown promise, the biochemical processes used can possibly change the structure and binding properties of growth factor binding molecules as well as the bioactivity of growth factors [29]. The systems investigated in this work are expected to enable BMP-2 to efficiently and adequately perform the intended osteoinductive biological effects, in order to reduce adverse effects and improve efficacy of BMP-2 therapies.

This work is *significant* because it examines delivery methods to help improve the efficacy of growth factor treatments, which may lead to the use of lower, safer doses. This project is expected to have the following outcomes: (1) lipid microtubes will maintain a sustained dose of an osteoinductive growth factor, (2) a heparinized matrix will enhance retention and bioactivity of an osteoinductive heparin-binding growth factor, and (3) the delivery of heparin and an osteoinductive heparin-binding growth factor will enhance functional bone regeneration in a critically-sized defect *in vivo*.

CHAPTER 2

LITERATURE REVIEW

2.1 Bone Structure and Function

Bone is a metabolically active, dynamic tissue that is constantly being renewed and remodeled. Apart from being the structural scaffold of the body, bone also has a large role in hematopoiesis (development of blood cells), maintaining mineral ion homeostasis, and protecting tissues and organs (i.e. lungs, heart, and brain). Bone remodeling and regeneration work cooperatively to maintain these physiological needs [4]. Renewal and adaptation of bone tissue occurs on four different surfaces in most mammals: periosteal, endocortical, trabecular, and Haversian (intracortical) [30]. These surfaces differ greatly in their surface area-to-volume ratios, which is largely dependent on the mechanical requirements of those surfaces.

Bone formation and the subsequent modeling or remodeling act cooperatively to define the proper skeletal geometry, maintain mineral ion concentrations, and repair damaged bone. These actions are regulated and carried out by osteoblasts and osteoclasts. Bone modeling usually only occurs during developmental phases in children, and reduces to an insignificant level after skeletal maturity is achieved. This modeling process consists of resorption by osteoclasts or formation by osteoblasts, but not both at the same location [30]. Bone remodeling includes both resorption and formation at a location by groups of cells from multiple sources called the basic multicellular unit (BMU). This remodeling process has a primary role in maintaining calcium homeostasis in the body [30, 31]. When calcium levels are low, osteoclast activity is stimulated by

parthyroid hormone to release minerals from the bone matrix. When calcium levels are above normal, osteoclast activity is inhibited by calcitonin secreted from the thyroid gland. These regulatory activities are constantly occurring in both immature and adult bones to maintain proper structure and function. Many metabolic bone diseases are attributed to interruptions in the normal BMU function (i.e. osteoporosis, osteoarthritis) [30, 32].

Bone formation occurs either by intramembranous ossification or endochondral ossification. Intramembranous ossification occurs when ostoeblasts differentiate within a mesenchymal or fibrous connective tissue, such as in the deep layers of the dermis, without formation of cartilaginous intermediates [33]. Osteoblasts cluster within the tissue and begin to secrete organic matrix, which then becomes mineralized. Flat bones, such as the mandible and clavicle, normally form by intramembranous ossification. Intramembranous bones may also form in abnormal locations in response to stresses or signals, resulting in heterotopic or ectopic bones. Endochondral ossification occurs when cartilaginous matrix is mineralized into bone tissue [33-35]. This process begins with undifferentiated progenitor cells differentiating into chondrocytes and subsequently secreting cartilaginous matrix. After the matrix calcifies and the chondrocytes within the matrix to undergo hypertrophy, osteoprogenitor cells and blood vessels invade the matrix. The progenitor cells then differentiate into osteoblasts and bone formation occurs on the calcified cartilage matrix. Most long bones, like the femur and tibia, are formed and repaired by endochondral ossification.

Mechanical stimuli have effects on bone remodeling, and research has that bone will adapt to the loads experienced [30, 36]. At the extremes, overuse and disuse both

result in stimulation of unbalanced bone turnover. In the case of disuse, or lack of use, bone resorption dominates bone formation on endocortical, cortical, and trabecular surfaces, resulting in rapid bone loss. This effect is often observed in astronauts and chronically ill patients on bed rest for extended periods of time. Overuse causes damage to the bone, which then stimulates bone remodeling to repair the microdamage. However, if damage accumulates faster than repair can occur, the microcracks can propagate and result in a fracture [37].

The major functions of bone are carried out by osteoblasts and osteoclasts. Osteoblasts are cells of mesenchymal lineage and secrete unmineralized bone matrix, called osteoid, which then mineralize to yield mature bone. Mesenchymal stem cells found in the marrow and periosteum are induced to differentiate into osteoblasts by a complex interaction of growth factors and transcription factors, such as Runx2/Cbfa1 and Msx2 [30, 38, 39]. Once these cells are committed to the osteoblastic lineage and become mature osteoblasts, they begin to express matrix proteins such as bone sialoprotein (Bsp), collagen type I, osteocalcin (OCN), and alkaline phosphatase (ALP). Some osteoblastic cells do not fully mature and instead begin to form long cytoplasmic processes through the osteoid and become osteocytes. Mature osteoblastic-formed tissue is maintained by osteocytes and bone-lining cells.

Osteoclasts are cells of hematopoetic cell lineage and resorb bone via secretion of acid and proteases. Osteoclastogenesis includes the stimulation of a hematopoetic stem cell to form mononuclear preosteoclast cells. These committed preosteoclast cells then enter the blood stream and travel to the site that is to be resorbed. The mononuclear preosteoclasts fuse together for form multinucleated osteoclasts. This fusion requires the

presence of macrophage colony stimulating factor (M-CSF) and receptor activator of nuclear factor κB (RANK-L) [30]. Mature osteoclasts resorb bone by secreting H+ ions to solubilize the mineral component and subsequently release proteases to degrade the organic matrix.

Mechanical stimuli have an affect on bone cell behavior via mechanotransduction, which involves ion channels, focal adhesions, and G-protein coupled receptors. Osteocytes and bone lining cells play important roles in communicating these mechanotransduction signals through the bone. Osteocytes have been shown to have an indirect response to mechanical stimuli, usually in the form of fluid flow caused by the mechanical loading event [30, 40]. This mechanical stimulation causes the osteocytes to release prostaglandins to signal cell responses. Osteoblasts are also involved in mechanotransduction, releasing prostaglandins and growth factors upon mechanical stimulation.

Bone extracellular matrix is very dense and heterogenous, largely composed of collagen and hydroxyapatite. Hydroxyapatite crystals are formed when calcium phosphate ($Ca(PO_4)_2$) interacts with calcium hydroxide ($Ca(OH)_2$), thereby maintaining mineral ion homeostasis [31, 41]. These crystals also incorporate other calcium salts, such as calcium carbonate, and ions such as sodium, magnesium, and fluoride. Hydroxyapatite crystals are very hard, but relatively inflexible and brittle. Collagen fibers, conversely, are strong and flexible and make up approximately 90% of the bone ECM [31]. These fibers can tolerate twisting, bending, compression and tension. The collagen fibers provide an organic framework for the formation of hydroxyapatite crystals. During osteogenesis, ascorbic acid and phosphates are in high demand to

synthesize collagen type I fibrils and subsequently form hydroxyapatite crystals. The bone matrix also contains proteoglycans and glycoproteins [31, 41]. Fibronectin and laminin are two of the main glycoproteins in bone ECM and bind other ECM components, such as collagens and proteoglycans. Matrix composition and structure is maintained by matrix metalloproteases (MMP), which cleave matrix proteins. Bone ECM proteins have a major role in regulating growth factor activity by limiting diffusion and blocking receptor-binding sites.

Bone ECM is then organized into woven or lamellar bone. Woven, or immature, bone has randomly arranged collagen bundles. This random organization causes the woven bone to be weaker, but more flexible than lamellar bone. During the remodeling process, woven bone is replaced by lamellar bone. Lamellar bone has tightly organized, parallel sheets of collagen bundles called lamellae. The lamellae are organized concentrically around a canal, which contains blood vessels and nerves, to create an osteon or Haversian system [30].

On a more global scale, bone has two main structures: compact bone and spongy bone. The matrix compositions of compact and spongy bone are the same, but they differ in the three-dimensional organization [30, 42]. Compact bone has a basic functional unit called osteon, or the Haversian system. The osteon consists of osteocytes arranged around a Haversian canal that contains blood vessels and run parallel to the surface of the bone. Perforating canals, or the canals of Volkmann, extend nearly perpendicular to the tissue surface and deliver blood to osteons deeper within the bone and in the marrow cavity. The periosteum is a layer of connective tissue that covers the surface of the compact bone and functions to isolate the bone from surrounding tissues, provide a route

for circulatory and nervous supply, and actively participates in bone growth and repair. Spongy or trabecular bone is present at the epiphyses of long bones and may extend into the marrow cavity, where the bones may experience stress from multiple directions [37, 43]. The spongy bone has an open structure consisting of struts and plates called trabeculae. This orientation and open structure reduces the weight of the skeleton while providing optimal mechanical integrity [30, 37, 43]. The trabeculae are covered by the endosteum, which is active in the modeling and remodeling of bone [30]. Nutrients reach osteocytes by diffusion along the canaliculi along the surfaces of the trabeculae, and not by blood vessels.

The mechanical properties of bone vary depending on the anatomic function and location, age, disease, and the amount of use. However, the mechanical properties of mammalian bone across species are similar [30]. Long bones, such as femurs, are thick-walled hollow cylinders. This allows for the long bones to remain strong while minimizing the weight. Much of the strength in long bones is in the periosteum, which increases the second moment of inertia and resists against bending or torsional loading [30]. Trabecular bone aligns with maximum stresses in bone, however anisotropy greatly increases the load-bearing capacity without increasing mass [30, 37, 43]. Collagen fibril alignment and cross-linking also greatly influences mechanical strength [43].

2.2 Fracture Healing

Bone is one of the few tissues in the body that maintains the ability to regenerate in adult life, which is required for fracture healing [44, 45]. The fracture repair process must restore the original geometry, biological matrix, and biomechanical properties to the damaged bone tissue. To meet these criteria, fracture healing involves the complex

cooperation of angiogenesis and osteogenesis stimulated by a combination of cells, cytokines, growth factors, hormones, and ECM components [4].

Fracture healing begins with the formation of a large blood clot, or fracture hematoma, at the site of fracture to close off the injured vessels [2]. This hematoma releases growth factors and cytokines from degranulated platelets and provides a fibrous framework at the damaged area for cells to attach and make new bone tissue. Cells from the periosteum migrate to the fracture site to form an external callus. These periosteal cells also rapidly produce BMPs in order to recruit progenitor cells to the site of fracture to proliferate rapidly and differentiate [46, 47]. Endogenous expression of BMPs is critical to adult bone formation [48]. Cartilage forms at the center of the external callus and the chondrocytes produce factors that induce osteogenesis [49, 50]. Blood vessels then begin to invade the callus, the cartilage cells hypertrophy, and cells begin to differentiate into osteoblasts. These osteoblasts secrete matrix and gradually replace the cartilage with bone. Osteoclasts and osteoblasts then remodel the region to integrate the newly formed bone with the surrounding tissue.

Fracture healing requires that vascular supply be adequately repaired in order to form the fracture callus and supply nutrients to the cells within the fracture callus [2]. This interdependency of angiogenesis, the regeneration of blood vessels, and bone repair has been recognized for many years and established in many studies [2, 51-53]. Vascular endothelial growth factor (VEGF) and bone morphogenetic proteins (BMPs) have been shown to have synergistic effects during fracture healing [54, 55]. Inhibition of angiogenesis significantly suppresses fracture healing in animal models [53]. Inhibition

of VEGF was shown to disrupt bone healing in femoral fractures and cortical bone defects by Street, et al. in both murine and rabbit fracture repair models [51].

Angiogenesis is a complex process regulated by multiple pathways. VEGF-related molecules mediate neo-angiogenesis and are mitogens specific for endothelial cells [56-58]. VEGF-stimulated angiogenesis involves migration of endothelial cells, inhibition of endothelial cell apoptosis, and up-regulation of endothelial-derived vasoactive molecules (i.e. tissue plasminogen activator and nitric oxide). Angiopoietin molecules regulate the formation of larger vessels and the development of co-lateral branches from existing vessels [52]. These angiogenic factors promote endothelial cell survival and vessel integrity. VEGF promotes new vessel formation by remodeling capillary basal lamina and stimulating endothelial cell migration and sprouting. However, the delivery of VEGF alone is not sufficient to complete angiogenesis and requires the delivery of other angiogenic factors to complete the process [59]. Inhibitors of angiogenesis, such as TNP-470 and thalidomide, also regulate blood vessel formation [53, 60]. Some of these negative regulators, or antiangiogenic factors, have been used in clinical trials to inhibit tumor growth and atherosclerosis [60].

Mechanical stimulation has been shown to be beneficial during fracture healing by regulating gene expression and differentiation of the surrounding tissue [36, 61, 62]. Several groups have demonstrated that displacement applied to a fracture results in the formation of a larger cartilaginous callous and earlier bone bridging [61]. A mechanically stable healing environment decreases the amount of cartilage formed at the fracture site, indicating that bone formation would occur primarily by intramembranous ossification in a stable fracture site [61]. However, when there is excessive motion at the

defect site the bone forms by endochondral ossification and the instability prolongs the cartilaginous phase [63].

Fracture repair is a highly regulated and coordinated activity, down to the cellular and molecular levels. Major advancements in bone biology have been made in recent years, revealing more information of the molecular mechanisms behind bone regeneration [39, 45, 64]. This information will be helpful in finding new treatments for bone fractures, congenital defects, and degenerative diseases. During osteogenesis, BMP-2 activates Smad signaling and regulation of osteogenic genes (i.e. ALP, type I collagen, osteocalcin, and bone sialoprotein). These genes are also regulated by expression of the transcription factor Runx-2. BMP-2 regulates Runx-2 expression through Smad signaling, which is required for the regulation of Osterix (Osx) expression [65-67]. This is known as the BMP-2-Smad-Runx2 axis in osteogenesis. Disruption of either BMP-2 or Runx-2 in this signaling cascade will result in a lack of bone formation and fracture repair [68, 69].

2.3 Bone Fracture and Clinical Intervention

There are many types of bone fractures, with varying clinical treatments. Fractures are typically classified based on the site of fracture, nature of the fracture, and the external appearance. These fractures can be a simple transverse fracture that typically requires no surgical intervention, or can be as severe as a comminuted fracture, which rarely heal spontaneously in patients and require some type of surgical treatment. Frequently, bone fractures experience impaired healing, in the form of delayed union or nonunion [34, 70]. This impaired healing is often due to inadequate mobilization of the fracture, distraction of the fracture by fixation devices, repeated manipulations, periosteal

damage during operative procedures, infections, or poor vascular supply [1, 34, 61]. Such defects can be treated with a graft to promote healing. However, impaired healing is not always due to severe fracture conditions. Diseases such as cancerous tumors in the bone (osteosarcoma) and chronic infections of the bone (osteomyelitis) are also very challenging for orthopedic treatments [71, 72].

Burwell showed over 40 years ago that fracture-healing was enhanced when cancellous bone grafts were implanted due to the presence of osteoprogenitor cells in the graft [73]. Autografts have been the standard treatment for bone fractures because the patient will not have a minimal immune response to their own cell source. However, the use of autografts is largely limited by the supply of available graft material. Typically, the graft is taken from the iliac crest of the pelvis, which only provides a small amount of material because removal of too much material may result in donor site morbidity, leaving the patient in a great amount of pain at both the donor site and at the fracture site. The material obtained from this site is also not structurally sound, being made of only small bone chips. Clinical trials have also utilized external stabilization of the graft material, often with a titanium chamber, or combining with other matrix components, such as calcium sulfate in order to improve the mechanical and biological environment [1]. However, these approaches often still result in re-fracture, non-unions, and/or repeat surgeries.

Allografts are also used in the treatment of large fractures. These grafts are obtained from cortical cadaver bone and devitalized to ensure sterility, minimize immune response, and prevent disease transmission. The processed graft is then void of all living material and bioactive factors that were originally stored in the bone matrix. Therefore,

the allograft serves mainly as a structural scaffold at the fracture site, and has no bioactive component to encourage healing and incorporation of the grafts [4, 74, 75]. Xie, *et al.* demonstrated a novel approach of combining structural allografts with genetically modified mesenchymal stem cells to improve fracture healing [74]. Allografts have shown some success in healing fractures, however are much less efficient than autografts and still have problems associated with infections, despite the extensive screening and decellularization techniques, as well as low osseointegration with host tissue [6, 76, 77]. The lower efficiency of allografts is mainly due to the low osteogenic activity, caused by the decellurization process, as well as the low porosity, leaving minimal space for revascularization and revitalization, leading to slow remodeling of the graft. This results in an accumulation of microdamage and ultimately leads to graft failure.

Tissue engineering may provide alternatives to allografts and autografts by restoring, maintaining, and/or improving tissue function [78]. This strategy typically includes a matrix or scaffold material, bioactive factors, and/or cells either transplanted or recruited to the fracture site. Some clinical studies have shown improved healing in spinal fusions and other osseous defects using tissue engineered constructs [79-81]. However, tissue engineering products have faced many challenges in becoming clinical treatments, including variability in product performance, clinical trial validation, and manufacturing scalability [4, 13, 42]. Tissue engineering remains a "development-stage" industry with many products failing to gain FDA approval [12, 14]. Therefore, grafting procedures remain the standard treatment for many organ and tissue problems, including bone fracture repair. The work presented in this thesis represents one tissue engineering

strategy to deliver bioactive factors within a porous polymer scaffold, with the aim to promote osseointegration of the scaffold into a bony defect site and enhance functional repair of the fracture site.

Table 2.1 Current and emerging therapeutic strategies for bone regeneration

AUTOGRAFTING	ALLOGRAFTING	XENOTRANSPLANTS	BIOMATERIALS/DEVICES	TISSUE ENGINEERING
Tissue transplanted to another area of the same patient	Tissue transplant from a matched donor	Transfer cells/tissues/organs from animal source to patient	Replicate tissue function with artificial materials	Restore structure and function to damaged tissue
Risks: Infection and pain at the donor site, high number of refracture	**Risks:** Tissue rejection and infection, donor shortages, poor tissue remodeling, high rate of refracture	**Risks:** Tissue rejection and infection, zoonotic disease transmission	**Risks:** Non-physiological behavior, material fatigue and fracture, toxicity	**Risks:** Still a developing science, very few FDA approved therapies
Benefits: Minimal immune response	**Benefits:** More tissue available than autografts, osteoconductive	**Benefits:** Tissue supply readily available	**Benefits:** Off-the shelf availability, control of material properties	**Benefits:** Functional repair

2.4 Growth Factor Therapy

Bone regeneration is regulated by a variety of signals including mechanical stimuli, cell-cell interactions, and soluble bioactive factors. Many proteins are involved in this signaling process, making them a potential therapy for various tissue engineering applications. Growth factors are proteins secreted by cells that specifically bind to membrane receptors to stimulate or inhibit a cellular function, such as differentiation. Multiple studies have shown that administering high concentrations of osteogenic growth factors promote fracture unions [33, 47, 82, 83]. The growth factor BMP-2 (bone morphogenetic protein-2) was selected for this thesis work to promote and accelerate bone tissue regeneration, because of its known osteoinductive capacities.

BMP-2 is the most widely used growth factor to stimulate osteogenesis [6]. Marshall Urist was the first to observe the osteoinductive effect of BMPs in 1965 and later found a method to extract BMPs from demineralized bone matrix (DBM) [84, 85]. BMPs increase the synthesis of structural components of ECM, decrease ECM

degradation, and increase proliferation. During fracture healing, BMP-2 expression is highest at the early stages to initiate and direct migration of progenitor cells for the formation of new bone, which is critical to the proper healing of damaged tissue [33, 64, 69, 86]. Only BMP-2, -6, and -9 are able to induce and maintain the entire bone formation cascade – chemotaxis, proliferation, and differentiation [9, 44, 84, 85]. Chemotaxis is the guided movement of cells, often mediated by up-regulation of integrins β1 and β3, in response to a chemical signal gradient [87, 88]. BMP-2 is endogenously expressed in MSCs, which stimulates osteogenic differentiation [89]. However, defects in BMP-2 expression may cause autosomal dominant fibrodysplasia ossificans progressiva (FOP), myositis ossificans, or osteogenic sarcoma [84].

BMP-2 is a low molecular weight glycoprotein in the TGF-ß family with a disulfide-linked homodimer structure. Native bone contains approximately 1-2 micrograms of BMP per kilogram of cortical bone [84, 90]. However, extraction is difficult, frequently yielding BMPs with high contamination and unpredictable behavior. Due to recombinant protein technology however, BMP-2 is readily available in a highly purified form. Yet, the clinical cost of these recombinant proteins is very high due to the limited yield obtained from mammalian Chinese hamster ovary (CHO) cells. One way to increase yield is to produce the proteins in *Escheria coli* (*E. coli*). However, the BMP-2 produced by *E. coli* lacks the posttranslational glycosylation sites and folding motifs seen in mammalian cell-derived BMP-2, and also has a slightly lower effect on osteogenic differentiation [91]. These posttranslational processes can be recreated using optimized renaturing procedures, but these processes are often complex and expensive [92].

Soluble BMP-2 is secreted from cells in an active form and then behaves in an autocrine or paracrine manner by binding the BMP I and II receptors (Ser/Thr kinase receptors) [34, 93]. Dimerized BMP-2 binds the receptor complex and the activated BMPRII phosphorylates BMPRI, which then recruits and phosphorylates Smads 1, 5, and 8. These Smads then associate with Smad 4 and translocate to the nucleus to activate transcription [44]. The dimeric conformation of BMP-2 is critical to the bioactivity, but is very sensitive to environmental conditions. Elimination of the disulfide bond between dimers renders the molecule inactive [94]. BMP-2 is the most soluble at pH < 5, however the solubility at pH > 6 (i.e. physiologic pH = 7.4) is greatly increased in solvents such as heparin solutions [95]. Heparin has also been shown to improve BMP-2 activity by protecting the protein from degradation and blocking antogonist suppression (**Figure 2.1**) [96].

Antagonists of BMP-2 include noggin and chordin, which directly bind BMP-2 and interfere with receptor binding, as well as Smad 6, which inhibits phosphorylation of Smads 1, 5, and 8 by BMPRI [93]. Other antagonists, such as fetuin, bind to the receptors, inhibiting proper receptor-ligand interactions [93]. Other research has suggested that BMP-2 and BMP-4 act as antagonists to each other due to their highly identical sequences (92% sequence similarity) causing each to bind to the other receptor [85].

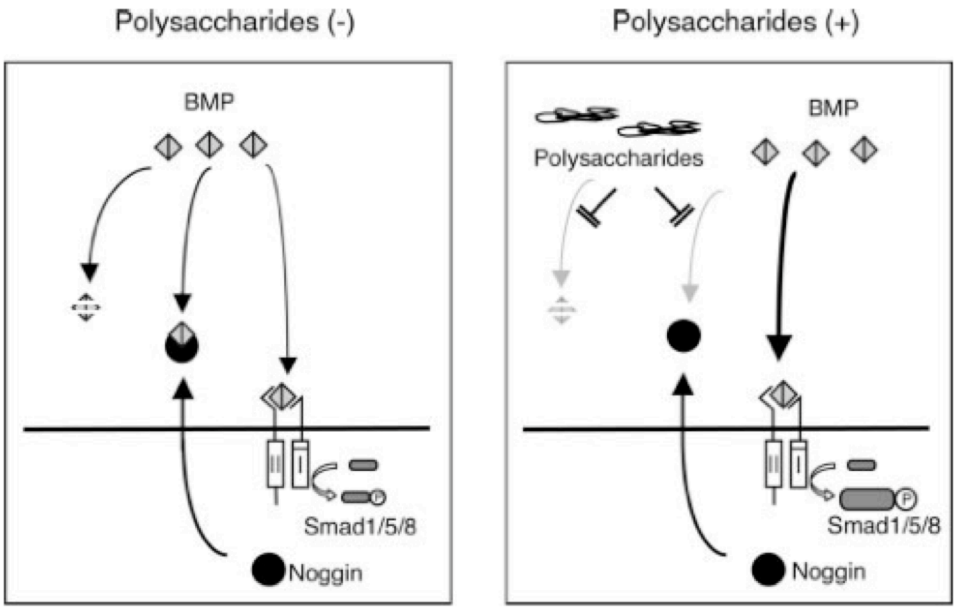

Figure 2.1 Mechanisms of heparin effects on BMP-2 activity (Image by Zhao, et al. [96]). Without heparin (left panel), BMP-2 is quickly degraded, suppressed by antagonists (i.e. noggin), or internalized after receptor binding. Heparin helps maintain extracellular concentrations of BMP-2 (right panel) by binding to the protein and protecting it from degradation and antagonist suppression, as well as keeping the BMP receptor continuously activated.

Research has shown that hMSCs endogenously express and secrete BMP-2, resulting in osteogenic differentiation [89]. However, the effects of BMP-2 are concentration dependent. Femtomolar concentrations of BMP-2 influences chemotaxis, nanomolar concentrations of BMP-2 influences proliferation, and micromolar concentrations of BMP-2 induces differentiation [34, 84, 97]. High doses of BMP-2 (100 µg/ml in rats), however, have been shown to cause excessive bone formation that spreads outside the native shape of the bone [97].

The FDA approved the use of rhBMP-2 in Medtronic's InFUSE™ Bone Graft (Medtronic Sofamor Danek, Memphis, TN, USA) for spinal fusion procedures to treat degenerative disc disease, and more recently approved for acute, open tibial fractures [98, 99]. The InFUSE™ Bone Graft delivered with a dose of 1.5 mg/ml BMP-2 in an absorbable collagen sponge (ACS) was shown to induce faster fracture healing and

reduce the risk of failure, as well as fewer infections and surgical interventions [11, 99]. Although, collagen is a biocompatible and resorbable carrier material, BMP-2 has a low affinity for collagen and has been reported to rapidly clear from the sponge when implanted [100-102]. This has caused clinicians to use high doses of BMP-2 in order to overcome the diffusion and stability limitations, resulting in extremely high costs and reports of adverse effects of the treatment. The risks initially reported by Medtronic included transient increases in BMP antibodies in 5-10% of patients, local edema, and accelerated bone resorption [6, 103]. Moreover, in July 2008 the FDA warned surgeons that it had received 38 reports in four years of life-threatening complications associated with off-label usage of the InFUSE™ device in the cervical spine [103, 104]. Many of these complications involved unwanted bone growths near nerves or in areas outside the targeted site of treatment leading to severe pain, swelling of the neck and throat, and breathing difficulties [104]. Many of these patients required emergency tracheotomies, feeding tubes, and repeat surgeries.

2.5 Growth Factor Delivery Methods

BMP-2 has been shown to promote fracture unions, however, delivery of BMPs alone is minimally effective and not reasonable for wide use clinically due to the extremely high doses needed, which may cause cyst-like bone voids [82]. Large, super-physiologic doses of growth factors are often necessary to overcome their short half-lives *in vivo* because of rapid denaturing of the protein structure by enzymes and other adverse conditions in the body (i.e. temperature, pH, ion concentration). These adverse *in vivo* conditions greatly affect the efficacy, bioavailability, and stability of the growth factor. Therefore, optimized drug delivery methods are needed in order to preserve the protein

structure in the unfavorable *in vivo* environment, as well as present the growth factor at the appropriate rate, duration, and location of exposure to promote cell responses. Three main approaches have been developed to deliver BMPs including: delivery of DNA encoding for BMPs, *ex vivo* gene therapy or overexpression of BMP genes in cells, and delivery of the protein itself in a carrier material [82, 105, 106]. Due to the advances in recombinant protein technology and safety concerns with gene therapy, delivery of the actual protein has become more widely used [100].

In order to attain optimal activity, growth factors should to be delivered in a manner that will closely relate to the regenerating tissue process of interest [101, 107, 108]. Thus, there are several important factors considered when designing a growth factor delivery system. First, the delivery method must target the desired cell population with minimal diffuse signaling into the surrounding tissue. Early applications administered growth factors via injections, however this approach proved to be insufficient due to the short half-lives of growth factors as well as transport away from the site of injection/implantation by convective transport (i.e. blood flow, fluid flow due to tissue deformation) or diffusion, resulting in effects on at undesired locations [90, 109]. This has led to the development of new formulations that address the pharmacological and therapeutic properties of the growth factor.

Next, the delivery system must help protect the structure and bioactivity of the growth factor. This has previously been achieved with various growth factors by encapsulating the protein [19, 22], thus protecting the structure from proteolytic degradation, and also by immobilizing growth factors into an ECM-like matrix to sequester the protein [26, 110]. Affinity-based delivery systems utilize unique binding

properties of the growth factor and immobilized molecules, to mimic the naturally occurring growth factor delivery system in the ECM. Binding of the growth factors with immobile molecules slows the rate of diffusion through the surrounding tissue as well as maintaining the protein structure. Molecules such as heparin and antibodies have been adsorbed onto or covalently linked to scaffold surfaces to sequester growth factors such as bFGF, TGF-ß2, BMP-2 and NGF [17, 20, 111-116]. Recently, chemical alterations have progressed to changing the BMP-2 amino acid sequence to improve collagen binding, using a known collagen binding domain from the vonWillebrand factor [21]. The delivery of growth factors in these affinity systems can be controlled by changing the overall affinity between the material and the growth factor (i.e. number of binding sites) or the rate of degradation of the matrix material. However, some of these approaches often still damage the protein due to the use of harsh solvents and high temperatures during the fabrication process.

Finally, the temporal and spatial release kinetics of the growth factor need to be controlled in order to most effectively act on the target cells [3]. These criteria have been addressed through various approaches including encapsulation, covalent linking and other chemical alterations, or co-delivery with other factors [21, 22, 96, 117]. Controlled release is often achieved by encapsulating the growth factor within a polymer to change the duration of bioactivity in order to maintain the concentration of growth factor at the implant site [22-24]. Release rates of proteins from the delivery vehicle are usually controlled by the diffusion properties of the protein and/or the degradation properties of the polymer. Proteins have been encapsulated in nano- or microparticles [22, 24, 25], electrospun nanofibers [118, 119], or lipid-based systems [120]. Controlled release can

also be achieved through matrix delivery systems (i.e. hydrogels) that have proteins uniformly dispersed in a biocompatible polymer carrier and release the protein as the matrix degrades [82, 112, 121]. In matrix systems, the release rate is driven by the degradation properties of the matrix material and the diffusion properties of the growth factor (i.e. concentration, molecular weight) [107].

In addition to the biochemical properties of the delivery system, the mechanical and physical properties (i.e. size, shape) have a role in the efficacy of growth factor delivery [122]. Physical properties can influence the interactions between the delivery system and the cells (i.e. endocytosis, circulation, targeting, immune response, adhesion), which may subsequently influence the efficiency of growth factor bioactivity [122, 123]. Previous research has shown that the surface topography of a material at either the nano- or micro-scales can alter the differentiation capabilities of osteogenic lineage cells [116, 124-126]. Many of the current BMP-2 delivery systems have focused on physical properties to meet the structural and mechanical requirements of bone regeneration. Recently, however, research has also focused on developing BMP-2 delivery systems with considerations for both biochemical and physical properties of the carrier.

Many different carriers have been developed for BMP-2, including the collagen carrier FDA approved for use in the Medtronic InFUSE™product [6, 79, 99]. Other BMP-2 carrier materials include PLGA, hydrogels, calcium phosphate (CaP) cement, hydroxyapatite (HA), demineralized bone matrix (DBM), and tricalcium phosphate (TCP) [8, 17, 83, 127-129]. These carrier systems allow for some control of the BMP-2 released and have been shown to improve BMP-mediated differentiation and mineralization *in vitro* and *in vivo*. However, some of these systems utilize harsh

chemical treatments during fabrication or still require large doses to induce a response. The work presented in this thesis examines different delivery methods for BMP-2 in order to enhance functional repair of bone tissue.

CHAPTER 3

SUSTAINED DELIVERY OF BMP-2 IN A LIPID-BASED MICROTUBE SYSTEM

3.1 Abstract

Sustained release systems have previously been developed for the use of growth factors in tissue engineering therapies. However, many of these systems continue to have limitations associated with low loading efficiencies and minimal biological activity after release. This aim focused on employing a previously developed lipid-based microtube delivery system for the sustained release of bone morphogenetic protein-2 (BMP-2). The lipid microtubes were fabricated using a self-assembly method, thus avoiding the use of harsh organic solvents that may cause damage to the protein. The microtubes were loaded with BMP-2 by rehydrating lyophilized microtubes in a concentrated BMP-2 solution and the subsequent release kinetics was measured using *in vitro* immunoassays. The capacity of this system to deliver biologically active BMP-2 was assessed *in vitro* using alkaline phosphatase assays, Von Kossa staining, and quantitative real time RT-PCR for osteogenic gene expression in human mesenchymal stem cell (hMSCs). The results demonstrated that the lipid microtube system provided sustained delivery of biologically active BMP-2, determined by the ability to enhance osteogenic differentiation over the control groups. However, when the sustained delivery system was compared to the delivery of a bolus dose of BMP-2, no significant advantage for cell differentiation was observed over the bolus.

3.2 Introduction

The interdisciplinary field of tissue engineering presents promising therapies to repair tissue and restore physiological function, with the potential to address many of the difficulties and limitations associated with grafting procedures. Tissue engineering therapies may include a combination of cell, protein, or gene therapies to restore and regenerate physiological tissue function. In particular, protein or growth factor therapies have shown promise in tissue engineering therapies due their highly specific actions [8, 82]. Growth factors have the ability to induce a variety of cell functions vital to tissue repair, such as proliferation, migration, and differentiation. However, protein therapies often require frequent injections at high doses to overcome poor protein stability, making these treatments dangerous to the patient and very expensive [9, 130]. Sustained delivery systems that are able to optimally control the rate and location of growth factor release, while also maintaining a concentration level within therapeutic limits are necessary in order to provide growth factor therapies safely and effectively to patients [131].

Existing growth factor delivery systems include lipid-based and polymeric vehicles [19, 132]. However, the fabrication processes of many of these systems often involve the use of harsh organic solvents, which may denature and deactivate sensitive proteins, resulting in low loading efficiencies and reduced bioactivity [9, 112, 120, 129]. Another limitation associated with current delivery systems is the occurrence of a large burst release of the growth factor soon after implantation [25, 132]. This release profile may not be optimal for tissue repair since the surrounding tissue sometimes requires prolonged exposure to the growth factor [133].

Bone morphogenetic proteins (BMPs) have been utilized widely in bone tissue engineering because of their ability to initiate and maintain the entire bone formation cascade (i.e. chemotaxis, proliferation, and differentiation) [8, 9, 82, 84, 85, 134, 135]. However, delivery of BMPs has been challenging due to the short half-life and rapid diffusion from the treatment site. Efforts to sustain BMP-2 activity have previously been approached by incorporating the protein in degradable carriers and/or co-delivery with other factors. The current carrier materials include collagen, tricalcium phosphate, demineralized bone matrix, hydrogels, and synthetic polymers [8, 9, 83, 134]. The delivery of BMP-2 in an absorbable collagen sponge is FDA approved for use in tibial fractures and spinal fusions. However, this system still requires large doses of BMP-2 at high costs and has unpredictable pharmacokinetic profiles [83, 103, 134]. Therefore, further development of carrier systems with consistent results and reduced doses is required.

Previous research has shown BMP-2 expression to vary spatially and temporally during fracture healing, with higher concentrations occurring in mature and hypertrophic chondrocytes and areas of active bone formation [64, 84, 86, 135]. However, the specific time period and mode of localization for optimal BMP-2 activity is still unclear. A carrier system may be designed to provide sustained, localized delivery of BMP-2 within the therapeutic limits throughout the course of tissue regeneration, ensuring that BMP-2 is present during the optimal time to induce a cell response [3, 83, 130].

The goal of this study was to establish if sustained release of BMP-2 from a lipid-based microtube delivery system would significantly enhance *in vitro* mineralization of human mesenchymal stem cells (hMSCs) in comparison to controls, empty microtubes,

and a bolus dose of BMP-2. The lipid-based microtube vehicle used in this study was previously developed for the delivery of neural growth factor, transforming growth factor-ß, and brain derived neurotrophic factor [120, 136, 137]. Lipid microtubes are a unique delivery system due to the self-assembly method used to fabricate this carrier system, which avoids the use of organic solvents, heat, and other harmful procedures that are often involved in processes utilized to produce growth factor delivery systems [5, 120, 138, 139]. These microtubes are also beneficial because they can either be injected for minimally invasive procedures or suspended in three dimensional gel structures for implantation [120, 136]. The hypothesis was that the lipid microtubes would provide sustained release of biologically active BMP-2, thereby enhancing mineralization of hMSCs. To test this hypothesis the system was analyzed using *in vitro* assays to monitor the release kinetics and bioactivity of BMP-2, and subsequently compare the sustained delivery system with a bolus dose.

3.3 Materials and Methods

3.3.1 Lipid microtube fabrication

Lipid microtubes were prepared using a self-assembly method described by Meilander et al. [120]. First, 10 mg of $DC_{8,9}PC$ lipid (Avanti Polar Lipids, Alabaster, AL, USA) (**Figure 3.1**) was dissolved in 10 ml of 70% ethanol at 55ºC. The lipid solution was held at 55ºC for 6 hours and then slowly cooled to 25ºC in a microprocessor-controlled refrigerated water bath (Isotemp Refrigerated Circulator, Fisher Scientific, Waltham, MA, USA). The microtubes were then stored at room temperature until further use. See **Appendix A** for a detailed protocol.

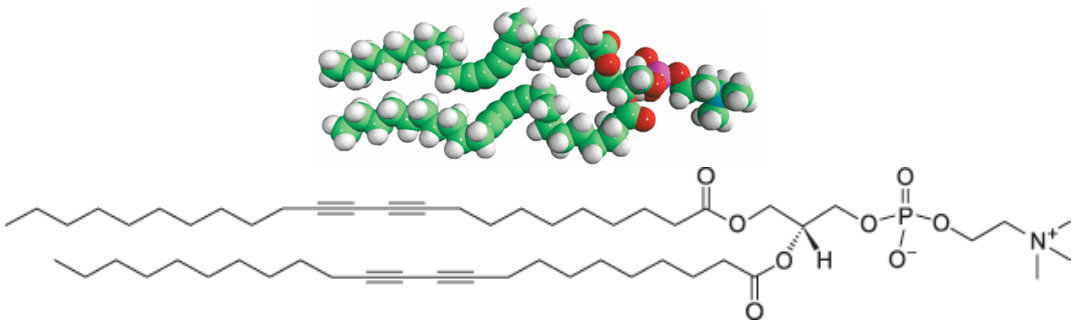

Figure 3.1 *1,2-bis(tricosa-10,12-diyonyl)-sn-3-phosphocholine* ($DC_{8,9}PC$) (Images courtesy of Avanti Polar Lipids, Alabaster, AL, USA) [140]

Prior to drying and using the microtubes in assays, the cryoprotectant trehalose (Sigma, St. Louis, MO, USA) was added to the solution at a concentration of 50 mM to preserve the tubular structure during the drying process. The microtubes were then washed in PBS and collected by centrifugation (1500 *g*, 10 min). Remaining solution in the microtubes was removed by lyophilization.

3.3.2 Characterization of lipid microtube dimensions and degradation

An aliquot of microtubes was placed on a glass slide with a cover slip to create a single layer of microtubes. The microtubes were imaged using a Zeiss Axiovert light microscope connected to an AxioCam digital camera (Carl Zeiss, Inc., Thornwood, NY, USA) and desktop computer running AxioVision software. The lengths of microtubes in at least 5 fields of view were traced from the captured images using the AxioVision software. The yield of microtubes was calculated from a dilution of microtubes counted on a hemocytometer.

To monitor the degradation, microtubes were incubated in 500 µl of phosphate buffered saline (PBS) or α-MEM (Invitrogen, Carlsbad, CA, USA) with 16% fetal calf serum (Atlanta Biologicals, Atlanta, GA, USA) and 2 mM L-glutamine, 100 units penicillin, and 100 µg streptomycin (Invitrogen). At the respective time points an aliquot

of microtubes was collected and the lengths were measured using the light microscope as described previously.

3.3.3 Protein loading and release kinetics

The microtubes were loaded with recombinant human BMP-2 (CHO-derived, carrier free, R&D Systems; Minneapolis, MN, USA) by rehydrating the dried microtubes in 40 μl of protein solution per mg of lipid. The microtubes were allowed to incubate in the protein solution overnight at 8°C. Unencapsulated growth factor was separated from the microtubes by centrifugation and collected for assay with an rhBMP-2 enzyme-linked immunosorbent assay (ELISA; R&D Systems). The loading efficiency was measured using microtubes that were counted on a hemocytometer and diluted to known concentrations. The microtubes were then incubated overnight in BMP-2 solution at a concentration of 2 μg/ml. The unencapsulated protein was separated from the microtubes by centrifugation and collected for assay with an ELISA (R&D Systems).

Microtubes loaded with BMP-2 were incubated in 500 μl of PBS to monitor the release kinetics. The microtubes were then separated by centrifugation and the supernatant was collected and stored at -20°C until assay. Microtubes were resuspended in 500 μl of fresh PBS at each time point. The amount of BMP-2 released was measured using an ELISA.

3.3.4 Bioactivity assay

The bioactivity of released BMP-2 was analyzed by determining its ability to induce alkaline phosphatase activity in human mesenchymal stem cells (hMSCs). Human mesenchymal stem cells, kindly provided by Tulane University, were harvested from bone marrow aspirates. Cells were passaged twice in α-MEM containing 16% FBS

(Atlanta Biologicals), 2 mM L-glutamine, 100 units penicillin, and 100 µg streptomycin (Invitrogen). The hMSCs were subcultured at a low density (500 cells/cm^2) and not allowed to expand past 70% confluency. The hMSCs were then trypsinized, counted, and seeded in collagen-coated 24-well tissue culture treated plates at a density of 10,000 cells/cm^2. The cells were allowed to reach confluency, usually requiring 1-2 days post-seeding. The cells were then differentiated in media supplemented with 6mM ß-glycerophosphate, 50 µg/ml ascorbic acid 2-phosphate (Sigma) (**Appendix B**). Cells layers were collected and analyzed at 7 and 28 days for alkaline phosphatase (ALP) activity. ALP activity was quantified using the *p*-nitrophenylphosphate method. Briefly, cell layers were washed with PBS, lysed with 0.1% TritonX-100/PBS and subjected to three freeze-thaw cycles to thoroughly disrupt the cell membranes. Subsequently, 50 µl of the supernatant was incubated with 50 µl *p*-nitrophenylphosphate solution (Sigma) for 30 minutes to 2 hours at 37ºC. The reaction was stopped by adding 100 µl 1M NaOH and the absorbance was read at 405 nm using a colorimetric plate reader. ALP activity was normalized to total DNA content. DNA content from cell lysates was quantified using the Pico Green® dsDNA Quantitation Kit (Molecular Probes). Briefly, samples from the cell lysates were added to a black 96-well plate in triplicate and incubated for 5 minutes with the Pico Green® working solution. The 96-well plate was then read on a fluorescent plate reader at an excitation of 485-nm, emission of 535-nm and manual gain of 60. Sample intensities were compared to a standard curve of known dsDNA concentrations.

Cell layers were also analyzed for phosphate deposits with the Von Kossa staining technique at 4 weeks. Cells were fixed in 70% ethanol and incubated under UV light

with 5% silver nitrate (Sigma) solution for 10 minutes. The cell layers were then rinsed in distilled water and treated with 2.5% sodium thiosulfate for 2 minutes.

Sustained delivery was compared to a bolus dose. Equivalent doses of BMP-2 (100 ng/ml) were either delivered encapsulated in the microtubes or as a bolus dose. The bolus dose was removed after 48 hours. BMP-2 microtubes were collected and reused throughout the study.

3.3.5 RNA isolation and quantitative RT-PCR

Cells monolayers were rinsed with PBS and then scraped from the tissue culture plates and stored in 500 µl RNAlater (Ambion, Austin, TX, USA) at -20°C. Cell pellets were then separated by centrifugation and resuspended in RLT buffer (Qiagen, Valencia, CA, USA) with 1% ß-mercaptoethanol (Sigma) and disrupted by passing through a Qiashredder (Qiagen) according to the manufaturer's protocol. RNA was isolated using the RNeasy spin columns (Qiagen) according to the manufacturer's protocol. RNA was quantified with a Nanodrop® ND-1000 spectrophotometer system. The RNA was then converted to cDNA using the Superscript III kit (Invitrogen). Samples were analyzed for alkaline phosphatase (ALP), bone sialoprotein (BSP), osteocalcin (OCN), and Runx2 mRNA levels using iQ SYBR Green Supermix (Bio-Rad, Hercules, CA, USA) on a Bio-Rad iCycler iQ5 real-time PCR instrument using the sequences listed in **Table 3.1** (Integrated DNA Technologies, Inc., Coralville, IA, USA) [32, 141]. Template concentrations from cDNA solutions were quantified using a linear standard curve of known template concentrations. Transcript levels were then expressed as femtomoles of transcript and normalized to total µg RNA. All results were confirmed to be the

amplification of a single transcript product by the presence of a single peak in the melt curve.

Table 3.1 Quantitative real-time PCR primers (5' to 3' direction)

Gene	Forward	Reverse
Alkaline phosphatase	CGTGGCTAAGAATGTCATCATGTT	TGGTGGAGCTGACCCTTGA
Bone sialoprotein II	GGCCTGTGCTTTCTCAATGAA	GCCTGTACTTAAAGACCCCATTTTC
Osteocalcin	GCAAAGGTGCAGCCTTTGTG	GGCTCCCAGCCATTGATACAG
Runx2	TGATGACACTGCCACCTCTG	GGGATGAAATGCTTGGGAAC

3.3.6 Statistical analysis

All data are presented as the mean ± standard error of the mean (SEM), unless otherwise stated. Statistical analysis was done using Prism 5 software (GraphPad Software, Inc., San Diego, CA, USA). Groups were compared using an ANOVA and Tukey's *post hoc* analysis for pairwise comparisons, with a p-value<0.05 considered statistically significant. Other statistical analyses used are stated in the results. When required, raw data was transformed using a logarithmic transformation to make the data normal and the variance independent of the mean [142, 143].

3.4 Results

3.4.1 Characterization of lipid microtube dimensions and degradation

The microtubes fabricated using the self-assembly method had an average length of 30 ± 14.71 μm (mean ± standard deviation, **Figure 3.2**) and median length of 27.82 μm. Over 75% of the microtubes had lengths between 10 and 40 μm, and nearly 20% of the microtubes were 40-70 μm. However, a small portion (less than 1%) of the microtubes reached lengths over 100 μm. Typically, 10 mg of $DC_{8,9}PC$ lipid yielded approximately $6x10^8$ microtubes.

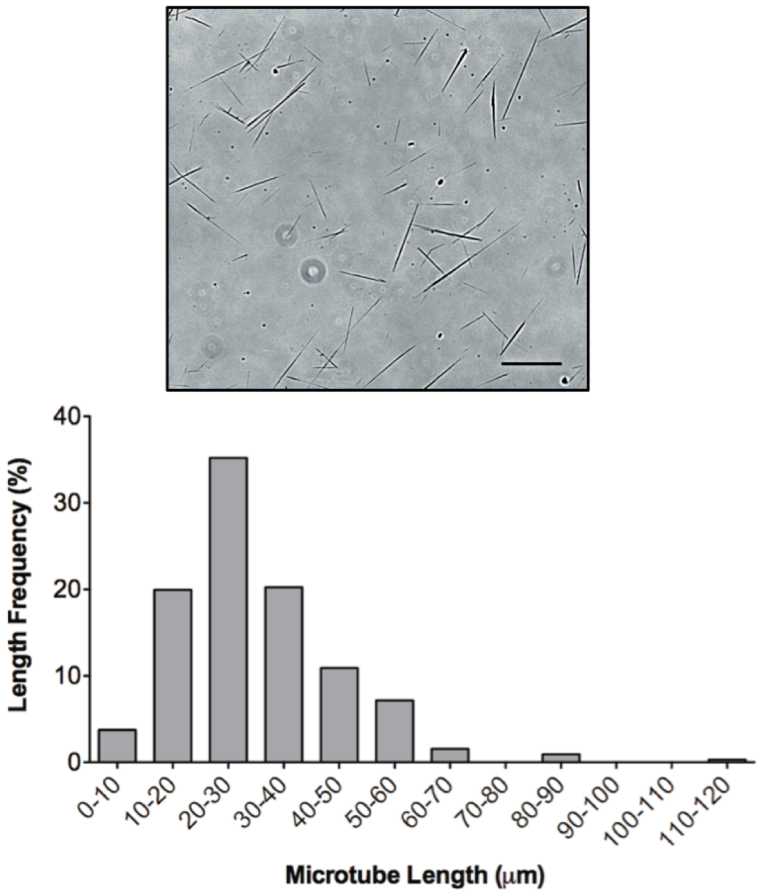

Figure 3.2 Lipid microtube characteristics. Representative light microscope image (top) of $DC_{8,9}PC$ lipid microtubes fabricated using the self-assembly method described by Meilander et al. [120]. Length distribution (bottom) of lipid microtubes measured from microscope images, average length of 30 ± 14.71 μm (mean ± SD).

Degradation was expected to occur from the ends of the microtubes due to the open lipid chains available to hydrolysis. This was confirmed by measuring the lengths of the microtubes incubated in cell culture media or PBS and performing a Kruskal-Wallis test for non-Gaussian distributions to determine if the distribution in lengths were significantly different. The lengths of the microtubes incubated in both PBS and media significantly decreased from day 0 to day 21 ($p<0.0001$), with the average lengths decreasing from 30 ± 15 μm to 17 ± 10 μm (**Figure 3.3A**). Microtubes in PBS appeared to degrade quicker than microtubes in media, with a significant decrease ($p<0.0001$) in lengths at each time point until day 10. Whereas microtubes in media had a slightly more

delayed degradation with no significant decrease in lengths until day 7 ($p<0.0001$). Although the microtubes in PBS degraded faster initially and had significantly shorter lengths than microtubes in media at days 4 and 10 ($p<0.0001$), by day 21 there was no difference in lengths of the microtubes in either solution. The microtubes had a tendency to aggregate in cell culture media due to the negatively charged ions exposed on the lipids during hydrolysis and the cations present in the media (**Figure 3.3B**).

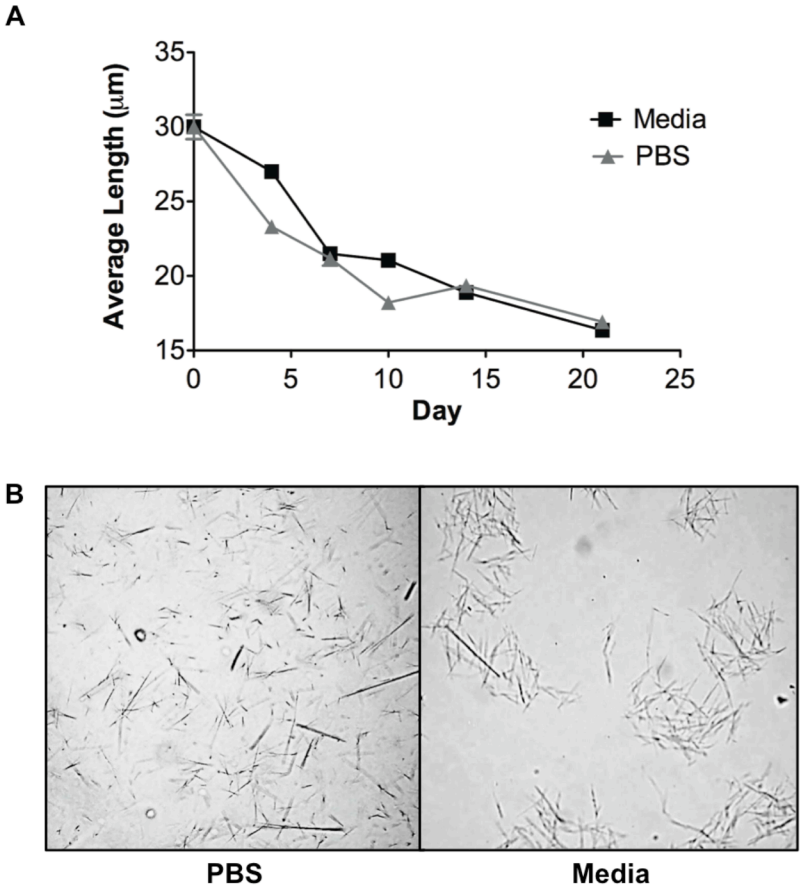

Figure 3.3 Lipid microtube degradation. **(A)** Average lengths of lipid microtubes incubated in PBS or media, measured from microscope images obtained at respective time points. Lengths decreased by approximately 50% during the 21-day period ($p<0.0001$). **(B)** Representative microscope images of microtubes after 4 days either in PBS or cell culture media conditions.

3.4.2 Protein loading and release kinetics

BMP-2 was effectively loaded into the microtubes. The loading capacity was represented as a ratio of the amount of protein encapsulated to the total amount of protein initially added to the microtubes (**Figure 3.4**). As expected, the amount of unencapsulated protein decreased with an increase in microtube concentration due to a larger available volume from the increasing microtube population. The lowest concentration of microtubes ($1x10^7$) encapsulated significantly less protein than all other microtube concentrations ($p<0.0001$). At concentrations above $4x10^7$ microtubes there was no significant decrease in unencapsulated protein indicating that there is a limit of a 90% loading capacity.

BMP-2 was then loaded into 10 mg of microtubes to monitor the release kinetics. Protein was released from microtubes for at least two weeks without a large initial burst release (**Figure 3.5**). Approximately 40% of the initial protein loaded was released over this period. The cumulative release was calculated as a ratio of the initially loaded protein, which was estimated using the approximate volume of microtubes and the concentration of the loading solution.

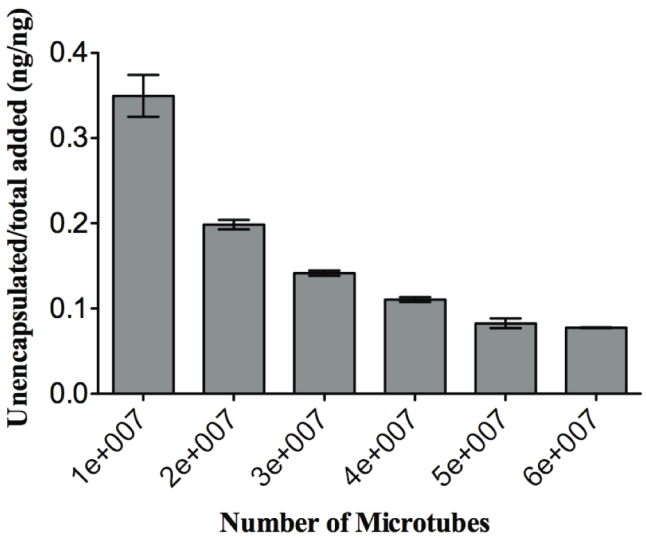

Figure 3.4 Loading capacity in relation to quantity of microtubes, represented as the ratio of unencapsulated protein to total protein added to the microtubes (n=3).

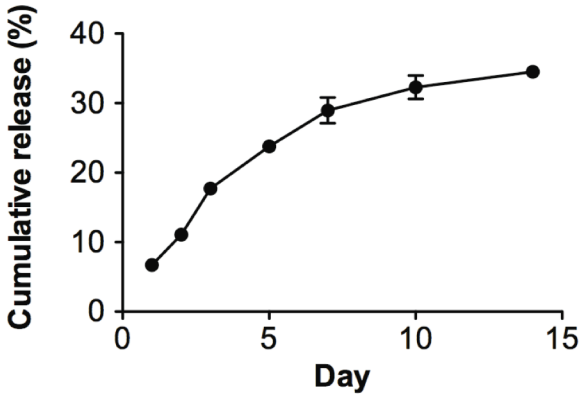

Figure 3.5 Release kinetics of BMP-2 measured with ELISA. Cumulative release calculated as the total amount released divided by the quantity of initially loaded BMP-2 (n=4).

3.4.3 Cell viability

Cell viability in the presence of microtubes was assessed using a LIVE/DEAD® Viability Kit (Invitrogen, Carlsbad, CA) to fluorescently label hMSC monolayers and imaged with a fluorescent microscope for viable cells (Calcein label—green) and dead cells (Ethidium homodimer label—red) (**Figure 3.6**). The images showed a minimal number of dead cells at all time points for each group. The highest concentration of microtubes had a larger number of dead cells at days 14 and 28 than all other groups, however the majority of the cells remained viable. DNA content was also not greatly affected by the presence of the lipid microtubes, measured by the Pico Green DNA quantification assay (**Figure 3.7**). DNA content at the highest concentration of microtubes ($24x10^5$ tubes/ml) was significantly less than the control (0 tubes/ml) only at day 14. However, by day 28 DNA content for the high concentration of microtubes significantly increased and was no longer less than the control. This indicates that the increase in cells was simply delayed by the high concentrations of microtubes, and cell number was not overall substantially hindered.

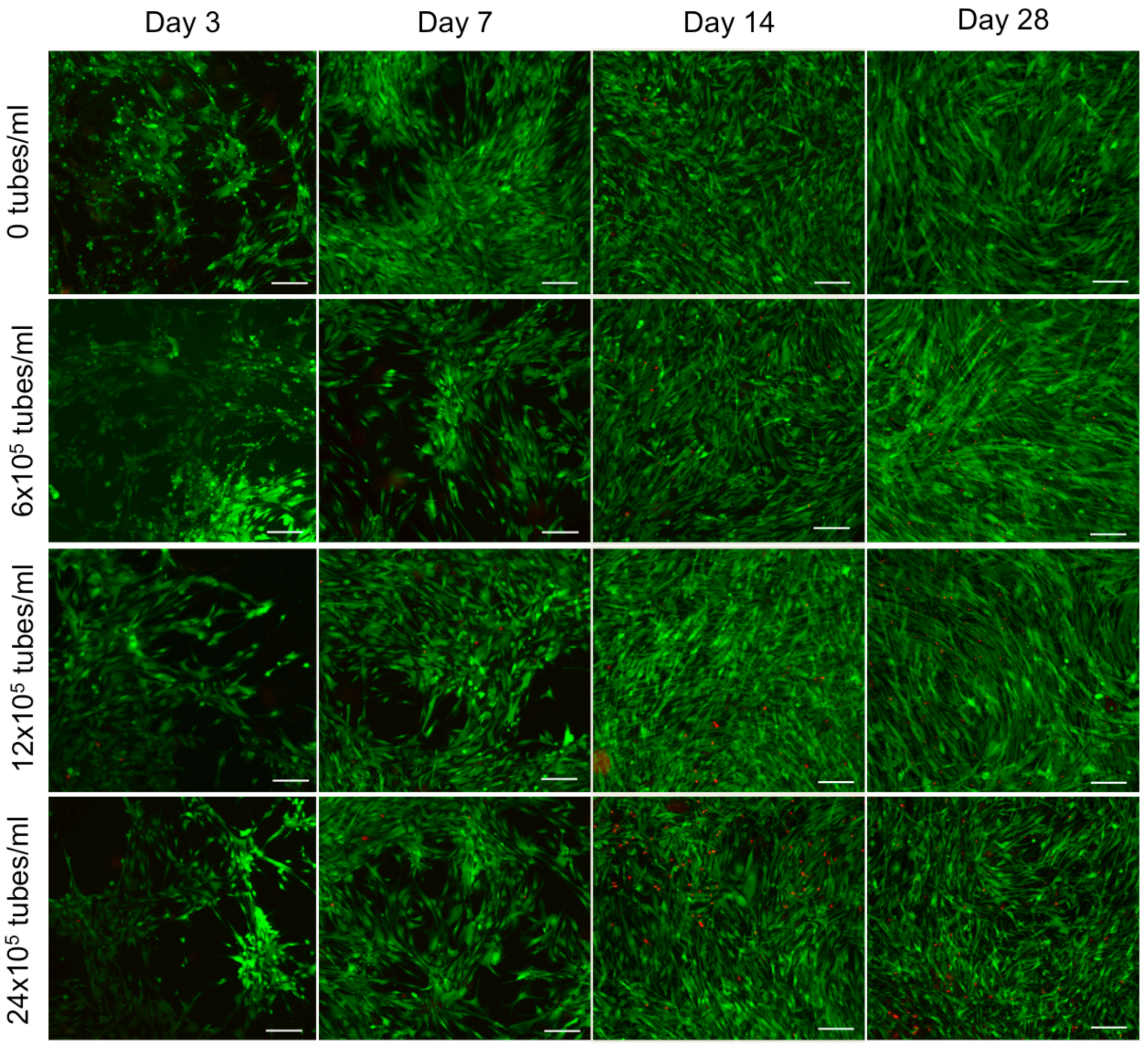

Figure 3.6 Cell viability in the presence of lipid microtubes. Microscope images of hMSC monolayers stained with a LIVE/DEAD® Viability Kit (RED = dead cells, GREEN = live cells; magnification 4x, scale bars = 200 μm).

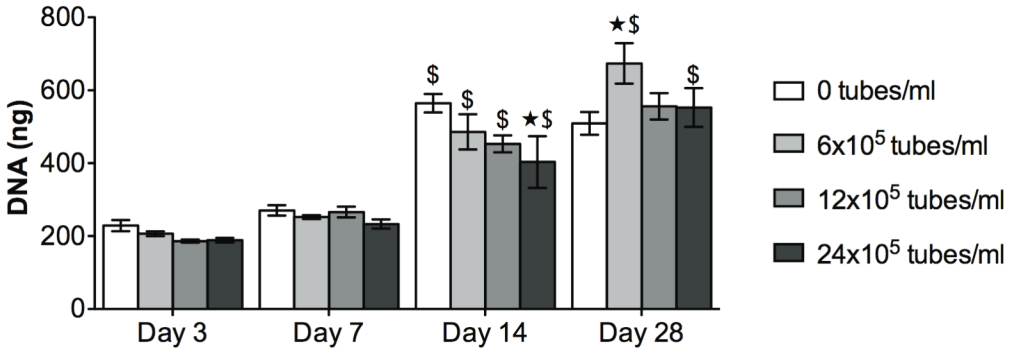

Figure 3.7 DNA quantification of hMSCs in culture with increasing concentrations of lipid microtubes (ANOVA: ★ $p<0.05$ compared to the control (0 tubes/ml) within each time point; \$ $p<0.05$ compared to the same group at the previous time point; n=4).

3.4.4 Post-release bioactivity assay

To ensure the BMP-2 released from the microtubes remained biologically active, the ALP activity of hMSCs was measured. The results demonstrate that BMP-2 releasing microtubes had significantly higher levels of alkaline phosphatase activity at 28 days compared to control microtubes ($p<0.01$), indicating a release of bioactive BMP-2 from the microtubes (**Figure 3.8**). Additionally, hMSCs in the presence of BMP-2 releasing microtubes had a significant increase ($p<0.0001$) in ALP activity from day 7 to day 28. The control PBS-loaded microtubes also significantly increased ($p<0.01$) from day 7 to day 28, however to a less extent than the BMP-2 microtubes.

Matrix mineralization was confirmed with von Kossa staining for phosphate deposits at day 28. Stained cell monolayers showed more phosphate deposits when hMSCs were cultured in the presence of BMP-2 releasing microtubes (**Figure 3.9**). These phosphate deposits exhibited nodule formation, indicating osteogenic differentiation of the hMSCs. Fewer mineralized regions were observed in monolayers treated with control microtubes.

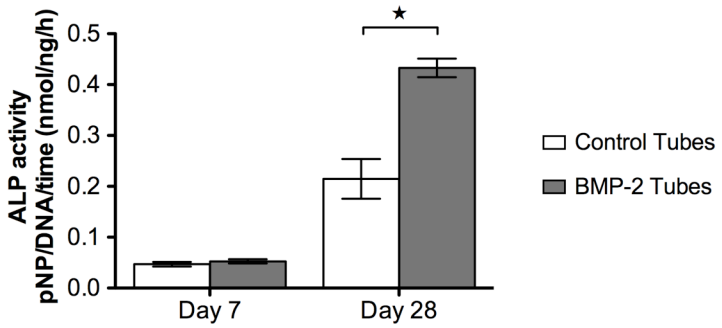

Figure 3.8 Alkaline phosphatase activity in hMSCs, measured by the *p*-nitrophenylphosphate assay, in response to BMP-2 releasing microtubes or control microtubes (n=6). Un-paired *t*-test: ★ $p<0.01$; each group is significantly different between time points ($p<0.01$ control tubes, $p<0.0001$ BMP-2 tubes).

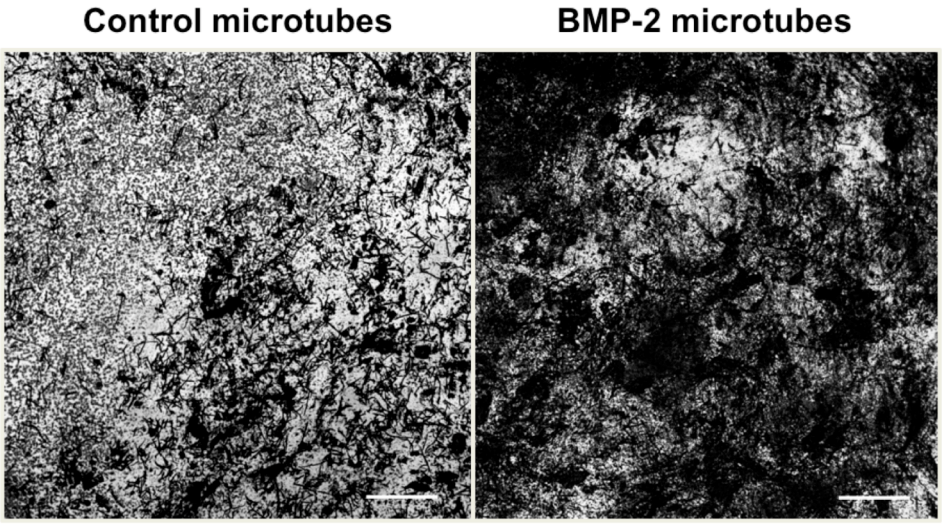

Figure 3.9 Von Kossa staining of hMSC monolayers after 28 days in culture with control or BMP-2 microtubes, scale bars = 100 μm.

3.4.5 Sustained release versus bolus dose of BMP-2

Further assessment of the efficacy of this system compared the differentiation of hMSCs in the presence of a bolus BMP-2 dose or BMP-2 releasing microtubes. The bolus BMP-2 dose was equivalent to the total amount of BMP-2 encapsulated in the microtubes. ALP activity was assessed at 7 and 28 days after bolus BMP-2 or BMP-2 microtubes were added to the cell culture media (**Figure 3.10**). After 7 days, the cells incubated with BMP-2 microtubes had significantly lower ALP activity than all other groups ($p<0.01$) and the bolus BMP-2 group was significantly lower than the control microtubes ($p<0.01$). Between day 7 and 28 the ALP activity in cells with bolus BMP-2 and BMP-2 microtubes increased significantly ($p<0.0001$). However, only the cells exposed to the bolus dose of BMP-2 had significantly higher ALP activity at 28 days than the cells incubated with control microtubes. The ALP activity at day 28 in cells incubated with BMP-2 microtubes remained higher than the control microtubes, however the differences detected by the ANOVA were not significant in this case.

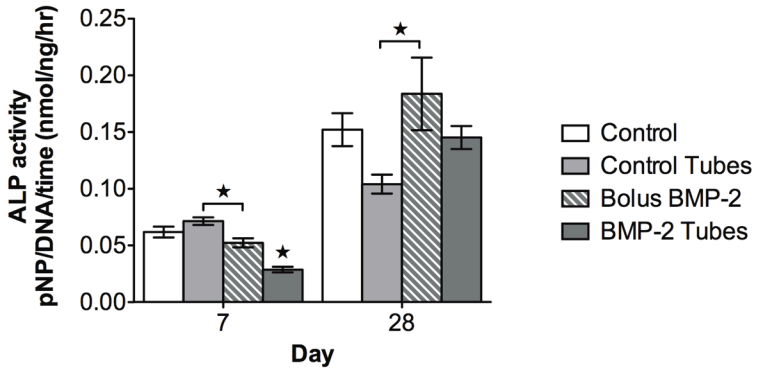

Figure 3.10 ALP activity in hMSCs, measured by the *p*-nitrophenylphosphate assay, in response to bolus dose BMP-2, BMP-2 microtubes or control microtubes (n=6). ANOVA: ★ $p<0.01$ within time-point. All groups significantly increased from day 7 to day 28 (un-paired *t*-test: $p<0.01$).

Gene expression was analyzed with RT-PCR at 7 and 28 days after bolus BMP-2 or BMP-2 releasing microtubes were added to the cell culture media. Expression levels for the osteogenic matrix proteins (bone sialoprotein, osteocalcin), transcription factor (Runx2), and mineralization-associated enzyme (alkaline phosphatase) were determined from linear standard curves (**Figure 3.11**). The bolus dose of BMP-2 significantly increased alkaline phosphatase, bone sialoprotein, and osteocalcin mRNA expression by day 28. BMP-2 microtubes significantly increased osteocalcin expression by day 7, however the level of osteocalcin expression remained the same at day 28 and was significantly lower than the expression in the cells exposed to the bolus dose. BMP-2 microtubes increased Runx2 expression compared to the control, however the control microtubes also increased Runx2 expression compared to the control. Therefore, the increase in Runx2 expression could not be attributed to the BMP-2 released from the microtubes.

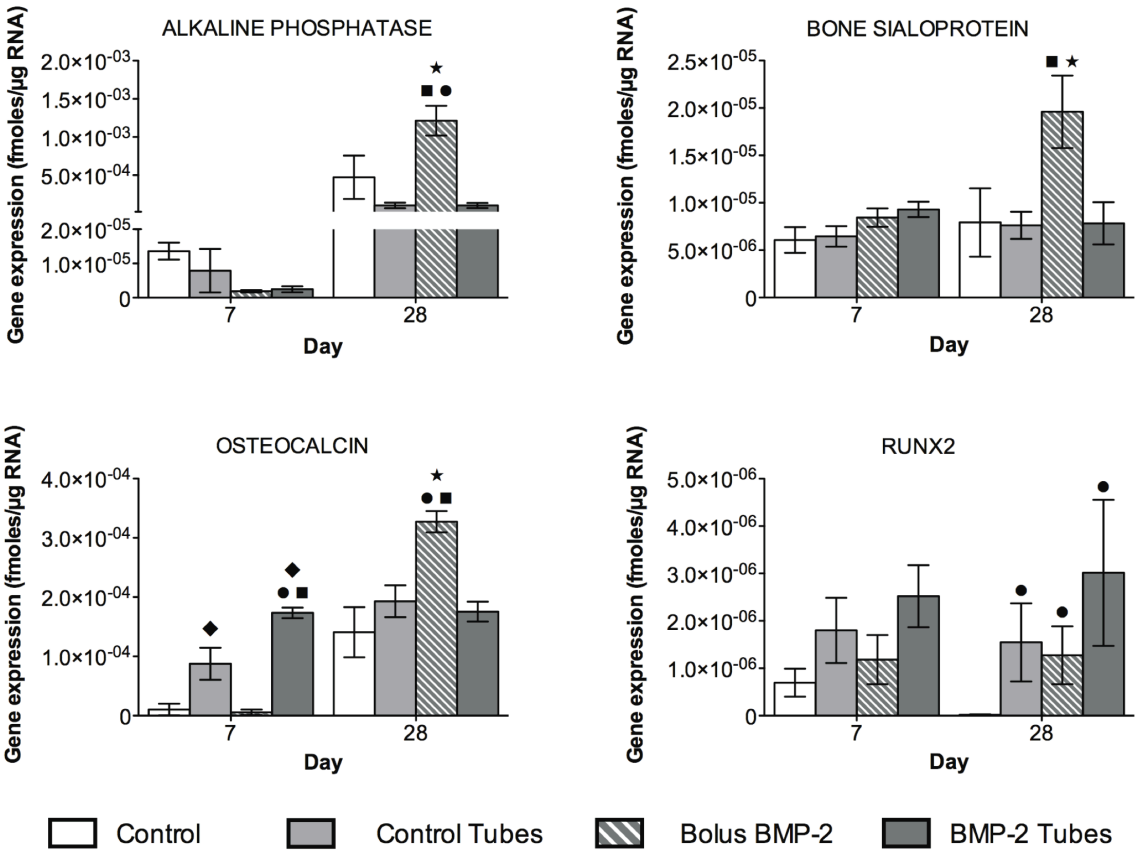

Figure 3.11 Osteogenic gene expression in response to bolus dose and BMP-2 microtubes. mRNA transcript levels were assessed by real time RT-PCR analysis for osteoblastic markers including alkaline phosphatase (ALP), bone sialoprotein (BSP), osteocalcin (OCN), and Runx2; (n=6). Data presented as femtomoles of mRNA transcript normalized to µg of total RNA. ANOVA: $p<0.05$ within each time-point • versus control, ■ versus control tubes, ◆ versus bolus BMP-2, ★ versus BMP-2 tubes.

Differences in matrix mineralization were assessed with von Kossa staining for phosphate deposits at day 28. Stained cell monolayers showed more phosphate deposits when hMSCs were cultured in the presence of BMP-2, either as a bolus or released from the microtubes (**Figure 3.12**). These phosphate deposits exhibited nodule formation, indicating osteogenic differentiation of the hMSCs. However, there were no large differences in matrix mineralization observed between the bolus BMP-2 and BMP-2 microtubes groups. Fewer mineralized regions were observed in control monolayers.

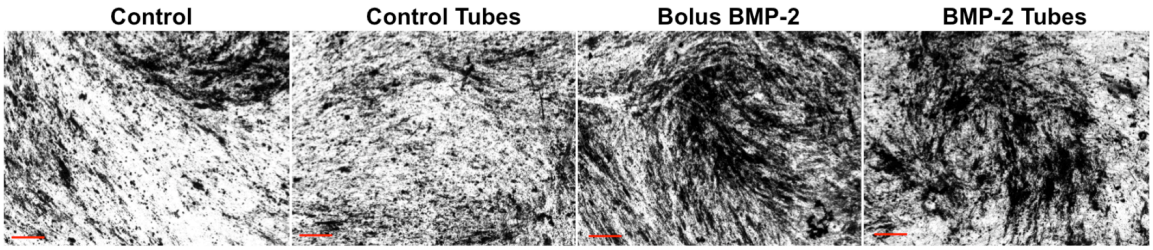

Figure 3.12 Von Kossa staining of hMSC monolayers after 28 days in culture to compare bolus BMP-2 and BMP-2 releasing microtubes, scale bars = 200 μm.

3.5 Discussion

Critical issues for effective therapeutic protein delivery include the stability of the proteins, time or duration of exposure, and effective dose. This has led researchers to develop sustained and controlled delivery systems [9]. However, the fabrication processes used for many of these carriers are extremely harsh and unfavorable for protein structure and function [9, 112, 120]. Additionally, many other sustained release systems, such as nanoparticles and microparticles, have unpredictable or unknown loading capacities leading to inconsistent results [24, 144-149]. In this study we utilized a lipid microtube system developed by Meilander, et al. for growth factor delivery [120]. However, the efficacy of these microtubes as a delivery vehicle may be growth factor dependent. We demonstrated the response of hMSCs to the sustained release of BMP-2 using the lipid microtube delivery system for bone tissue engineering applications. We

found that although the microtubes provided sustained release of bioactive BMP-2, there was no significant benefit for hMSC differentiation over exposure to a bolus dose.

Lipid microtubes were successfully fabricated using the self-assembly method previously described, with an average length of 30 ± 15 μm [120, 138]. Although the large dimensions of the microtubes restrict their use for drug delivery applications in the vasculature (i.e. injectable delivery), they are suitable for applications in which localized delivery within tissues is desirable. The large size will also restrict endocytosis by cells in the surrounding tissue, which is a process that may render a drug inactive due to the external localization of some receptors on the cell membrane. Smaller drug delivery systems, such as nanoparticles, can be quickly taken up by cells, resulting in the release of the drug within the cell [150, 151]. Although this may not be a problem for drugs with intercellular receptors, such as steroid hormones or gene therapies, BMP-2 requires binding to extracellular domains of the BMP receptors [95, 152].

The microtubes were observed to degrade from the ends, as indicated by the significant decrease in average length. Carlson, et al. suggested that the degradation of $DC_{8,9}PC$ lipid microtube structures is dominated by the heterogenous bilayer packing at the open microtube ends [153]. However degradation is not limited to the open ends and can occur at any location of non-uniform bilayer packing along the walls of the microtubes where the lipid molecule is exposed to potential hydrolytic activity [153]. Due to this hydrolytic degradation, the microtubes were observed to form aggregates in the cell culture media as the negatively charged fatty acids produced during hydrolysis were electrostatically attracted to cations and other positively charged molecules in the media [138].

Sustained release of BMP-2 from the lipid microtubes was observed for at least two weeks without a large initial burst release, as shown by the release profile. Other studies have shown that these microtubes provide release for over 50 days [154]. Meilander, et al. determined that molecular weight of the loaded protein affects the rate of release, with smaller molecules releasing faster than the larger molecules [120]. It was also shown that the higher concentrations of protein initially loaded in the microtubes caused a larger amount to be released each day [120]. This leads to the ability to more accurately assess the performance of the delivery system and potentially predict the release of various proteins.

The viability of hMSCs was not substantially affected in the presence of high concentrations of lipid microtubes. Previous studies have shown that lipid microtubes were biocompatible and safe for use in *in vitro* tissue culture experiments [120]. Other research has also shown that implanting microtubes for *in vivo* rodent assays did not induce a significant inflammatory response as compared to saline injections [120, 136]. Some polymeric delivery systems have demonstrated chronic inflammatory responses and low biocompatibility due to the biproducts resulting from degradation as well as residual chemicals from the fabrication process [155]. The lipid microtube system avoids both of these criteria, with free fatty acids being produced during degradation and no harsh chemicals used during fabrication.

BMP-2 released from the microtubes was able to increase alkaline phosphatase (ALP) activity in hMSCs after four weeks in culture compared to cells incubated with control microtubes, indicating that the microtubes provided sustained release of biologically active BMP-2 [156]. However, ALP activity was not significantly different

when compared to a bolus dose of BMP-2. BMP-2 microtubes also did not significantly increase gene expression compared to a bolus dose of BMP-2. The results seen in ALP activity and osteogenic gene expression may be due to the response of hMSCs to different kinetics of BMP-2 exposure and lower concentrations of BMP-2 released from the microtubes [157]. Although the initial dose of BMP-2 loaded in the microtubes was equivalent to the bolus dose, the cumulative exposure of BMP-2 released from the microtubes was lower than the bolus dose. Previous research has shown that osteoinduction is dependent on the pharmacokinetics of the BMP-2 delivery system [16, 128, 129, 158, 159]. Maeda, et al., demonstrated that faster releasing systems resulted in more bone formation *in vivo*, while other work has shown that a burst release followed by a sustained release profile is more beneficial [16, 158-160].

The poor stability of the BMP-2 structure upon release from the microtubes may also contribute to the reduced osteogenic activity. BMP-2 structure and bioactivity is known to be highly sensitive to environmental conditions (i.e. temperature, pH, solubility, proteolytic degradation) [96, 161]. While encapsulated in the microtube system, BMP-2 is protected from many of the factors that denature or deactivate the protein. However, upon release from the microtubes, BMP-2 is subject to all of the adverse environmental factors that have been shown to damage the protein and reduce its bioactivity. This rapid degradation of the protein can cause the bioactivity of the small amount of released BMP-2 to be reduced, resulting in minimal signaling to induce a cell response. We showed that a dose greater than 25 ng/ml is required in order to induce a significant osteogenic response in hMSCs *in vitro* (**Appendix C**). In addition to the poor stability of BMP-2 upon release from the microtubes, the encapsulation within the

microtubes does not fully protect the BMP-2 from denaturing conditions such as temperature. Therefore, even while the BMP-2 is encapsulated within the microtubes, it is potentially subject to denaturing and subsequent reduced bioactivity. The drastic reduction of BMP-2 bioactivity can be taken into consideration when designing a future sustained delivery system, with the possibility of co-delivering BMP-2 and stabilizing factor, such as heparin. Zhao, et al., showed that the half-life of BMP-2 was only 1-3 hours *in vitro*, but could be prolonged 20-fold by using protective agents such as heparin and other sulfated polysaccharides [96].

Previous research has indicated that sustained release at low doses will be more effective than a large bolus dose, and will pose a lower risk of side effects [3, 133]. The aim of this study was to determine if sustained release of BMP-2 from the lipid microtube system would provide a significant benefit to inducing mineralization compared to the current clinical standard, which usually provides a large bolus dose of BMP-2 to the surrounding tissue. The lipid microtube sustained delivery system was designed to acquire prolonged exposure of BMP-2, with the expectation that sustained delivery of BMP-2 will result in greater mineralization. However, the prolonged exposure to lower amounts of BMP-2 did not exhibit a significant improvement over a brief exposure to a larger dose of BMP-2 in the differentiation response of hMSCs. Some research has suggested that a burst release followed by sustained release of BMP-2 is most desirable [100]. Nevertheless, the efficacy of the lipid microtube delivery system is protein dependent and may still be beneficial for applications that have low therapeutic concentration requirements, as was previously shown for the delivery of brain-derived neurotrophic factor (BDNF) [136].

3.6 Conclusions

In this study, we characterized the sustained release of BMP-2 from lipid microtubes and showed that the biological activity is retained after release from the microtubes. These results indicate that lipid microtubes can be used to provide sustained release of BMP-2 for bone tissue engineering. However, sustained delivery of BMP-2 was not sufficient to significantly enhance osteogenic differentiation compared to a bolus dose over a 28-day period. These data suggest that the microtube sustained delivery system is able to deliver active BMP-2, however the sustained release of low doses may not be significantly advantageous. Another approach for BMP-2 delivery will be investigated in Specific Aim II.

CHAPTER 4

INCORPORATION OF HEPARIN IN A COLLAGEN MATRIX TO IMPROVE BMP-2 RETENTION AND BIOACTIVITY

4.1 Abstract

The binding affinity of BMP-2 and the current FDA approved collagen carrier is low, resulting in rapid diffusion from the implant *in vivo*. This can cause ectopic bone formation in surrounding tissues as well as other systemic effects. Research has recently concentrated on improving the affinity of BMP-2 to the carrier material. The focus of this aim was to incorporate heparin in a collagen matrix to improve the retention and bioactivity of BMP-2 for bone tissue engineering applications. The ability to retain BMP-2 and the osteoinductive capacity of this delivery system was assessed *in vitro* using immunoassays and confocal microscopy to quantify BMP-2 content, and micro-CT analysis of cell-mediated mineralization. The results indicate that incorporation of heparin in the collagen matrix improves BMP-2 retention. This corresponded to slower release kinetics from collagen/heparin matrices. Three-dimensional mineralization of hMSCs was also significantly enhanced when heparin and BMP-2 were present in the collagen matrix. These results indicate that incorporating heparin in the collagen matrix improves BMP-2 retention, delays the release, and potentiates the bioactivity *in vitro*. Therefore, incorporation of heparin in a collagen matrix for the delivery of BMP-2 may be beneficial for bone tissue engineering.

4.2 Introduction

Growth factor therapies have gained considerable attention in recent years because of their highly specific activity and ability to induce a variety of cell functions vital to tissue repair, such as proliferation, migration, and differentiation. However, proteins often have low stability and rapidly diffuse from the treatment site, resulting in frequent injections at high doses. In Specific Aim I, we demonstrated that the sustained delivery of BMP-2 in a lipid microtube system was able release biologically active BMP-2, but the sustained release system did not provide a significant benefit compared to a bolus dose. These results indicate that a different type of delivery system may be more beneficial for BMP-2 therapies.

BMPs have been used in combination with various carrier materials in efforts to efficiently deliver and retain the BMP molecule at the treatment site. These carrier materials mainly include collagen and demineralized bone matrix (DBM) [15, 16]. Yet, few delivery approaches have addressed the biological interactions between BMP-2 and the carrier, and have mainly been designed to meet structural/biomechanical and immunogenic requirements. Currently, the FDA has only approved collagen as a carrier for BMP-2. Yet research has shown that BMP-2 has low affinity for collagen, leading to rapid diffusion from the construct [15]. Researchers have claimed that BMP-2 mediated bone formation not only depends on the initial concentration of BMP-2, but also is largely controlled by the subsequent retention within the carrier [15, 159]. Therefore, recent efforts have focused on enhancing the binding affinity of BMPs either by immobilizing heparin or other ECM molecules in the carrier, or biochemically altering the BMP-2 molecule [17, 20, 21].

BMPs were originally isolated from demineralized bone matrix using heparin affinity columns due to their inherent binding properties [162]. In addition to the high binding affinity, research has suggested that heparin is involved in BMP-mediated differentiation [17, 95, 96, 117, 163]. This effect has been shown to be in part due to heparin promoting protein-receptor binding with higher specificity and maintaining the structural conformation necessary for receptor-ligand binding [95, 117]. Heparin has also been shown to protect the ligand from suppression by antagonists such as noggin and chordin [96, 164].

Heparin is a sulfated polysaccharide, which is located on the cell surface as well as in the bone extracellular matrix (ECM). It is known to be a potent stimulator of proliferation in human mesenchymal stem cells (hMSCs) [112, 163]. Low molecular weight heparins have been shown to enhance osteoblast differentiation in a dose dependent manner by serving as a multifunctional regulator of growth factors expressed during bone repair [96, 112, 117, 163, 165]. These attributes of heparin may prove to be useful for bone tissue engineering.

Heparin has been used as an anti-coagulant and as a preventative treatment for thromboembolic episodes after orthopedic surgeries [166]. Without treatment, deep vein thrombosis occurs in 50-70% of patients that have undergone total hip arthroplasty, total knee arthroplasty, acute fixation of hip fractures, and in patients that have acute spinal cord injury or multiple injuries [166]. However, standard unfractionated heparin has been shown to have deleterious effects on bone formation when administered daily [166-168]. These effects include osteoporosis, increased calcium loss, and decreased bone turnover. Low molecular weight heparins, derived from unfractionated heparin, reduce

these risks by about 50% without the side effects seen with standard unfractionated heparin and have become the standard treatment for thromboembolism, [166, 169]. However, high doses of low molecular weight heparin administered daily can reduce cancellous bone volume and delay fracture healing [166]. Therefore, these effects must be considered when designing growth factor delivery systems that utilize heparin.

Crystal structure analyses indicate that heparin directly binds BMP-2 via electrostatic interactions among the negatively charged sulfate groups on the heparin molecule and the high concentration of positively charged amino acid residues at the N-terminus of BMP-2 [95, 117, 164, 170, 171]. Approximately 5-6 BMP-2 molecules can bind one heparin molecule with dissociation constant (K_d) of about 15-20 nM [95]. Ruppert, et al. showed that an 11 amino acid sequence at the N-terminus is critical for heparin binding, but this region is outside the cysteine rich area necessary for receptor binding, therefore does not inhibit receptor binding (**Figure 4.1**) [95]. This N-terminus region normally causes non-specific binding of BMP-2 to other receptors, however, when this region is bound to heparin, BMP-2 is able to bind more specifically to the BMP receptor [95]. Heparin binding also improves growth factor activity by inducing a conformational change in the proteins, leading to higher resistance to thermal denaturing, enzymatic degradation, and inactivation at acidic pH [172].

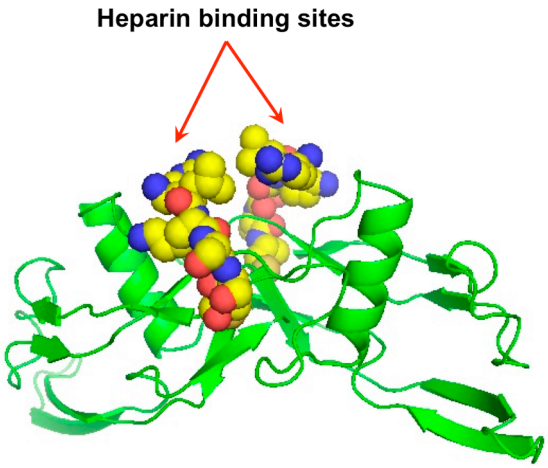

Figure 4.1 Dimerized BMP-2 structure with heparin binding sites indicated by the space-filling structures. Protein structure generated using PyMOL Molecular Viewer software with amino acid sequences acquired from the Protein Data Bank [95, 171].

A major limitation of current clinical BMP-2 treatments is the rapid diffusion from the implant site, causing a significant decrease in local concentration. Furthermore, soluble or free BMP-2 loses its bioactivity quickly due to enzymatic degradation and other physiologic conditions (i.e. pH, temperature, salt concentration). Studies have shown that immobilized growth factors retain their biological function and remain localized to the surface of the construct [26, 173, 174]. Research is currently investigating the incorporation or immobilization of heparin into implant materials to stabilize and localize heparin-binding growth factors at the implant site [17, 20, 111, 112, 175, 176]. Additionally, immobilizing heparin to the scaffold retains the heparin molecule locally, reducing the side effects caused by systemic exposure to heparin (i.e. loss in bone density, abnormal bleeding) [27].

The overall goal of Specific Aim II was to develop a delivery system for BMP-2 utilizing the binding properties with heparin to enhance the retention and osteoinductive activity. A lyophilized collagen matrix previously described by Porter, et al. was modified to incorporate heparin for the delivery of BMP-2 [177]. The hypothesis was that

BMP-2 would bind with higher affinity to the collagen/heparin matrix, retaining the growth factor within the matrix for a longer period of time, thereby enhancing mineralization. To test this hypothesis the system was analyzed using in vitro assays to monitor the retention of BMP-2 within the matrix and the bioactivity of BMP-2.

4.3 Materials and Methods

4.3.1 Effect of heparin on BMP-2 stability

To assess the stability of BMP-2 in the presence of heparin, BMP-2 content remaining in the cell culture media after three days was measured using an enzyme-linked immunosorbent assay (rhBMP-2 ELISA; R&D Systems). BMP-2 (carrier free, CHO cell expressed; R&D Systems) was incubated with low molecular weight heparin (porcine intestinal mucosa; Sigma) for 30 minutes prior to adding to cell culture media. The cell culture media was then collected from the cell layers after three days and assayed with the ELISA.

4.3.2 Differentiation of hMSCs in the presence of BMP-2 and heparin

BMP-2 mediated differentiation was analyzed by determining osteogenic gene expression in human mesenchymal stem cells (hMSCs). The hMSCs that Tulane University kindly provided were harvested from bone marrow aspirates. Cells were passaged twice in α-MEM containing 10% FBS (Atlanta Biologicals), 2mM L-glutamine, 100 units penicillin, and 100 μg streptomycin (Invitrogen). The hMSCs were sub-cultured at a low density (500 cells/cm^2) and not allowed to expand past 70% confluency. The hMSCs were then trypsinized, counted, and seeded in collagen-coated 6-well Nunc-tissue culture treated plates at a density of 10,000 cells/cm^2. The cells were allowed to reach confluency, usually requiring 1-2 additional days after seeding. The cells were

then differentiated in media supplemented with 6 mM ß-glycerophosphate and 50 µg/ml ascorbic acid 2-phosphate (Sigma) and the additional 100 ng/ml BMP-2 and/or 10 µg/ml heparin. Cells layers were collected and analyzed at 7, 14, and 21 days for expression of alkaline phosphatase (ALP), bone sialoprotein (BSP), osteocalcin (OCN), and Runx2 mRNA levels with real-time RT-PCR. RNA isolation and quantitative PCR methods are detailed in Chapter 3. Cell number was assessed using the Pico Green® dsDNA Quantitation Kit (Molecular Probes) at days 7, 14, and 21 as described previously in Chapter 3. Cell layers were also analyzed for matrix mineralization with the Von Kossa staining technique, also described in Chapter 3, for phosphate deposits at day 21.

4.3.3 Incorporation of heparin into lyophilized collagen matrix

Synthetic polycaprolactone (PCL) scaffolds (Osteopore, Singapore) were cut from a lattice sheet using a biopsy punch (Miltex, York, PA, USA) and incubated in 5 M NaOH for 8 hours at 37°C to increase the surface roughness of the polymer. Scaffolds were rinsed twice in DI H_2O and sterilized by 70% ethanol evaporation overnight in a laminar flow hood. Type I rat tail collagen (Vitrogen, Palo Alto, CA, USA) was mixed with low molecular weight heparin (Sigma,) and lyophilized into the pore space of the PCL scaffolds. Briefly, 100 parts collagen/heparin (1.4 mg/ml collagen + 10 µg/ml heparin) in 0.05% acetic acid was combined with 9 parts sodium bicarbonate (71.2 mg/ml in DI H_2O). One hundred microliters of the solution was deposited on each scaffold and allowed to polymerize at room temperature for 30 minutes. The scaffolds were then transferred to a -80°C freezer for 60 minutes and then lypophilized overnight (Labconco, Kansas City, MO, USA) (**Figure 4.2**).

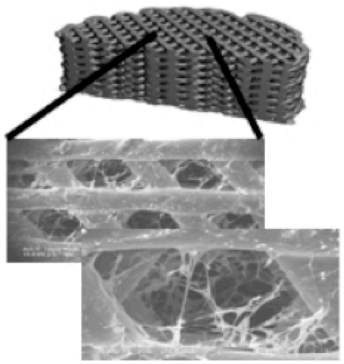

Figure 4.2 Micro-CT image of synthetic polycaprolactone (PCL) scaffold with SEM images of lyophilized type I rat tail collagen matrix

4.3.4 Fluorescently labeled BMP-2 and heparin on collagen matrices

BMP-2 was labeled with fluorescein isothiocyanate (FITC) using a Pierce® FITC antibody labeling kit (Thermo Scientific, Rockford, IL, USA). Briefly, the BMP-2 was resuspended in an amine-free borate buffer at pH 8-9. The FITC molecule suspended in the labeling reagent crosslinked to primary and secondary amines on the protein and excess, un-conjugated FITC molecules were separated from the labeled protein in purification resin and spin columns.

Labeled protein was then added to collagen or collagen/heparin matrices at a concentration of 5μg/ml (0.5 μg/construct). For comparison BMP-2 pre-incubated with heparin (10 μg/ml) was added to collagen matrices. The fluorescent protein on the matrices was imaged and quantified using a confocal laser scanning microscope (CLSM) Zeiss 510 with a 488 nm emitting laser (Carl Zeiss, Inc., Thornwood, NY, USA). See **Appendix C** for detailed confocal image quantification protocol.

4.3.5 hMSC culture on 3D heparinzed collagen matrix

hMSCs were subcultured for 1 week at a low density (500 cells/cm^2) and not allowed to expand past 70% confluency. The hMSCs were then trypsinized, counted, and seeded on collagen or collagen/heparin scaffolds, with or without 0.5 μg BMP-2. One

million cells were suspended in cell culture media and deposited on each scaffold in a 12-well plate (Nunc, low cell binding surface). Cells were allowed to attach to the scaffold for 1 hour prior to adding cell culture media, supplemented with 6 mM ß-glycerophosphate and 50 μg/ml ascorbic acid 2-phosphate, to each well. Acellular controls were prepared by adding 100 μl of cell culture media to the scaffolds and subsequently cultured in the same way as the cellular samples. After 48 hours constructs were incubated on a rocker plate to enhance perfusion of nutrients into the center of the scaffold. Consistent scaffold orientation while on the rocker plate was maintained by placing the constructs in a holder consisting of sterile ¾" Teflon disks in the 12-well tissue culture dish [178].

Cell-seeded scaffolds were harvested at 2 and 5 days post-seeding, rinsed with phosphate buffered saline (PBS), and incubated in 4 μM calcein-AM and 4 μM ethidium homodimer-1 (Molecular Probes) in PBS for 45 minutes under gentle agitation. Cell viability in the constructs was then assessed with a Zeiss LSM 510 confocal microscope (Carl Zeiss, Inc.) through a 10x objective lens.

After 3 and 5 weeks in culture, the constructs were removed from cell culture media and inserted into a sterile polycarbonate chamber for micro-CT analysis as previously described by Porter, et al. [177, 179]. In vitro mineralization was quantified using a Scanco Medical Viva-CT scanner (Basserdorf, Switzerland). Samples were evaluated at a global threshold of 78, filter width of 1.2, and filter support of 2. The mineralized matrix volume was determined for each sample. After imaging, samples were removed from the sterile polycarbonate chamber and returned to the Teflon construct holders for further culturing.

4.3.6 Statistical analysis

All data are presented as the mean ± standard error of the mean (SEM), unless otherwise stated. Statistical comparisons using Prism 5 software (GraphPad Software, Inc., San Diego, CA, USA) were based on an ANOVA and Tukey's *post hoc* analysis for pairwise comparison of three or more groups within each time point and p-value < 0.05 was considered statistically significant. Other statistical analyses used are stated in the results. When required, raw data was transformed using a logarithmic transformation to make the data normal and the variance independent of the mean [142].

4.4 Results

4.4.1 Effect of heparin on BMP-2 levels in cell culture media and BMP-2 mediated osteogenic differentiation

Analysis of cell culture media with an ELISA indicated significantly more BMP-2 remained in the media after 3 days when heparin was present at a concentration of 10 μg/ml compared to 0 and 2 μg/ml heparin (**Figure 4.3**). Less BMP-2 remained present in the media when incubated with 20 μg/ml heparin compared to 10 μg/ml heparin, however this difference was not significant. There was a slight detection of BMP-2 without the addition of exogenous growth factor to the media due to the growth factor content in the serum as well as the endogenous expression of BMP-2 in hMSCs, which has been shown previously by Seib, et al. [89]. However, the quantities of exogenous BMP-2 detected with the ELISA were significantly higher than when no BMP-2 was added to the media ($p<0.05$). These results confirm that heparin helps protect BMP-2 from degradation, thereby maintaining higher concentrations of BMP-2 in culture for prolonged periods.

Based on these results, we chose a heparin concentration of 10 μg/ml for future experiments.

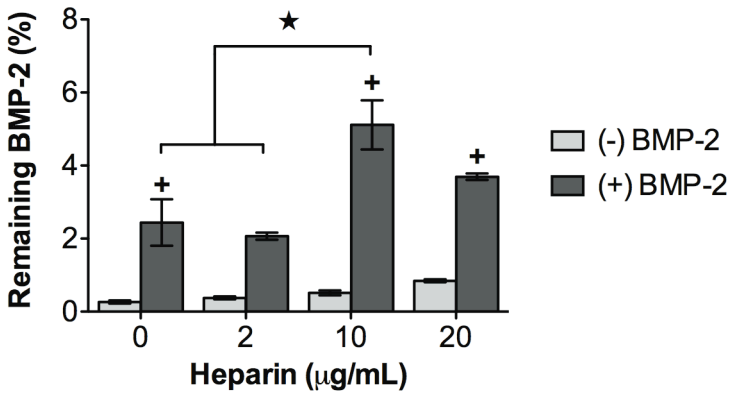

Figure 4.3 BMP-2 remaining in cell culture media after 3 days in the presence of heparin detected with an ELISA (ANOVA: ★ $p<0.05$, ✚ $p<0.05$ compared to no BMP-2 with the same heparin concentration).

The combined osteogenic activity of BMP-2 and heparin was confirmed using *in vitro* cell monolayer assays. First, gene expression was analyzed at 7, 14, and 21 days after addition of heparin (10 μg/ml) and/or BMP-2 (100 ng/ml) to the cell culture media for alkaline phosphatase, osteogenic matrix proteins: bone sialoprotein and osteocalcin, and Runx2 transcription factor (**Figure 4.4**). Alkaline phosphatase was significantly increased compared to the control by heparin, BMP-2, and the combination of both BMP-2 and heparin at day 14. Bone sialoprotein was also significantly increased in the presence of the BMP-2 and heparin combination at day 14. Early changes in osteocalcin expression were induced by the combination of BMP-2 and heparin, compared to the control at day 7. Both BMP-2 and the BMP-2/heparin complex significantly increased Runx2 expression compared to the control and heparin groups at day 14.

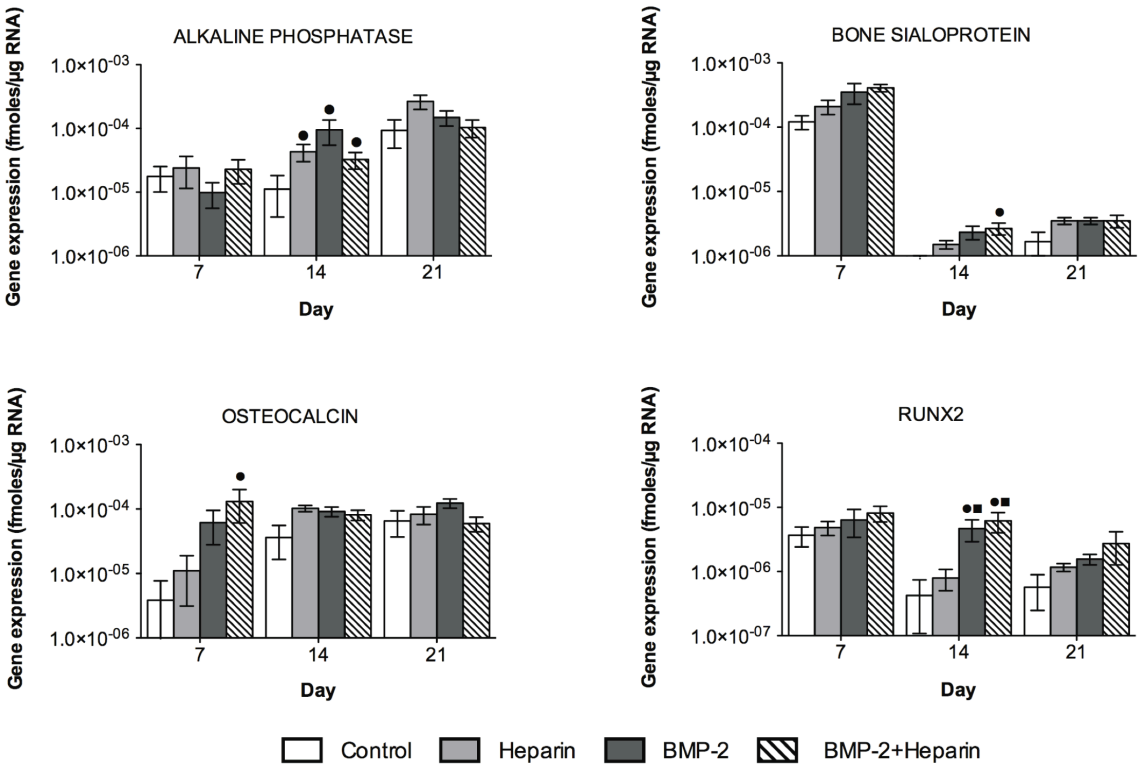

Figure 4.4 Osteogenic gene expression in response to BMP-2 and heparin was assessed by real time RT-PCR analysis of osteoblastic markers including alkaline phosphatase (ALP), bone sialoprotein (BSP), osteocalcin (OCN), and Runx2; (plotted on logarithmic y-axes; ANOVA: • $p<0.05$ versus control, ■ $p<0.05$ versus heparin).

The effect of BMP-2 and heparin on variations in cell number was assessed at days 7, 14, and 21 with the Pico Green DNA assay (**Figure 4.5**). The results indicate that all groups experienced a significant increase in DNA content between days 14 and 21 ($p<0.001$). However, hMSCs incubated with BMP-2 had significantly less cells at day 21 than all other groups, suggesting that BMP-2 without heparin causes a decrease in the proliferation rate.

Matrix mineralization was confirmed by von Kossa staining for phosphate deposits in hMSC monolayers after 21 days. Staining demonstrated that phosphate deposition was enhanced when cells were culture in the presence of both BMP-2 and heparin (**Figure 4.6**). A small number of mineralized regions were observed in control and heparin treated cell layers. Interestingly, cell layers cultured with BMP-2 exhibited a small

amount of phosphate deposition. Microscope images of these cell layers showed substantial amounts of phosphate nodules in the BMP-2/heparin group, indicating osteogenic differentiation of the hMSCs.

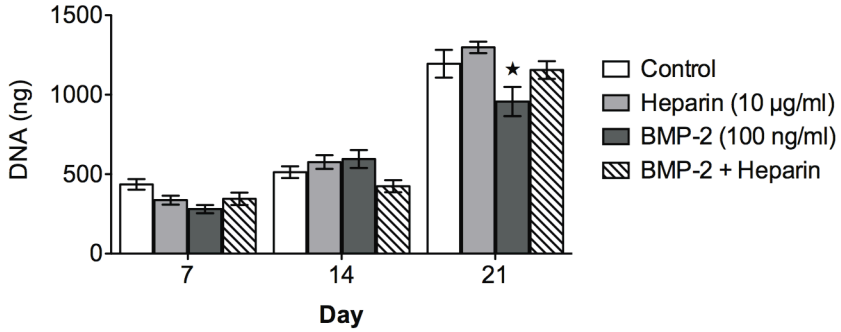

Figure 4.5 Effect of BMP-2 and heparin on hMSC number. DNA was quantified using the Pico Green assay (ANOVA: ★ $p<0.05$ compared to all groups at the same time point).

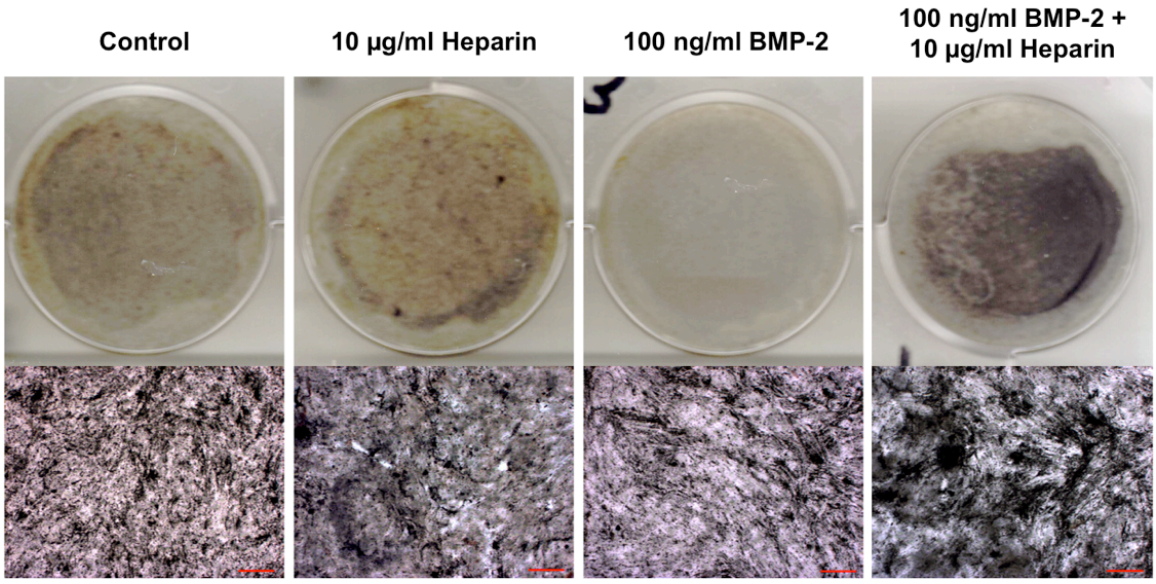

Figure 4.6 von Kossa stain on hMSC layers treated with BMP-2 (100 ng/ml) and/or heparin (10 µg/ml) at day 21. Scale bars = 200µm.

4.4.2 Incorporation of heparin in a lyophilized collagen matrix

Heparin was incorporated within a lyophilized type I collagen matrix on PCL scaffolds. PCL scaffolds were selected due to their widespread use in tissue engineering applications and the structural properties necessary during bone regeneration. Heparin content within the collagen matrix was confirmed with DMMB dye for sGAG content (**Figure 4.7A**). BMP-2 was added to scaffolds and incubated for 1 hour before adding PBS to wells to measure the release kinetics. A burst release of almost 75% of the initial BMP-2 was measured from the collagen scaffolds within the first day and nearly 100% was released by two weeks (**Figure 4.7B**). Additionally, large variations in BMP-2 released from collagen scaffolds were observed, with each scaffold releasing at different rates. Conversely, the release of BMP-2 from collagen/heparin scaffolds did not experience a large burst release and the kinetics among samples had very little variation. Less than 50% of the initial BMP-2 was released from the collagen/heparin scaffolds by two weeks, suggesting that most of the BMP-2 was retained within the matrix.

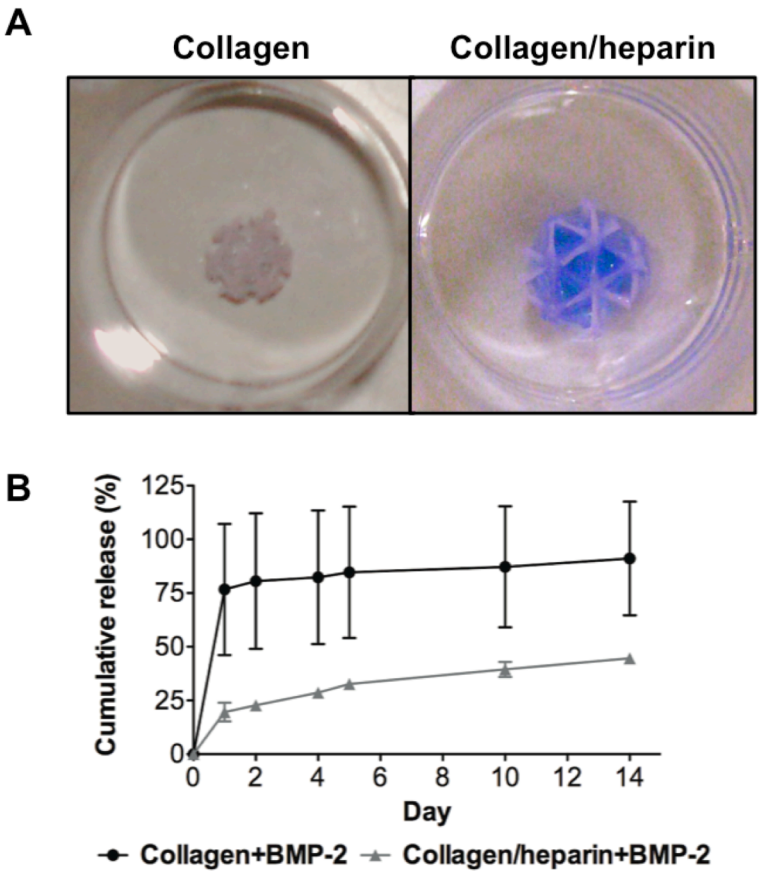

Figure 4.7 Incorporation of heparin in a lyophilized collagen matrix. **(A)** Heparin content confirmed by DMMB dye on PCL scaffolds with lyophilized collagen matrices (scaffold dimensions: ø 6 mm x 4.5 mm); **(B)** BMP-2 release kinetics from collagen and collagen/heparin matrices in PCL scaffolds measured by an ELISA.

4.4.3 Quantification of fluorescently labeled BMP-2 and heparin

BMP-2 was labeled with FITC in order to quantify and image the spatial distribution of BMP-2 within the scaffolds. A detailed protocol for quantification of fluorescently labeled proteins using confocal microscopy is described in **Appendix D**. In order to confirm that the collagen and collagen/heparin matrices did not interfere with the FITC fluorescent signal, scaffolds without FITC BMP-2 were imaged and compared to scaffolds with FITC BMP-2 (**Figure 4.8A**). Quantification of the fluorescent area and mean intensities in the confocal images indicated that the fluorescent signal was significantly greater in samples containing FITC BMP-2 compared to the non-FITC

controls (**Figure 4.8B and C**). The mean fluorescent intensity measurement was more sensitive to the presence or absence of FITC BMP-2 ($p<0.001$ compared to non-FITC control for each matrix type).

A major advantage of the confocal microscope is the ability to collect accurate measurements of fluorescent signals within thick specimens. We demonstrated the capability of the confocal microscope for optical sectioning of the three-dimensional collagen and collagen/heparin matrices at different depths within the construct to compare the overall spatial distribution of BMP-2 (**Figure 4.9A and B**). The FITC-labeled BMP-2 was observed to be more evenly distributed throughout the collagen/heparin matrices compared to the collagen matrix, indicating that BMP-2 binds more consistently to the collagen/heparin matrix (**Figure 4.10A and B**).

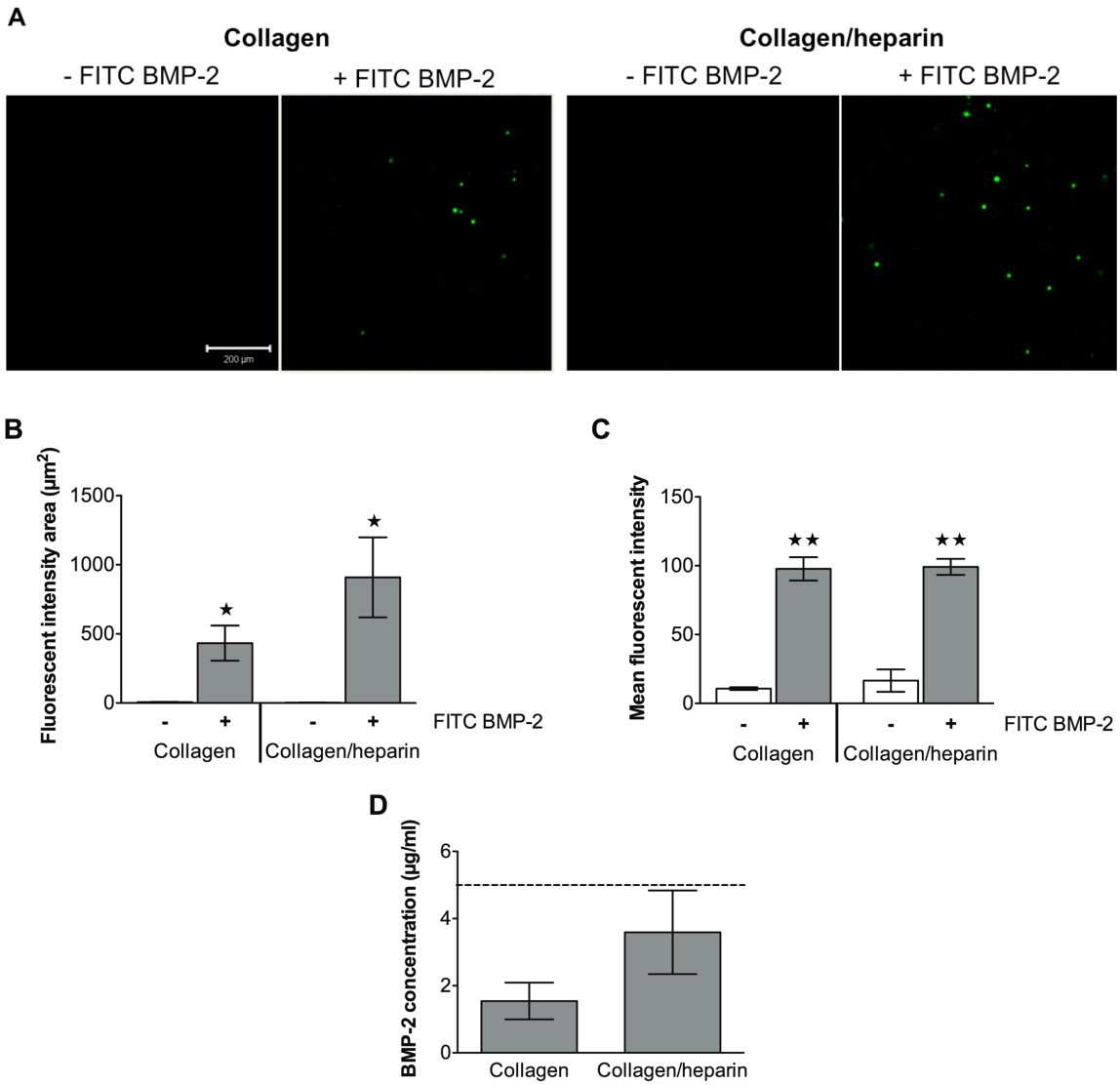

Figure 4.8 Collagen and collagen/heparin matrices do no interfere with FITC BMP-2 fluorescent signals. **(A)** Confocal laser scanning microscope images of control samples without FITC and samples with FITC BMP-2 on collagen and collagen/heparin matrices (scale bar = 200 µm, applies to all images). **(B)** Quantification of fluorescent intensity areas of control scaffolds without FITC BMP-2 compared to scaffolds with FITC BMP-2 **(C)** Mean fluorescent intensity of scaffolds with and without FITC BMP-2. **(D)** BMP-2 concentrations on collagen or collagen/heparin 3D matrices calculated from the standard curve obtained previously, correlating fluorescent intensity area to BMP-2 concentration. Dotted line indicates the concentration of the original loading solution (5 µg/ml). (n = 4, each sample averaged over 30 image slices; t-test: ★ $p<0.05$ and ★★ $p<0.001$ compared to non-FITC control)

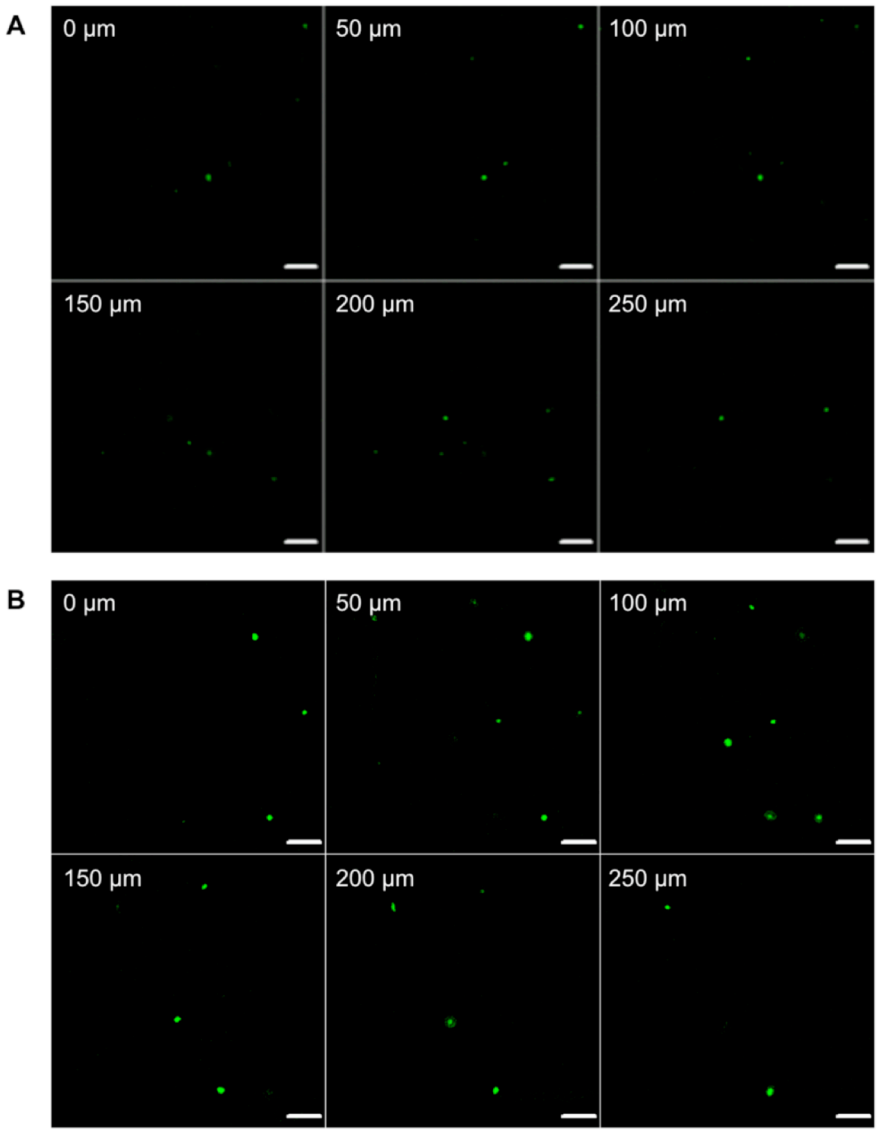

Figure 4.9 Representative confocal image slices along the z-axis for **(A)** collagen matrix with FITC BMP-2, and **(B)** collagen/heparin matrix with FITC BMP-2. Scale bars = 100 µm.

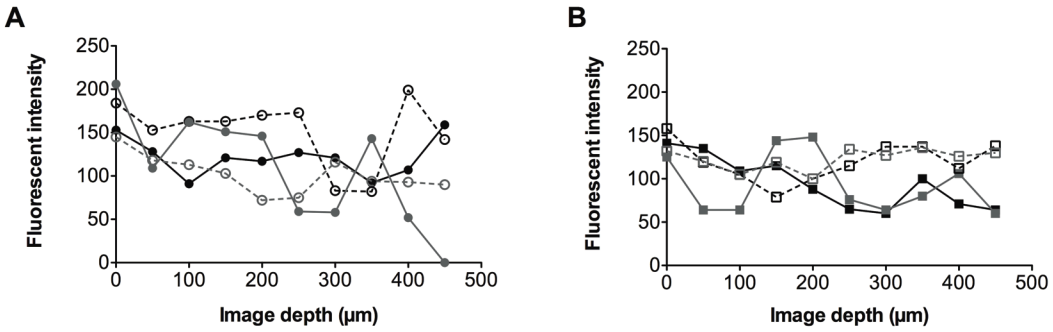

Figure 4.10 Patterns of fluorescent intensity along the z-axis for **(A)** collagen matrix with FITC BMP-2, and **(B)** collagen/heparin matrix with FITC BMP-2. Each line represents a different sample.

Heparin concentrations within the collagen matrix were then varied to determine the effect of heparin content on BMP-2 retention within the matrix (**Figure 4.11A and B**). The highest concentration of heparin (20 μg/ml) seemed to abrogate the binding effects of BMP-2 and heparin, and had BMP-2 levels similar to the collagen matrices without heparin. Still, the lower heparin concentrations (0-10 μg/ml) followed a trend of BMP-2 content increasing with heparin concentration. Generally, it is presumed that the fluorescent intensity is directly proportional to the amount of fluorescence present. However, we saw that although the fluorescent area was different among the varying heparin concentrations, the fluorescent intensity did not demonstrate any differences. This indicates that fluorescent intensity measurements are not highly sensitive to changes in the concentration of fluorescence present; rather it mainly detects the overall presence or lack of fluorescent signals and not gradients of fluorescent signals.

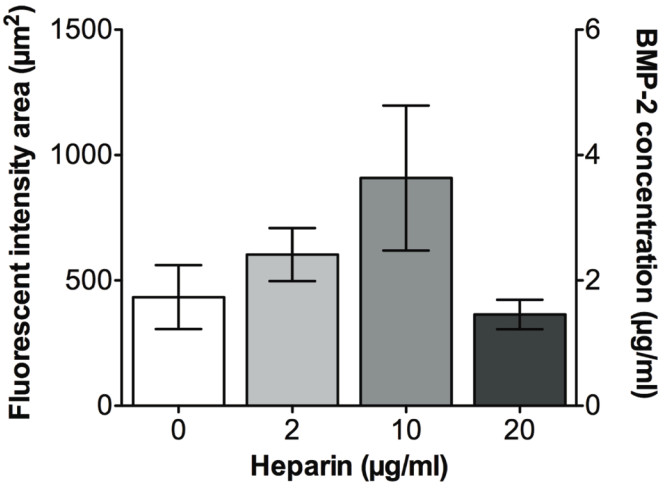

Figure 4.11 BMP-2 content on collagen matrices is influenced by heparin concentration. Quantification of fluorescent intensity area of FITC-labeled BMP-2 on lyophilized collagen matrices with varying concentrations of heparin (n=4; each sample averaged over 30 image slices)

Confocal microscopy was then used to assess the capacity of collagen and collagen/heparin matrices to retain BMP-2. Collagen and collagen/heparin scaffolds with FITC BMP-2 were imaged before and after a 30-minute wash in PBS on a shaker plate (**Figure 4.12A**). Image analysis indicated that only about 50% of the BMP-2 remained on the collagen matrix after the wash treatment, while nearly 100% of the BMP-2 remained on the collagen/heparin matrix after the wash treatment (**Figure 4.12B and C**). Both the fluorescent area and mean fluorescent intensity were significantly different between pre- and post-wash for the collagen matrices. The decrease in fluorescent intensity further confirms that the decrease in fluorescent area was in fact due to an overall loss of BMP-2 content and not just a decrease in BMP-2 concentration.

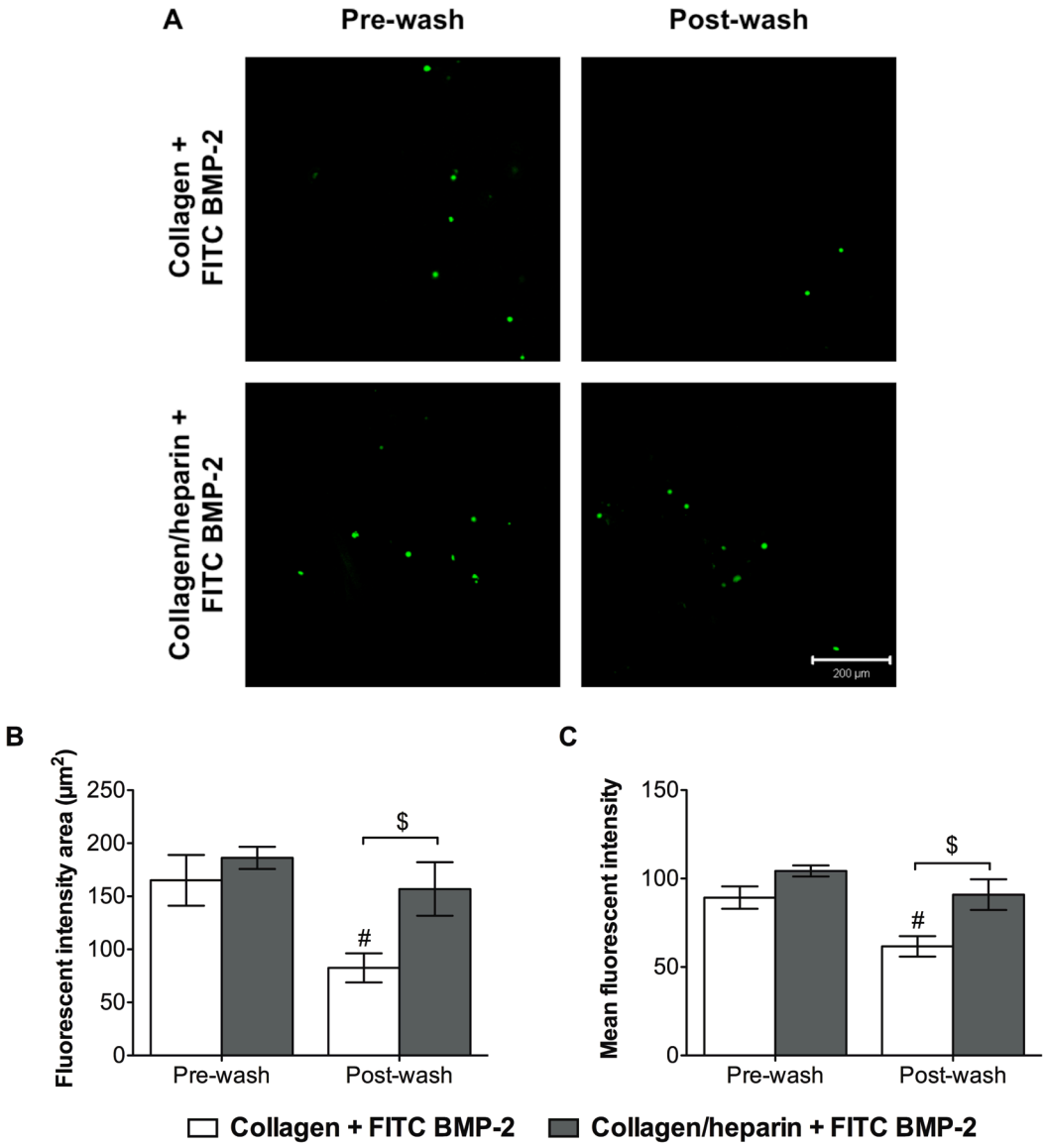

Figure 4.12 Collagen/heparin matrices retain higher amounts of BMP-2. **(A)** Confocal image slices of FITC-labeled BMP-2 on collagen or collagen/heparin lyophilized matrices before and after a 30-minute wash treatment (scale bar = 200µm, applies to all images); Quantification of BMP-2 on collagen or collagen/heparin matrices: **(B)** fluorescent area and **(C)** fluorescent intensity of FITC-labeled BMP-2 on collagen or collagen/heparin lyophilized matrices before and after a 30-minute wash treatment. (n=4, each sample averaged from 55-60 image slices; ANOVA: $ $p<0.05$, # $p<0.01$ compared to pre-wash)

Further, in a separate experiment, the retention of pre-complexed BMP-2 and heparin was analyzed. FITC BMP-2 and heparin were pre-bound for 30 minutes prior to adding to the collagen matrix. Confocal imaging showed that the BMP-2/heparin complex did not have a significant decrease in BMP-2 content after the 30-minute wash (**Figure 4.13**), as BMP-2 alone on the collagen matrix did previously. It seems that the BMP-2/heparin complex has an interaction to some extent with the collagen matrix even when heparin is not directly incorporated into the matrix. However, the levels of BMP-2 detected after washing still decreased, unlike the BMP-2 levels previously detected on the collagen/heparin matrices.

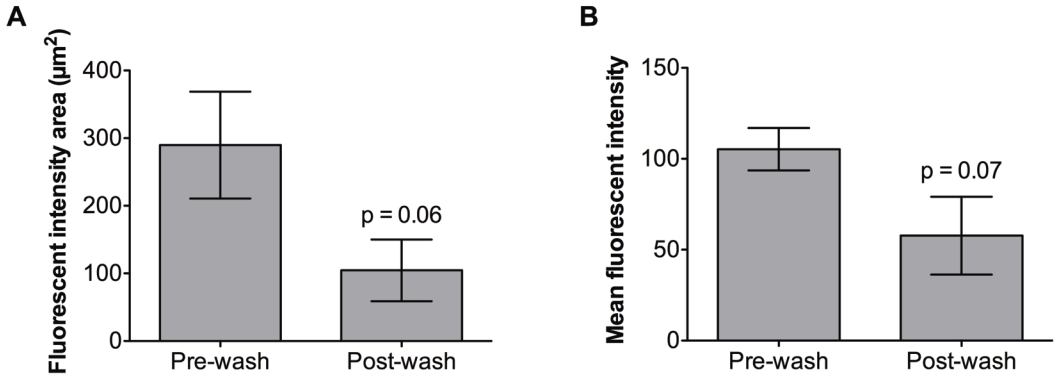

Figure 4.13 Quantification of the BMP-2/heparin complex on collagen matrix: **(A)** average fluorescent area and **(B)** mean fluorescent intensity of FITC-labeled BMP-2 pre-complexed with heparin on collagen lyophilized matrices before and after a 30-minute wash treatment. (n=4, each sample averaged from 55-60 image slices; groups compared with paired t-test)

4.4.4 Effect of heparin in lyophilized collagen matrix on BMP-2 mediated differentiation of hMSCs in 3D in vitro culture

One million hMSCs were seeded on collagen and collagen/heparin matrices with or without BMP-2 and cultured *in vitro* under static conditions. Cell attachment and viability were assessed after 2 and 5 days using live/dead staining and confocal microscopy. After 2 days in culture, live/dead staining showed that matrix composition did not have a major effect on cell adhesion, distribution, or morphology (**Figure 4.14**). However, differences in cell localization were observed among scaffolds with or without BMP-2, with cells located largely on the struts when BMP-2 was present. However, by 5 days cells on all matrix types with or without BMP-2 filled the scaffolds. The cells on all scaffolds were also observed to have high cell viability.

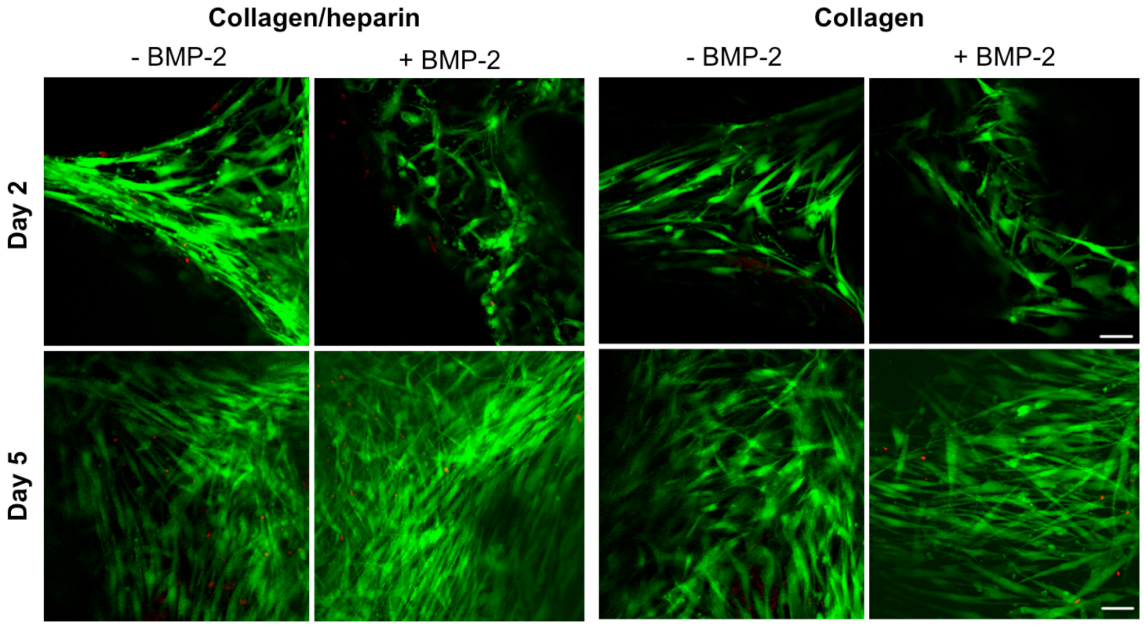

Figure 4.14 Viability of hMSCs in collagen and collagen/heparin matrices. Cell viability, distribution, and morphology were determined with live (green)/dead (red) staining of cells seeded on collagen and collagen/heparin scaffolds and imaged on a confocal microscope after 2 and 5 days. Scale bars = 50 μm, applies to all images.

BMP-2 mediated mineralization within collagen and collagen/heparin matrices was quantified using micro-CT analysis at 3 and 5 weeks (**Figure 4.15A and B**). Cells on collagen/heparin scaffolds with BMP-2 deposited significantly greater amounts of mineral compared to collagen scaffolds with BMP-2 as well as collagen/heparin scaffolds without BMP-2. Mineral deposition was also increased on collagen/heparin scaffolds with BMP-2 at both 3 and 5 weeks compared to acellular collagen/heparin scaffolds, indicating that the mineralization observed was due to cell-mediated matrix deposition and not due to precipitation of media components onto the scaffolds. In contrast, collagen matrices with BMP-2 showed no significant increase at either 3 or 5 weeks compared to acellular and non-BMP-2 groups. Collagen matrices with the pre-bound BMP-2/heparin complex had less mineral formation than collagen/heparin + BMP-2 matrices, however this difference was not significant.

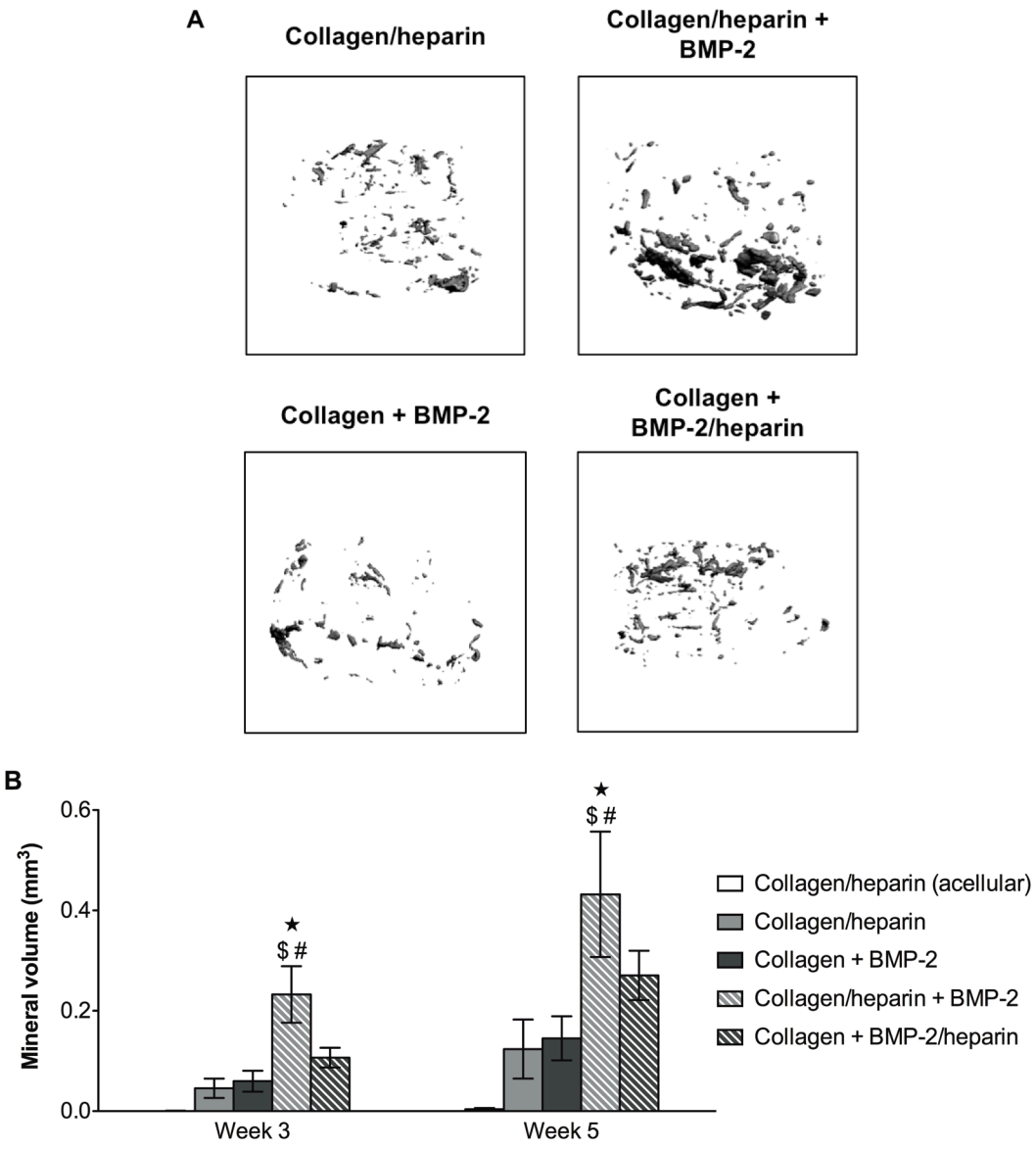

Figure 4.15 BMP-2 mediated mineralization capacity of hMSCs on collagen or collagen/heparin matrices. **(A)** Representative micro-CT images of hMSCs seeded on collagen and collagen/heparin matrices with or without BMP-2 after 5 weeks *in vitro*. **(B)** Quantification of mineral volume by micro-CT image analysis after 3 and 5 weeks *in vitro* (ANOVA: $p<0.05$ ★ compared to collagen/heparin (acellular), # compared to collagen/heparin, $ compared to collagen + BMP-2)

4.5 Discussion

The use of BMP-2 in tissue engineering has exhibited potential for bone regeneration, however is largely limited by the short half-life due to degradation and rapid diffusion from the implant site. In Specific Aim I we showed that the sustained delivery of BMP-2 from a lipid microtube system did not provide a significant benefit for hMSC mineralization compared to a bolus dose of BMP-2. In this study, we investigated the incorporation of heparin in a collagen matrix in order to improve the retention and bioactivity of BMP-2. We showed that incorporating heparin into a collagen matrix delivery system delays diffusion of BMP-2 from the scaffold and enhances BMP-2 mediated mineralization.

Biomaterials are often modified to improve bioactivity and biocompatibility. Incorporating matrix molecules, such as heparin, in the biomaterial closely mimics the natural ECM leading to improved retention of many growth factors, including BMP-2. Matrix-bound growth factors are temporarily retained *in vivo* by sGAGs, such as heparin, in the ECM protecting the growth factor from proteolytic degradation and delaying diffusion into the surrounding tissue [94, 180]. Low molecular weight heparin has previously been shown to be a useful molecule in stabilizing the BMP-2 structure as well as enhancing the BMP-2 activity [96, 117]. It has also been shown that heparin in the ECM sequesters BMP-2 at the cell surface, near the receptors, and mediates internalization of the protein, which further mediates BMP-2 activity [180]. This matrix/growth factor interaction was employed in this study by incorporating heparin in a collagen matrix system to improve the retention and bioactivity of BMP-2.

In the presence of heparin, higher levels of BMP-2 were maintained in the cell culture media after three days, confirming that the heparin protected the BMP-2 molecule from proteolytic degradation as well as thermal denaturing. Zhao et al. previously demonstrated this stabilizing effect, where the half-life of BMP-2 was prolonged by almost 20-fold in the presence of heparin [96]. The higher levels of BMP-2 remaining in the media corresponded with a significant increase in osteogenic differentiation of hMSCs, as indicated by increased osteogenic gene expression as well as more phosphate deposits detected by Von Kossa staining. These results support previous work with C2C12 myoblasts that indicated heparin enhances the biological activity of BMP-2 [96, 117].

We demonstrated that the collagen/heparin matrices delayed the release of BMP-2 as shown in the release kinetics. Collagen matrices had highly variable and rapid release of BMP-2, with nearly 75% being released within the first day, and almost 100% by 2 weeks. Conversely, collagen/heparin matrices released less than 50% of the BMP-2 by 2 weeks and had very consistent release kinetics across samples. The variability observed in the BMP-2 release kinetics from the collagen matrices could induce significant variability during clinical trials, which may result in variable healing responses and side effects [6, 83, 90, 97]. Uludag, et al. has previously shown that BMP-2 releases rapidly from collagen sponges implanted in an ectopic site, in which approximately 60% of the initial BMP-2 remained three hours after implantation and less than 5% remained in the sponges two weeks after implantation [158]. They later demonstrated that improved BMP-2 retention within the carrier increases bone formation [18]. Therefore, we

hypothesized that delivery of BMP-2 in the collagen/heparin matrix would enhance mineralization.

Confocal imaging of FITC-labeled BMP-2 also demonstrated that collagen matrices had poor retention of BMP-2 after a 30-minute wash treatment. BMP-2 concentrations remained the same after washing when heparin was incorporated in the collagen matrix. Further, when BMP-2 and heparin were pre-bound prior to adding to a collagen matrix, retention was not as good as observed in the collagen/heparin matrix. However, the decrease in BMP-2 content was not as drastic on the collagen matrix when BMP-2 and heparin were pre-complexed. This effect may be due to the larger size of the BMP-2/heparin complex compared to BMP-2 alone, thus reducing the diffusion from the collagen matrix [111]. Additionally, this effect may be caused by the inherent interactions of heparin with other ECM components, thereby causing the BMP-2/heparin complex to have an affinity for the collagen matrix [31]. However, this affinity of the BMP-2/heparin complex with collagen does not improve the BMP-2 retention as much as incorporating the heparin within the matrix. Release of BMP-2 from these systems can happen as a result of various events including the dissociation of BMP-2 from the matrix molecules, diffusion of the matrix molecules, or degradation of the matrix. Similar to our study, Visser, et al. demonstrated that BMP-2 had poor retention in collagen sponges after a wash treatment, unless the system was altered to improve binding of BMP-2 to collagen [21].

We also demonstrated that high concentrations of heparin (20 μg/ml) reversed the effects of heparin on BMP-2 binding and stability. Analysis of the cell culture media samples after 3 days showed that the high dose of heparin had no added effect on

remaining BMP-2 over 10 μg/ml heparin, and had BMP-2 concentrations similar to samples without any heparin. Moreover, confocal imaging of the 3D collagen/heparin scaffolds indicated that 20 μg/ml heparin did not enhance binding of BMP-2 to the matrix over 10 μg/ml heparin, and again had BMP-2 concentrations similar to the collagen matrix without heparin. Similarly, high heparin concentrations have previously been shown to inhibit growth factor activity, as well as reduce cell number and matrix deposition [181, 182]. This effect has been attributed to multiple causes, such as non-specific competition with endogenous sGAGs, however no clear reason has been determined for this inhibitory activity. Other studies have demonstrated use of heparin to protein molar ratios between 1:25 and 1:500, and showed that a moderate ratio of protein to heparin was most beneficial for bioactivity [111]. Our results in combination with the previous work indicate that lower heparin concentrations will be beneficial for BMP-2 delivery.

Cell attachment and morphology on scaffolds are key factors when evaluating cell proliferation and differentiation. Previous work has shown that immobilized growth factors cause changes in cell attachment and morphology, which is critical for cell differentiation [174, 183]. Our results clearly demonstrated that there were no differences in cell attachment, morphology, or growth on collagen or collagen/heparin matrices when BMP-2 was present. However, the consistent presence of BMP-2 within the collagen/heparin matrix resulted in a significant increase in BMP-2 mediated mineralization of hMSCs. The differences in mineralization may be due to the quick diffusion of BMP-2 from the collagen matrices, before the cells reached confluency and were able to begin differentiating. We showed by live/dead staining that the cells are not

confluent immediately after seeding, and required more than two days to fully populate the scaffold. Seib, et al. showed that MSCs require higher cell densities (>10, 000 cells/cm^2) for significant osteogenic differentiation [89]. Therefore, osteoinductive factors need to be present when the cells have reached this state in order to induce osteogenic differentiation. The collagen/heparin matrices retained the BMP-2 for longer periods of time, ensuring that the growth factor was still present when the hMSCs reached confluency and were able to begin differentiating. Acellular collagen/heparin matrices did not exhibit any mineral deposition, indicating that the mineral formation observed in other groups was due to cell-mediated mineral deposition and not the precipitation of media components. Similarly, Peister, et al. demonstrated that no mineralization occurred in acellular collagen matrices [178].

Other biomaterial approaches for growth factor delivery have directly linked either the proteins or the heparin to the material through chemical reactions that create covalent bonds between the molecule and the biomaterial [26, 173, 174, 184]. However, direct surface coupling of proteins and the biomaterial often result in drastic conformational changes in the protein, which can compromise the protein activity and may cause an adverse response *in vivo* due to the foreign protein structure [185]. Conformational changes may also affect the binding affinity of proteins with their receptors or other molecules, resulting in suboptimal activity [29, 183]. Osmond, et al. showed that different methods for chemical immobilization of heparin affected the binding capacity of heparin and a protein [29]. The work in this Aim is beneficial because the collagen/heparin system utilizes no chemical alterations to the heparin or BMP-2 in order to improve retention.

4.6 Conclusions

In this study, we developed an affinity-based delivery system to retain BMP-2 within bone tissue engineering constructs. We utilized the binding properties of BMP-2 and heparin to delay diffusion of the growth factor from the scaffold. The results demonstrated that heparin incorporation into collagen matrices improves BMP-2 retention and delays the release. Subsequently, BMP-2 mediated differentiation of hMSCs was significantly enhanced when heparin was incorporated in the collagen matrix. These results suggest that the collagen/heparin matrix delivery system may be beneficial as a bone tissue engineering therapy. In Specific Aim III we assess the performance of this delivery system *in vivo* in a clinically relevant animal model.

CHAPTER 5

EVALUATION OF A BMP-2 DELIVERY SYSTEM IN AN IN VIVO SEGMENTAL DEFECT MODEL

5.1 Abstract

The collagen/heparin delivery system developed in Chapter 4 was quantitatively evaluated *in vivo* using a previously developed critically-sized rat segmental defect model. BMP-2 was delivered in the collagen or collagen/heparin matrices on PCL scaffolds promote bone regeneration within the critically-sized defects. A group delivering pre-complexed BMP-2/heparin in a collagen matrix was also included for comparison. A previously developed fixation design was used to consistently stabilize the defect as well as provide an imaging window for longitudinal *in vivo* two-dimensional x-ray and three-dimensional micro-CT analysis of bone formation. After 12 weeks, the femurs were explanted and analyzed for functional bone regeneration with torsional mechanical testing. Sequential *in vivo* micro-CT imaging demonstrated that there was significantly more mineralized tissue within the defect site when treated with BMP-2. *Post-mortem* analyses showed that only the pre-complexed BMP-2/heparin delivered in the collagen matrix restored mechanical properties to levels near age-matched intact femurs. The *in vitro* micro-CT analyses demonstrated that the mineralized tissue was more organized when pre-complexed BMP-2/heparin was delivered to the defect, indicating mature bone formation. The results from this study indicate that the co-delivery of BMP-2 and heparin may be a potential therapy for defect repair.

5.2 Introduction

Although structural allografts are currently the standard treatment for bone defects, these treatments experience unacceptably high rates of failure due to incomplete revascularization and bone remodeling. Tissue engineering therapies that include growth factors, such as BMP-2, provide a possible alternative to bone graft substitutes. BMPs were originally identified as molecules that could induce ectopic bone formation when implanted in subcutaneous or intramuscular sites, classifying them as osteoinductive proteins. Thus, the *in vivo* rodent subcutaneous or intramuscular ectopic implantation assay is the standard model to demonstrate BMP-2 activity in initiating and maintaining the bone formation cascade [17, 106, 186]. However, the ectopic assay does not provide a clinically relevant *in vivo* model for fracture healing. A segmental defect model will be utilized in this study to assess the performance of the BMP-2 delivery system developed in Specific Aim II for fracture healing applications.

Many *in vitro* models and assays have been developed to examine BMP-2 mediated osteogenesis, however these methods are oversimplified and do not account for systemic factors, thus still requiring validation *in vivo*. The *in vivo* ectopic implantation model has been the standard assay for evaluating BMP-2 activity; nevertheless it does not serve as a clinically relevant model. Therefore, other research has tried to assess the efficiency of BMP-2 in healing critically-sized defects in rat, rabbit, sheep, and dog models [83, 84, 187, 188]. However, the necessary dose for fracture healing exceeds the therapeutic window and may result in severe adverse effects. One approach to address growth factor dosing issues has been to deliver genetically modified cells to over-express the desired growth factor [74, 105]. These approaches are often controversial due to the

viral vectors necessary to genetically modify the cells [7]. Other approaches for growth factor therapies have included sustained delivery and affinity-based systems [17, 22]. The delivery of growth factors in materials that promote the growth factor activity while also delaying protein denaturing *in vivo* may result in enhanced bone formation at lower doses.

BMP-2 activity *in vivo* is largely mediated by transiently binding to glycosaminoglycans (GAGs), such as heparin, in the bone extracellular matrix (ECM). Thus, heparin has been incorporated into BMP-2 delivery systems to improve the affinity and release properties [17, 20, 115]. These delivery systems have been evaluated *in vivo* to assess improvement in bioactivity and retention of BMP-2 for bone regeneration therapies. In 2008, von Walter, et al. reported the benefit of a heparinized collagen system for the delivery of BMP-2 in a rabbit bone defect model, in which a cylindrical defect was created laterally in the femoral condyle [20]. Other studies have used subcutaneous and intramuscular implantation models to demonstrate the improved ability of BMP-2 to induce ectopic bone formation when delivered with heparin [17, 96, 186]. However, the ectopic assays simply assess matrix mineralization and not bone repair. The potential of heparin-binding delivery systems have not yet been evaluated in a segmental femoral defect, which provides a clinically relevant and robust test bed for evaluating bone repair.

The standard rat segmental defect model was modified to an 8 mm defect dimension in order to achieve a stable fixation of a critically-sized defect, while also allowing *in vivo* micro-CT and X-ray imaging [82, 189, 190]. This model is highly reproducible and utilizes a large, stable defect for evaluation of tissue engineering

strategies for load-bearing situations. The majority of segmental defect animal models utilize qualitative radiographic analyses and end-point histological methods to evaluate healing. However, more quantitative measures of functional, integrated bone healing is necessary to thoroughly evaluate bone tissue engineering strategies. Micro-CT based methods have been established to quantify the 3D distribution of mineralized matrix growth into the defect [82, 191, 192]. Biomechanical testing has also been used to evaluate the restoration of bone function [82, 192, 193].

In Specific Aim II (Chapter 4) we showed that collagen/heparin matrix retained BMP-2 longer and improved BMP-2 mediated mineralization *in vitro*. The purpose of this aim was to test the BMP-2 delivery system developed in Aim II in a challenging and clinically relevant *in vivo* model in order to determine the potential of this delivery system to induce new bone formation. The hypothesis was that the collagen/heparin matrix would improve BMP-2 retention *in vivo* compared to delivery in a collagen matrix, thereby enhancing bone regeneration.

5.3 Methods and Materials

5.3.1 Collagen/heparin matrix for the delivery of BMP-2

Nine millimeter thick PCL scaffolds (Osteopore, Singapore) were cut from a lattice sheet using a 5 mm biopsy punch (Miltex, York, PA) and incubated in 5M NaOH for 8 hours at 37°C to prepare the polymer surface for matrix incorporation. Scaffolds were rinsed twice in deionized H_2O and sterilized by 70% ethanol evaporation overnight in a laminar flow hood. Type I rat tail collagen (Vitrogen, Palo Alto, CA) was mixed with low molecular weight heparin (porcine intestinal mucosa; Sigma) and lyophilized into the pore space of the PCL scaffolds as described in Chapter 4. Two hundred microliters of

the collagen solution was deposited on each scaffold and allowed to gel at room temperature for 30 minutes. The scaffolds were then transferred to -80°C for 60 minutes and then lypophilized overnight (Labconco, Kansas City, MO).

A volume of 175 µl containing 3 µg of rhBMP-2 (carrier free, CHO-derived, R&D Systems, Minneapolis, MN, USA) was pipetted onto the collagen matrices at least 30 minutes prior to implanting into the defect. BMP-2 was also pre-incubated with 10 µg/ml heparin for 30 minutes prior to adding to the collagen scaffold.

5.3.2 Surgical technique

All surgical procedures were reviewed and approved by the Institutional Animal Care and Use Committee (IACUC) at the Georgia Institute of Technology (Protocol #A08032). The surgical technique and analysis previously described by Oest, et al. was used [82]. Female Sasco Sprague-Dawley rats (Charles River Labs, Wilmington, MA) aged 13 weeks were anesthetized with isoflurane and bilateral incisions were made along the length of the hind limbs. A modular fixation plate consisting of a polysulfone plate and two stainless steel plates was directly secured to the femur using four miniature screws (**Figure 5.1**). Bilateral full-thickness diaphyseal segmental defects, 8 mm in length, were created using a small oscillating saw and flushed with saline. Defects were filled with PCL scaffolds containing one of the following treatments: collagen matrix (n=5), collagen/heparin matrix (n=7), collagen matrix + BMP-2 (n=9), collagen/heparin matrix + BMP-2 (n=9), and collagen matrix + BMP-2/heparin complex (n=9). All groups receiving BMP-2 had a dose of 3 µg. Animals received 0.05 mg/kg buprenorphine subcutaneously every 12 hours for the first 48 hours post-op. Within 2-3 days post-op, the animals resumed normal ambulation and showed no signs of pain or distress.

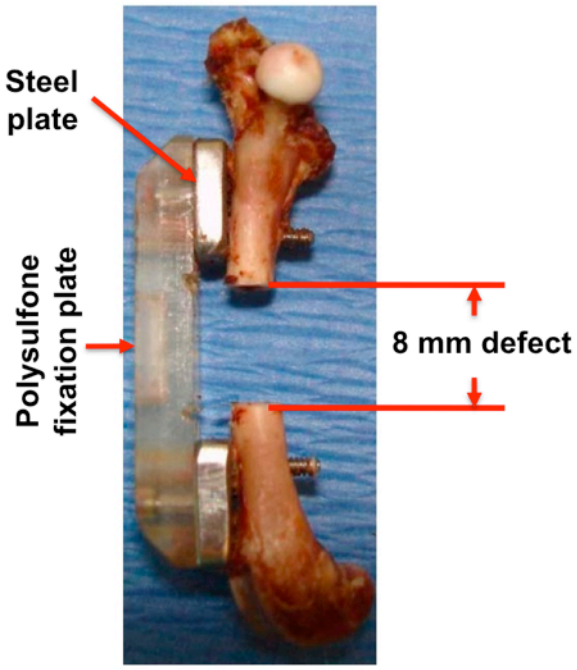

Figure 5.1 Rat femur with 8 mm defect and fixation plate assembly

5.3.3 2D X-ray and 3D Micro-CT imaging

In vivo digital x-rays (Faxitron MX-20 Digital; Faxitron X-ray Corp., Wheeling, IL) were obtained at 2, 4, 8, and 12 weeks post-op to provide a two-dimensional qualitative assessment of healing and defect stability over time. The radiolucent properties of the polysulfone fixation plate allowed for clear imaging of the defect. Qualitative assessment of bone regeneration was determined by two blinded observers and classified according to the extent of defect bridging.

Quantitative 3D analysis of bone regeneration in the defects was performed at 4, 8, and 12 weeks post-op using an *in vivo* micro-CT system (Viva-CT 40; Scanco Medical, Bassersdorf, Switzerland) following the technique described by Oest, et al. [82]. The defect region was scanned at a 38.5 μm voxel resolution, a voltage of 55 kVp and a current of 109 μA. A constant volume of interest (VOI) centered over the defect site was used for analysis of all samples (100 slices thick for *in vivo* scans and 300 slices thick for

in vitro scans). A Guassian filter (sigma = 1.2, support = 1) was used to reduce noise levels in the VOI prior to applying a global threshold. Appropriate threshold levels for *in vivo* and *in vitro* scans were determined by examining individual slices to detect newly formed mineralized tissue and to exclude soft tissue, the PCL scaffold, and the polysulfone plate.

5.3.4 Mechanical Testing

Animals were euthanized at 12 weeks post-op and samples were harvested and wrapped in saline-soaked gauze for storage at -20°C. Thawed samples were subjected to torsion testing immediately after *in vitro* micro-CT scanning, using a Bose ElectroForce system (ELF 3200, Bose EnduraTEC, Minnetonka, MN) with a 2 N-m torsional load cell. First, the femur ends were embedded in end blocks using Wood's metal (Alfa Aesar, Ward Hill, MA) and pinned through the potting blocks for extra stability in the end blocks. The polysulfone fixation plates were removed without disrupting the defect and the samples were tested at a rate of 3°/s to failure. Torque and rotation were recorded and exported for analysis. Unbridged samples displayed a gradual increase in torque and did not experience an abrupt failure point due to stretching of the soft tissue. For these samples the failure torque was measured in the first 60° in order to exclude the forces generated due to soft tissue deformation. Stiffness was calculated by determining the slope of a straight line fitted to the linear portion of the torque-rotation plot prior to failure.

5.3.5 Statistical analysis

All data are presented is the mean ± standard error of the mean (SEM), unless otherwise stated. When necessary, raw data was transformed using the Box-Cox method

to make the data normal and the variance independent of the mean [194]. Statistical comparisons using Minitab® 15 software (MiniTab Software, Inc., San Diego, CA, USA) were based on an ANOVA using a general linear model and Tukey's *post hoc* analysis for pair-wise comparison of three or more groups. Differences were considered statistically significant for $p < 0.05$ and a trend for $p < 0.10$.

5.4 Results

During the course of the study one animal was euthanized 48 hours post-op due to rapid weight loss and minimal activity, indicating pain or distress. Another animal was euthanized at 7 weeks post-op due to bacterial infections in both limbs, which caused substantial necrosis of the surrounding tissue.

5.4.1 Qualitative analysis of digital x-ray images

Digital two-dimensional x-ray images were used to qualitatively assess the progression of bone regeneration into the defect (**Figure 5.2**). In non-BMP-2 controls, there was a minimal amount of bone formation observed in the defects throughout the study. Conversely, x-ray images of groups with BMP-2 or BMP-2/heparin demonstrated bone regeneration in the defects. Collagen + BMP-2/heparin appeared to have more mineralized tissue at 2 weeks than other groups, with one defect already demonstrating full bridging and four more defects with a substantial amount of bone formation (**Table 5.1**). The collagen + BMP-2 group also had one defect fully bridged by two weeks, but the majority of the defects in this group still had minimal bone formation at this time point. By 4 weeks, all groups treated with BMP-2 had similar bridging rates. At both eight and twelve weeks post-op, about 60% (15 of 25) of the defects treated with BMP-2 had complete bridging compared to only 9% (1 of 11) of the non-BMP-2 groups. Chi-

square (χ^2) analysis of the ratios revealed that the bridging rates between all groups was not significantly different ($p=0.065$), but were significantly different when comparing groups treated with BMP-2 to the non-BMP-2 controls ($p=0.0046$). Moreover, disconnected areas of bone formation occurred outside the defect region when treated with collagen + BMP-2 scaffolds, indicating diffusion of BMP-2 out of the scaffold. Defects treated with collagen/heparin + BMP-2 or collagen + BMP-2/heparin scaffolds appeared to have more localized bone formation.

Table 5.1 Bridging rates assessed from 2D x-ray images

Group	2 weeks	4 weeks	8 weeks	12 weeks
Collagen	0/5	0/5	0/5	0/5
Collagen/heparin	0/7	0/6	1/6	1/6
Collagen + BMP-2	1/9	3/9	5/9	5/9
Collagen/heparin + BMP-2	0/9	4/9	5/9	5/9
Collagen + BMP-2/heparin	1/8	4/7	5/7	5/7

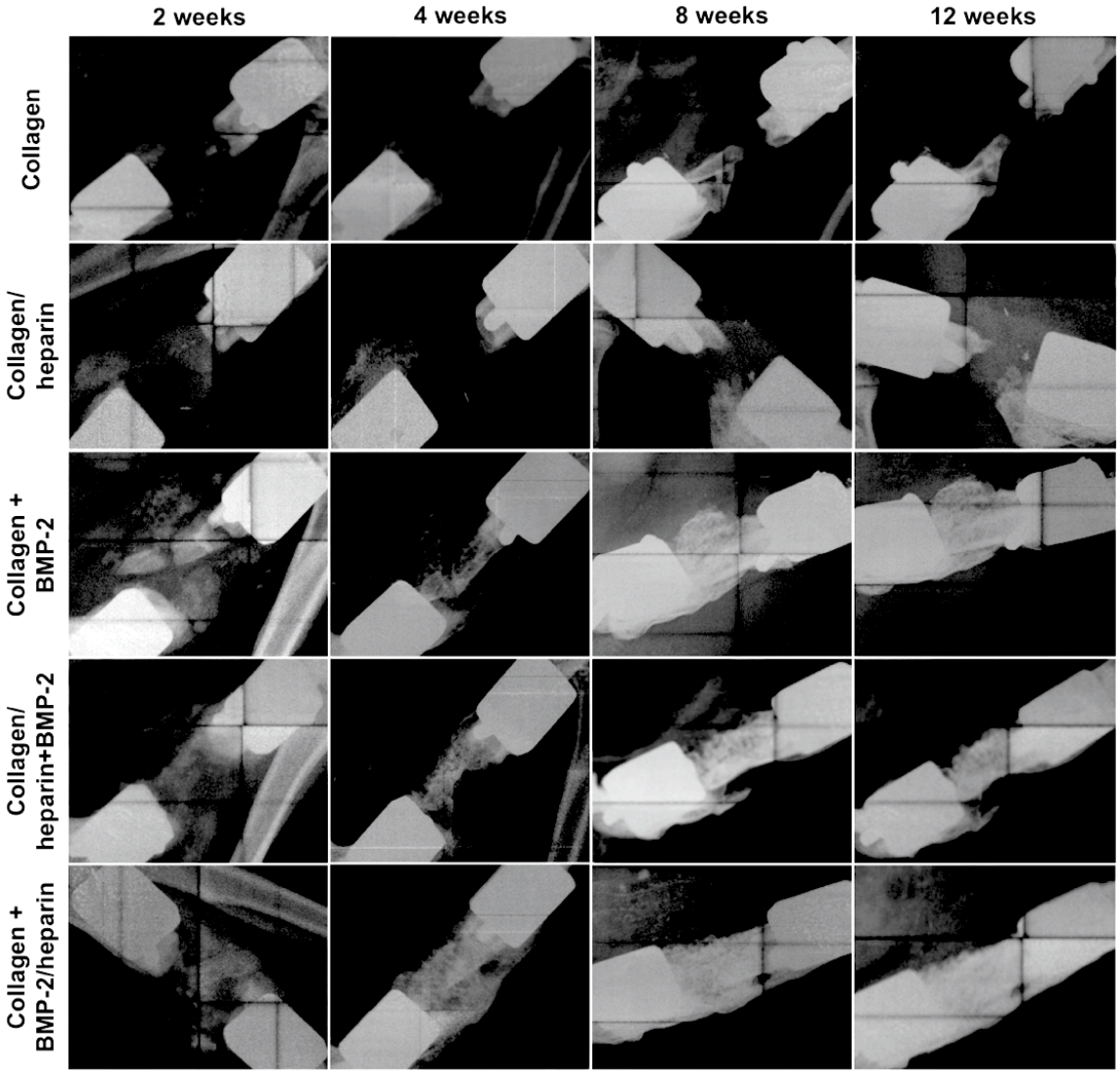

Figure 5.2 Representative *in vivo* 2D x-ray images of defect sites obtained at 2, 4, 8, and 12 weeks post-op.

5.4.2 In vivo quantitative micro-CT analysis of bone formation

Evaluation of *in vivo* micro-CT scans allows for the quantification of bone formation in the defect region within the same animal at multiple time points. The volume of mineralized tissue was quantified within a consistent volume of interest (VOI) centrally located within the 8 mm defect at 4, 8, and 12 weeks post-op (**Figure 5.3**). Delivery of BMP-2 and BMP-2/heparin on the collagen matrix significantly increased mineral formation at 4 weeks compared to non-BMP-2 controls, and remained significantly higher than the collagen only group at 12 weeks (**Figure 5.4A**). BMP-2 delivered in the collagen/heparin matrix had slightly lower mineral formation than BMP-2 and BMP-2/heparin in collagen matrices, however the differences between these groups were not significant. Collagen + BMP-2 had the largest increase in volume from 4 to 8 weeks, significantly higher than both non-BMP-2 control groups. However, all groups produced less new mineral from 8 to 12 weeks, as indicated by the small changes in volume within the last 4 weeks of the study (**Figure 5.4B**).

Mean density and connectivity density of the regenerated bone was also evaluated at 4, 8, and 12 weeks from *in vivo* micro-CT scans. Both collagen + BMP-2 and collagen/heparin + BMP-2 groups had significantly lower hydroxyapatite densities at 8 and 12 weeks compared to the collagen only group (**Figure 5.5A)**. It should be noted that this quantity is the actual density of the mineralized tissue and not the apparent mineral density of the entire volume. The bone density significantly increased from week 4 to week 8 ($p<0.001$) in all groups indicating maturation of the newly formed mineralized tissue. Between 8 and 12 weeks, all groups containing BMP-2 continued to significantly increase in density ($p<0.05$). At 4 and 8 weeks, the connectivity density was

significantly higher in the collagen + BMP-2 group compared to the collagen only group. Additionally, the collagen + BMP-2/heparin group had significantly higher connectivity density at 4 weeks compared to collagen and collagen/heparin groups (**Figure 5.5B**). Among time points, the connectivity density did not significantly change in any of the groups.

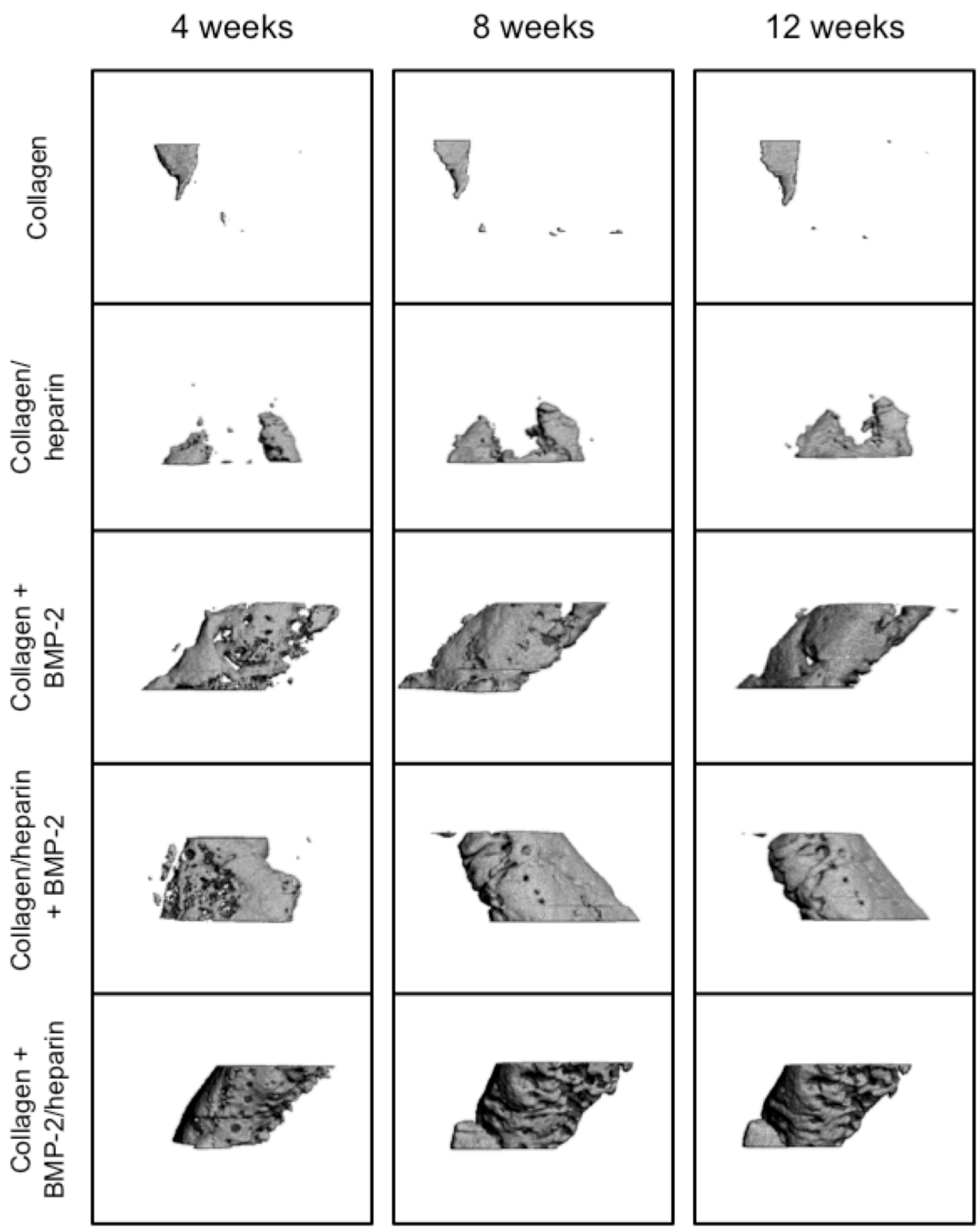

Figure 5.3 Three-dimensional *in vivo* micro-CT images at 4, 8, and 12 weeks post-op. The images were analyzed over a volume of interest (VOI) 100 slices thick that was centrally located within the 8 mm defect.

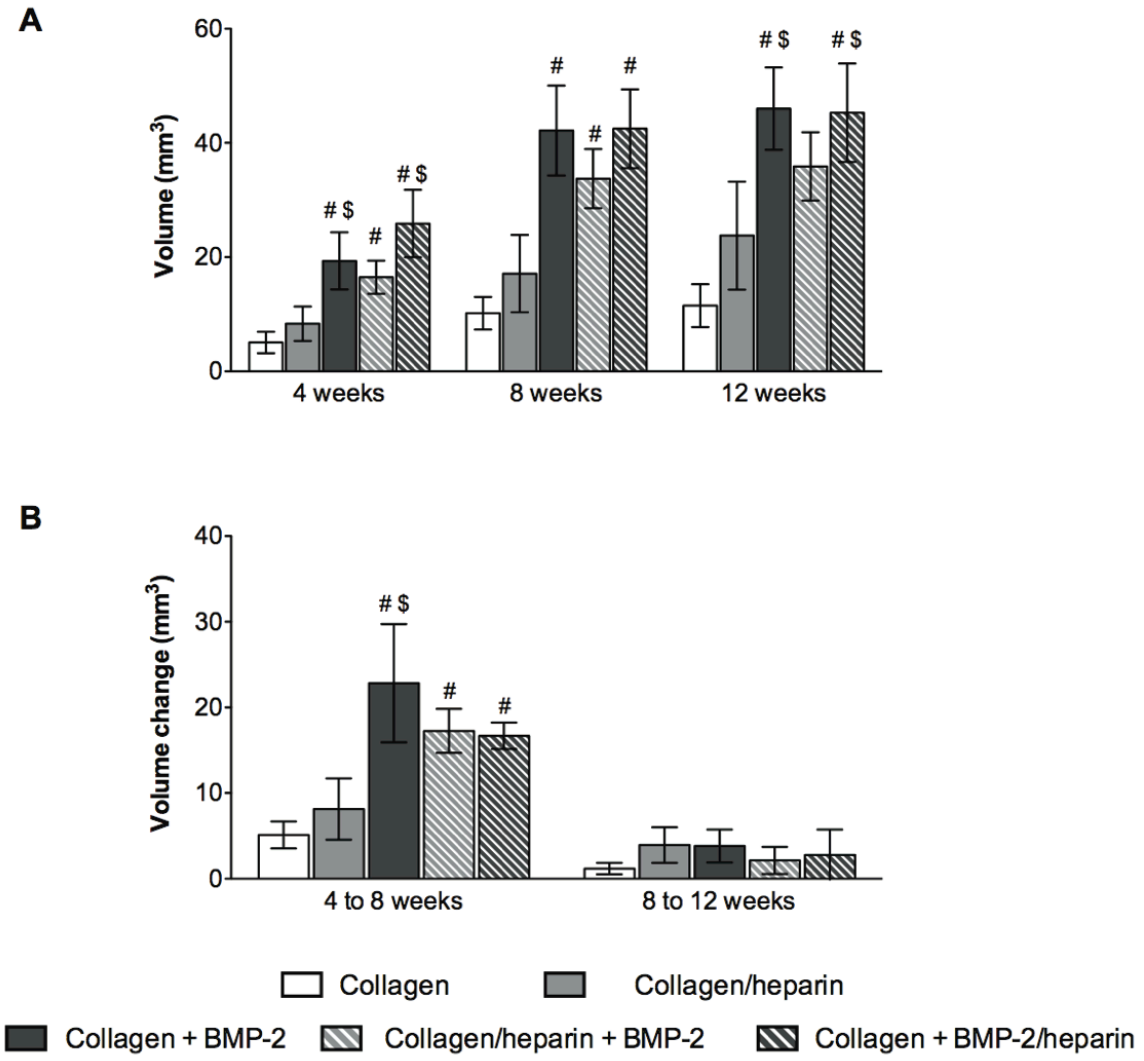

Figure 5.4 Quantitative evaluation of *in vivo* bone formation from micro-CT images at 4, 8, and 12 weeks post-op. **(A)** Volume of mineralized tissue (mm^3). **(B)** Volume change of mineralized tissue (mm^3) between time points. # $p<0.05$ compared to collagen, $ $p<0.05$ compared to collagen/heparin.

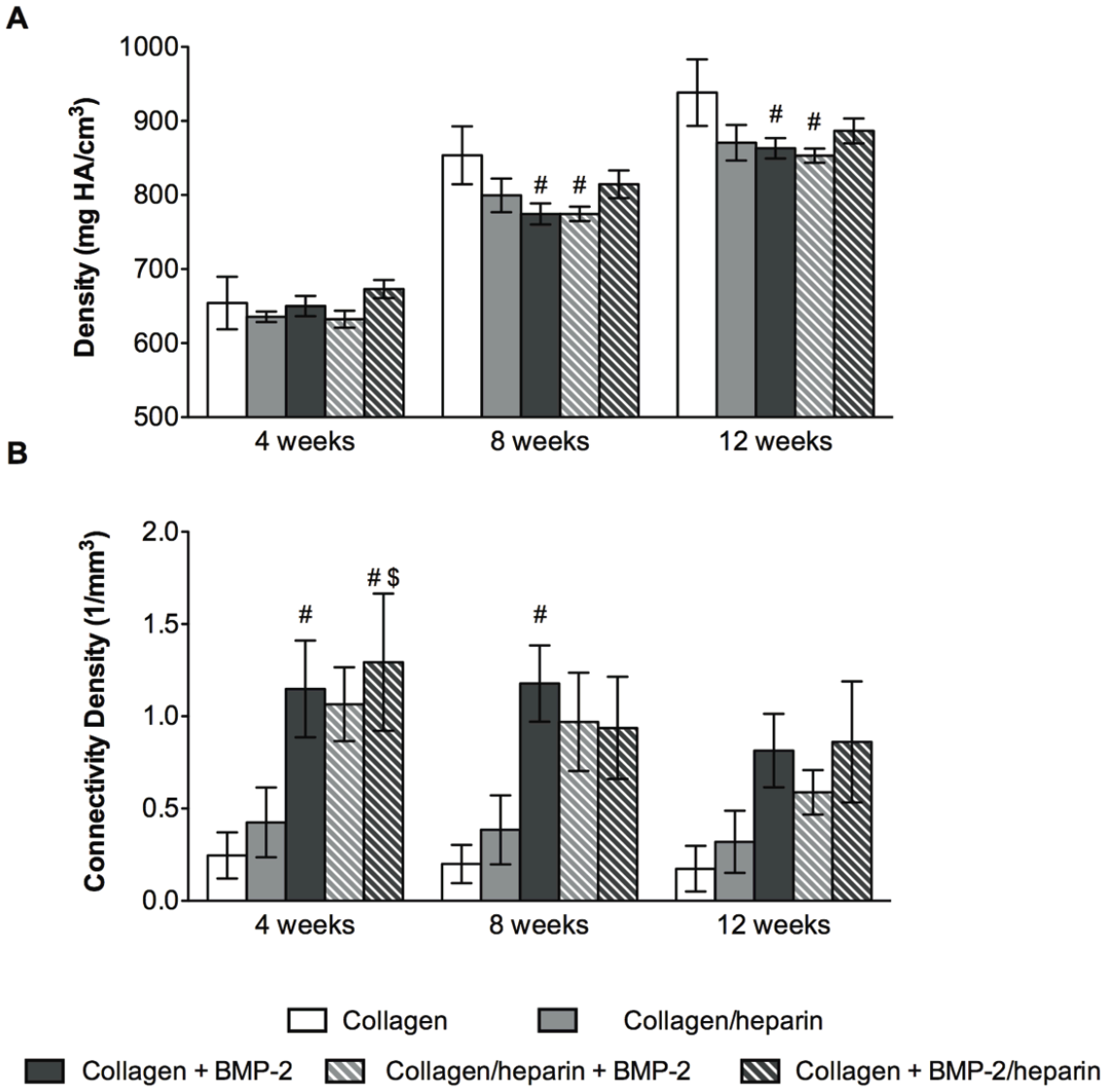

Figure 5.5 Quantitative evaluation of density and connectivity density from *in vivo* micro-CT images at 4, 8, and 12 weeks post-op. **(A)** Mean hydroxyapatite density (mg HA/cm^3) and **(B)** Connectivity density (1/mm^3) between time points. # $p<0.05$ compared to collagen, \$ $p<0.05$ compared to collagen/heparin.

5.4.3 In vitro quantitative micro-CT analysis of bone formation in segmental defect

Quantitative micro-CT analysis was performed *post-mortem* on the explanted femurs prior to mechanical testing (**Figure 5.6A and B**). Consistent with the 12 week *in vivo* scans, all groups with BMP-2 had significantly more mineralized tissue in the defect region than the collagen only group ($p<0.05$). The group that received pre-complexed BMP-2/heparin in the collagen matrix had the highest volume of mineralized tissue, however the differences between the groups with BMP-2 were not significant. The pre-complexed BMP-2/heparin group also had the highest connectivity density, indicating a more interconnected mineralized structure, although this difference was not significant. As expected, the mineralized tissue volume and connectivity density quantities were dominated by the contributions from the fully bridged samples, indicating that these measures are good assessments of defect healing (**Figure 5.6C and D**). Interestingly, the differences between connectivity density in bridged and unbridged samples from the collagen/heparin + BMP-2 group were not as great as seen in the other BMP-2 treated groups.

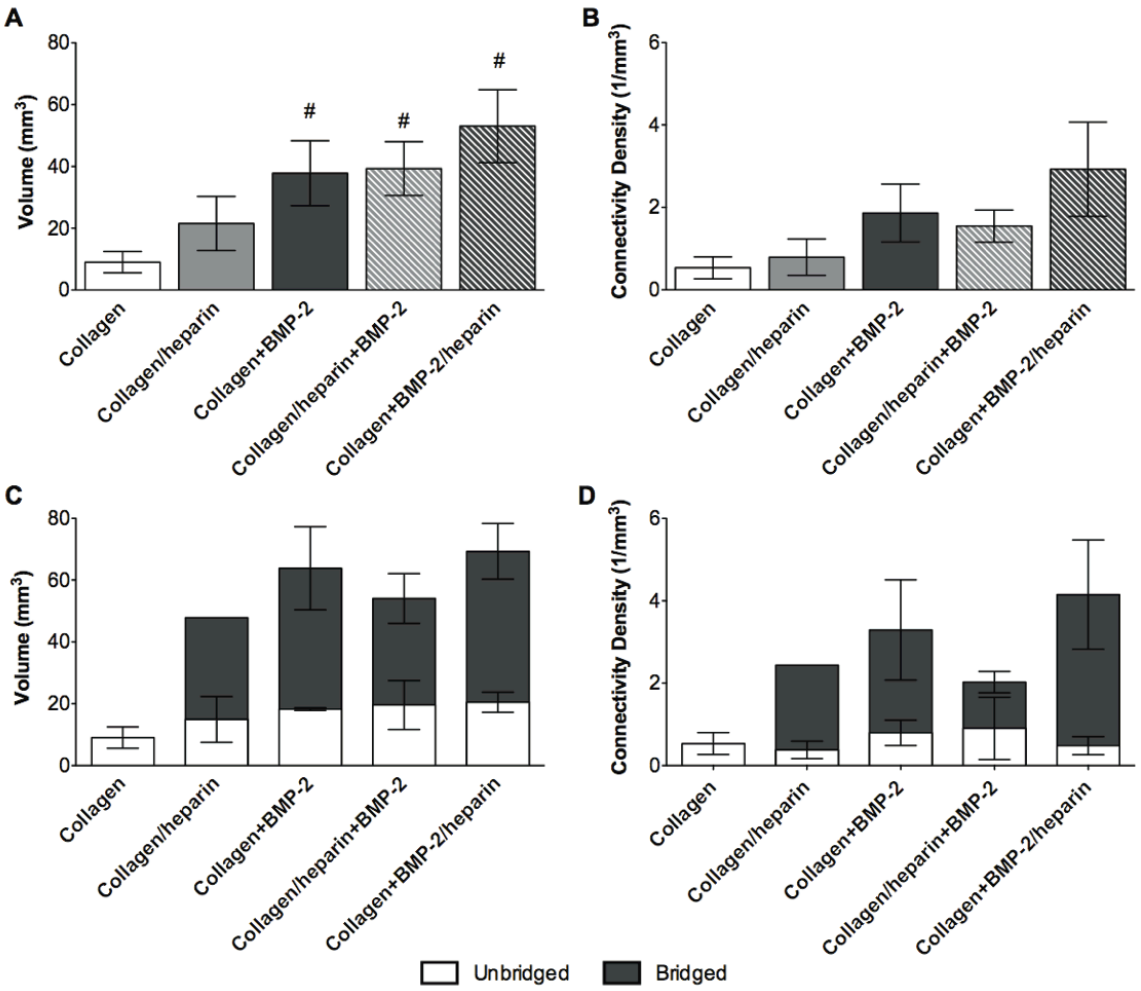

Figure 5.6 Quantitative evaluation of mineralized tissue volume and connectivity density from *in vitro* micro-CT images of 12 weeks *post-mortem* samples: **(A)** Volume of mineralized tissue (mm^3) and **(B)** Connectivity density ($1/mm^3$). **(C)** Contributions of unbridged and bridged samples to mineralized tissue volume. **(D)** Contributions of unbridged and bridged samples to connectivity density. (# $p<0.05$ compared to collagen)

5.4.4 Post-mortem mechanical testing

Torsional testing was performed on explanted samples at 12 weeks post-op to determine the functional integration of the regenerated bone. A plot of torque versus angular displacement was generated for each sample in order to calculate the maximum torque and stiffness. Defects treated with BMP-2/heparin on the collagen matrix had the highest strengths, reaching an average maximum torque of 0.204 ± 0.079 N-m (mean ± SEM), which was only slightly below the torsional strength of age-matched intact bones (0.31 ± 0.016 N-m [189, 195]), and the only group that was not significantly different from intact bone. The maximum torque for this group (collagen + BMP-2/heparin) was significantly greater than both non-BMP controls (collagen and collagen/heparin). Defects treated with BMP-2 on either the collagen or collagen/heparin matrix had lower maximum torques of 0.053 ± 0.023 and 0.079 ± 0.047 N-m, respectively (**Figure 5.7A**). The collagen/heparin + BMP-2 group was significantly greater than only the collagen group. The collagen + BMP-2 was not significantly greater than either non-BMP control group. Upon further consideration of the results for maximum torque we noted that a majority of the torsional strength could be attributed to the bridged samples, and the unbridged samples demonstrated the torsion curve patterns of soft tissue and polymer material (**Figure 5.7C**). The maximum torque of bridged samples in the collagen+BMP-2/heparin group was not significantly different than that of intact bone. When only the bridged samples were compared, the intact bone was significantly different from the collagen+BMP-2 group.

Similar trends were observed in the torsional stiffness. Control groups (collagen and collagen/heparin without BMP-2) had minimal resistance to the torsional

deformation induced (**Figure 5.7B**). Defects treated with BMP-2/heparin in the collagen matrix had the highest stiffness of 0.014 ± 0.006 N-m/deg (mean ± SEM), approximately 50% of the intact bone stiffness previously measured [189, 195], however this difference was not significant. Intact bone had significantly higher stiffness than the other groups. Delivery of BMP-2 in either collagen or collagen/heparin matrices yielded torsional stiffness an order of magnitude lower than intact bone (0.005 ± 0.002 and 0.0043 ± 0.003 N-m/deg, respectively). Additionally, we observed that the bridged samples contributed the majority of torsional stiffness, yet the collagen+BMP-2 and collagen/heparin+BMP-2 bridged samples were still significantly lower than intact bone (**Figure 5.7D**).

Although all groups delivering BMP-2 had similar volumes of bone formation, only delivery of BMP-2/heparin in the collagen matrix was able to restore mechanical properties to levels similar to those of intact bone. Therefore, in order to assess if the bone volume and connectivity density had an effect on biomechanical properties, we performed linear regression analyses between the variables. First, we examined bone volume in relation to maximum torque and stiffness (**Figure 5.8, Table 5.2**). When data from all groups were pooled together for analyses, the regressions were significant (slopes were significantly non-zero) but had weak correlations (low R^2 values). Among the bridged samples only, the correlations with maximum torque and stiffness did not improve (R^2 = 0.56 and 0.52, respectively). However, when each treatment group was analyzed separately, the collagen + BMP-2/heparin group demonstrated a strong correlation between volume and maximum torque (R^2 = 0.93), as well as between volume and stiffness (R^2 = 0.92). Conversely, the bone volumes in the collagen/heparin + BMP-2 group did not correlate as powerfully to maximum torque and stiffness. This suggests

that although the amount of bone regenerated in this group was similar to the collagen + BMP-2/heparin group, the geometry and orientation of that newly formed bone may not have provided optimal mechanical stability.

Analysis of the relationship between the connectivity density and mechanical properties demonstrated similar results. Overall, the pooled data demonstrated significant regressions, but the correlations were weak (**Figure 5.9, Table 5.3**). Analysis of only the bridged samples did not exhibit any improvement in the correlations with maximum torque and stiffness (R^2 = 0.35 and 0.40, respectively). Separately, the groups showed differences in their correlations between connectivity density and mechanical properties. The collagen + BMP-2/heparin group had weaker correlations than observed with the volume relationships (R^2 = 0.84 and 0.77), however the correlations were still significant. The collagen/heparin + BMP-2 group did not exhibit any significant correlation between connectivity density and maximum torque and stiffness.

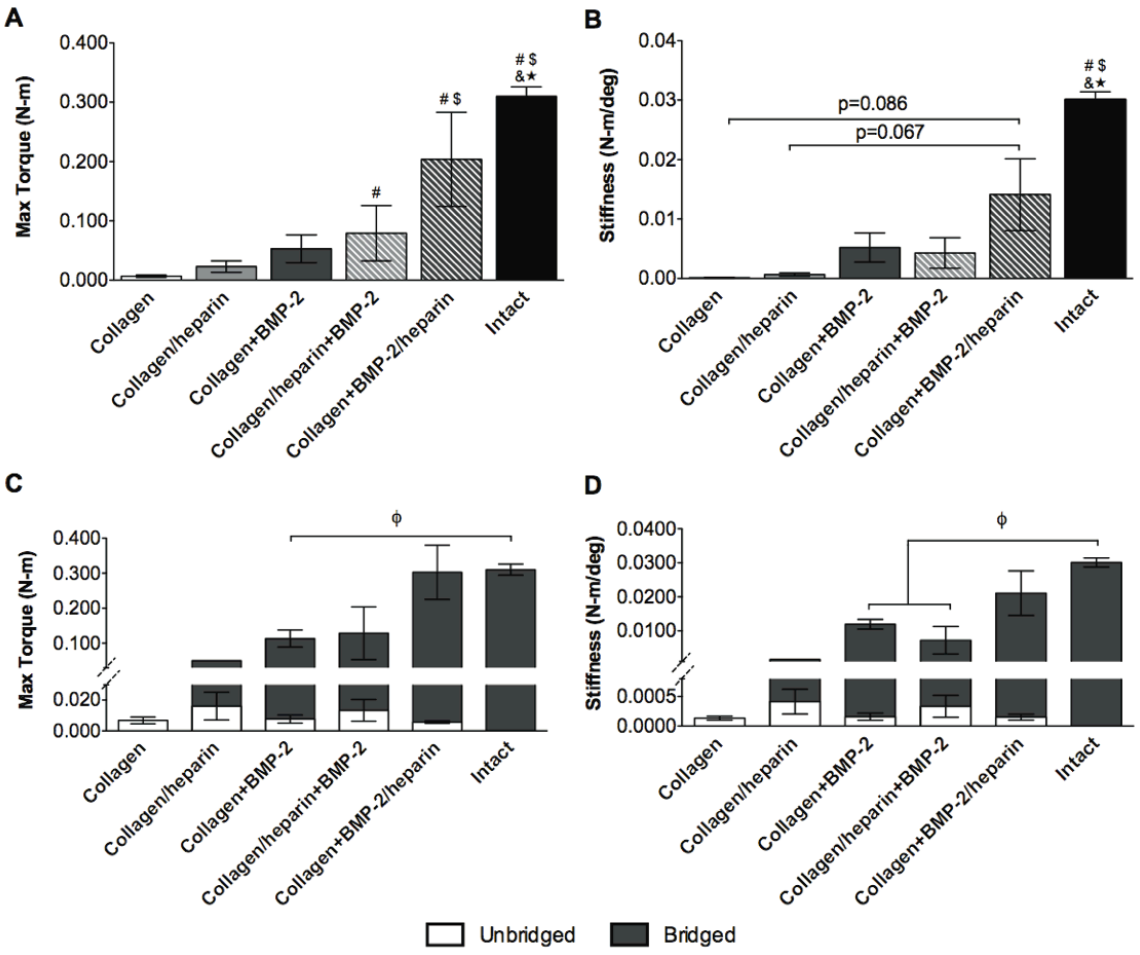

Figure 5.7 Evaluation of mechanical properties of 12 weeks *post-mortem* samples: **(A)** Maximum torque (N-m), **(B)** Torsional stiffness (N-m/deg), **(C)** Contributions of unbridged and bridged samples to maximum torque, **(D)** Contributions of unbridged and bridged samples to torsional stiffness. ANOVA: # $p<0.05$ compared to collagen, $ $p<0.05$ compared to collagen/heparin, & $p<0.05$ compared to collagen+BMP-2, and ★ $p<0.05$ compared to collagen/heparin+BMP-2. Mann-Whitney test: Φ $p<0.05$.

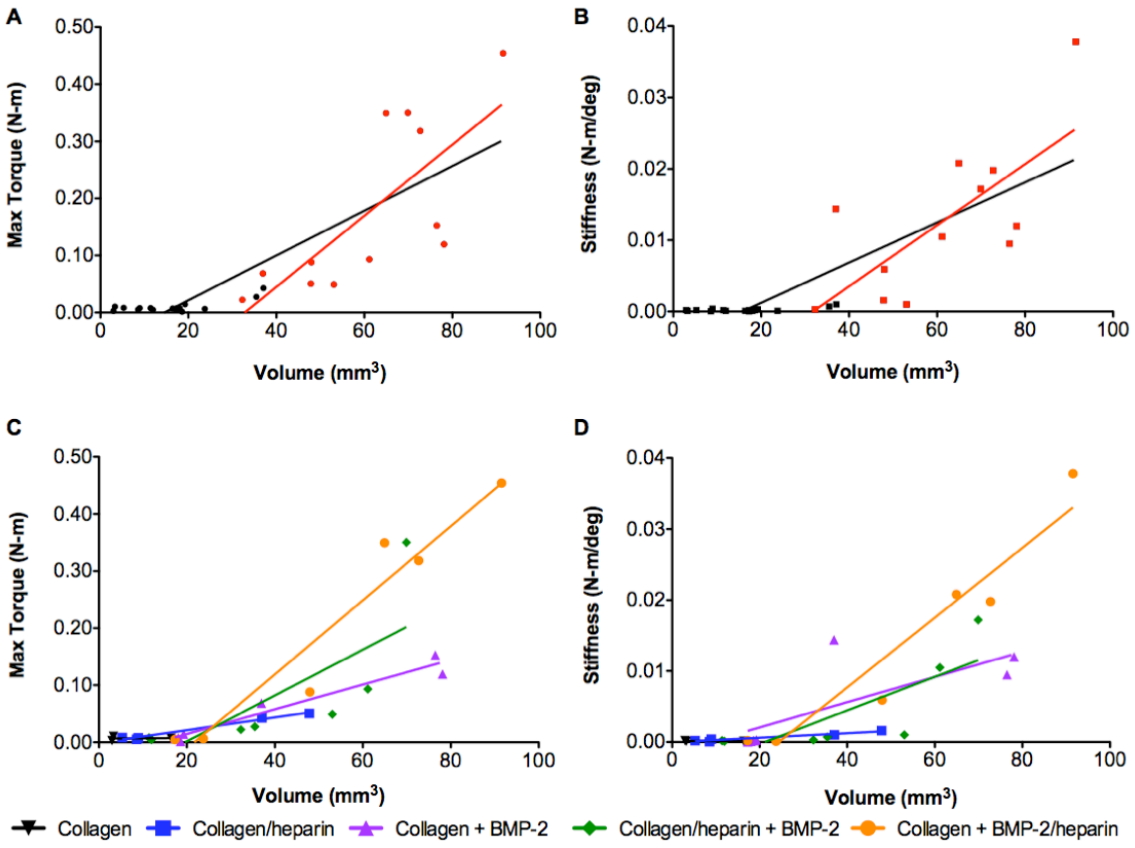

Table 5.2	Volume (mm^3) vs. Max Torque (N-m)		Volume (mm^3) vs. Stiffness (N-m/deg)	
	R^2	*p*-value	R^2	*p*-value
All groups	0.67	< 0.0001	0.66	< 0.0001
Collagen	0.01	NS	0.27	NS
Collagen/heparin	0.98	< 0.001	0.94	< 0.01
Collagen + BMP-2	0.95	< 0.001	0.59	< 0.05
Collagen/heparin + BMP-2	0.56	NS	0.64	< 0.05
Collagen + BMP-2/heparin	0.93	< 0.01	0.92	< 0.02

Figure 5.8 Correlations of mineralized tissue volume to mechanical properties: **(A & B)** Linear regression analysis of combined data from all groups (bridged samples highlighted in red); **(C & D)** Linear regression analysis of each treatment group. **Table 5.2** Goodness of fit values for linear regression correlating volume to max torque and stiffness; *p*-values for significant correlations (NS = no significance).

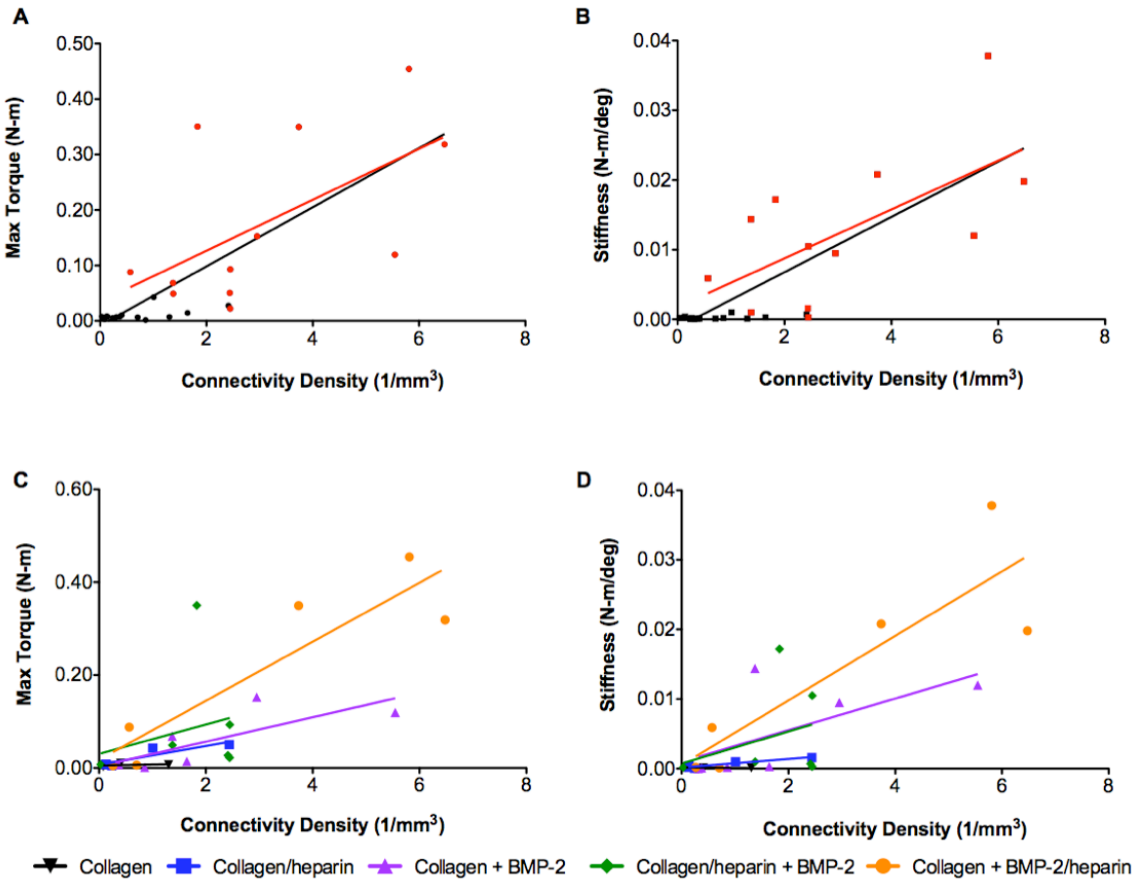

Table 5.3	Connectivity Density (1/mm³) vs. Max Torque (N-m)		Connectivity Density (1/mm³) vs. Stiffness (N-m/deg)	
	R^2	*p*-value	R^2	*p*-value
All groups	0.58	< 0.0001	0.61	< 0.0001
Collagen	0.12	NS	0.50	NS
Collagen/heparin	0.83	< 0.05	0.91	< 0.05
Collagen + BMP-2	0.63	< 0.05	0.42	NS
Collagen/heparin + BMP-2	0.07	NS	0.12	NS
Collagen + BMP-2/heparin	0.84	< 0.05	0.77	< 0.05

Figure 5.9 Correlations of connectivity density to mechanical properties: **(A & B)** Linear regression analysis of combined data from all groups (bridged samples highlighted in red); **(C & D)** Linear regression analysis of each treatment group. **Table 5.3** Goodness of fit values for linear regression correlating connectivity density to max torque and stiffness; *p*-values for significantly non-zero slopes (NS = no significance).

Analysis of *in vitro* micro-CT images was able to demonstrate the density distribution of the mineralized tissue within the defects (**Figure 5.10**). These images further validate the mechanical testing results. The samples with the highest mechanical properties were in the collagen + BMP-2/heparin group, which were shown in the density maps to have more organized dense tissue distributed around the perimeter in a manner similar to native cortical bone. The defects treated with collagen + BMP-2 or collagen/heparin + BMP-2 had disorganized dense tissue; with dense areas occurring in the center around the PCL scaffold struts and disconnected from other dense areas.

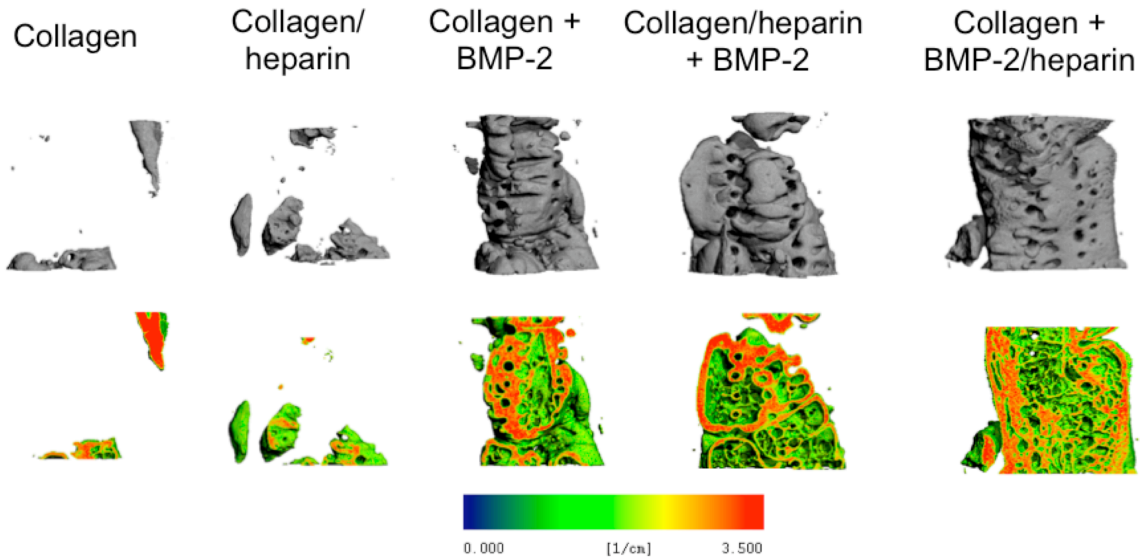

Figure 5.10 Representative *in vitro* micro-CT images with corresponding density maps (bottom row) sectioned longitudinally. The color scale at the bottom correlates to the attenuation, which corresponds to the tissue density. Red indicates the higher density bone and green indicates lower density bone.

5.5 Discussion

A number of *in vivo* studies have recently demonstrated the ability of heparinized BMP-2 delivery systems to improve retention and bioactivity. However, these systems have mainly been tested in ectopic assays and have not been quantitatively evaluated in a more clinically relevant model for assessment of fracture repair. Von Walter, et al. implanted heparinized collagen sponges with BMP-2 in a cylindrical defect in rabbit condyles [20]. Other groups have utilized the ectopic bone formation assay to assess the efficacy of incorporating heparin into BMP-2 delivery systems [17, 115, 133, 186]. We evaluated the delivery system developed in Specific Aim II (Chapter 4) in an *in vivo* segmental defect model to further determine the potential for the collagen/heparin matrix to deliver BMP-2 in bone tissue engineering applications.

The dose delivered in this work was increased to 3 μg BMP-2 due to the increased dimensions of the implanted constructs, as well as consideration of previous work demonstrating that higher doses are necessary to promote consistent bone regeneration in an *in vivo* segmental defect model [189, 190]. Nevertheless, the dose used in this study (0.02 mg/ml) was orders of magnitude lower than the 1.5 mg/ml dose used clinically in the InFUSE™ graft system and in the lower range of doses administered (2-20 μg) in similar rodent segmental defect studies [127, 187, 196].

Quantitative micro-CT analysis was performed at 4, 8, and 12 weeks *in vivo*, as well as *post-mortem* to assess bone ingrowth into the defect region. Measures included mineralized tissue volume, hydroxyapatite density, connectivity density, maximum torque, and stiffness. Collectively, these measurements can demonstrate the extent of functional bone regeneration within the defect for a given treatment. *In vivo* analyses

showed that treatment of defects with BMP-2 resulted in significantly higher amounts of bone formation compared to non-BMP-2 controls, however no significant differences among the groups treated with BMP-2 were observed. Further analysis of the femurs *post-mortem* demonstrated that defects treated with collagen + BMP-2/heparin had the greatest amount of bone formation within the defect, significantly higher than the collagen only group, as well as the highest connectivity density. Connectivity density is defined as the number of connections per unit volume, or the maximum number of connections per unit volume that can be broken before failure [197]. It is generally understood that native bone is highly connected, however during bone formation and fracture healing isolated regions of bone form [197]. Eventually these isolated areas of mineralized tissue develop connections and form highly connected bone. We observed in this study that connectivity densities were highest when pre-complexed BMP-2/heparin was delivered in the collagen matrix, indicating regeneration of a more interconnected bone structure and therefore higher mechanical stability, however these differences were not significant.

The mechanical properties of the femurs were substantially less than those of intact bone, with the exception of femurs treated with collagen + BMP-2/heparin. Both maximum torque and stiffness in the collagen + BMP-2/heparin group were not significantly different from the properties seen in age-matched intact bone (0.31 N-m and 0.03 N-m/deg) [189, 195]. The biomechanical properties in this group were also greater than values seen in previous studies using PCL scaffolds in the same segmental defect model [192]. The higher mechanical properties seen in the collagen + BMP-2/heparin may have been attributed to the higher rate of bridging, 71% compared to 56% in both

the collagen + BMP-2 and collagen/heparin + BMP-2 groups, however upon analysis of the bridged samples the collagen + BMP-2 group remained significantly lower than the intact bone. The collagen + BMP-2/heparin group was also observed to have the highest connectivity density, which strongly correlated to the higher biomechanical properties. Other groups had weaker correlations between connectivity density and biomechanical properties, indicating that the organization of the mineralized matrix in these groups did not provide optimal mechanical integrity. The matrix in these groups may still be immature bone and require more time to organize into more mature bone, whereas the collagen + BMP-2/heparin may have accelerated defect bridging resulting in more time for bone remodeling.

Previously, we showed *in vitro* that BMP-2 mediated mineralization was significantly increased when heparin was incorporated in the collagen matrix, while the delivery of pre-complexed BMP-2 and heparin in the collagen matrix had less mineralization. The observations of bone repair *in vivo* resulted in different conclusions. First, the *in vitro* and *in vivo* assay systems have different experimental designs, and therefore may result in differing conclusions. Also, the differences observed may have been caused by the many additional factors present *in vivo* that are not in the controlled *in vitro* environment, such as inflammatory responses, endogenous growth factors and antagonists [39, 64]. This complex *in vivo* environment often compounds the interactions between growth factors, receptors, and matrix components such as heparin. For example, previous work has shown that activation of macrophages causes a decrease in local pH to below 5 [198]. This decrease in pH causes a significant decrease in BMP-2 binding and results in rapid clearance of the growth factor, as shown in work performed by Friess, et

al. [15]. *In vivo* the pre-complexed BMP-2/heparin group was the only condition to restore properties, indicating that stabilizing the BMP-2 molecule provides a significant advantage in the *in vivo* environment.

The release kinetics of growth factors are also drastically different *in vivo*, as shown by Kempen, et al. [22]. They demonstrated that their scaffolds had a larger burst release and overall faster release of BMP-2 *in vivo* compared to similar release experiments *in vitro* [22]. Other research has shown that release properties are very dependent on the conditions in the immediate environment (i.e. pH, chemical composition, temperature) [149]. Therefore the release of BMP-2 *in vivo* may be very distinct from *in vitro* release kinetics, as well as varying kinetics at different sites *in vivo*, thereby having a different effect.

Growth factors delivered bound to the matrix results in no circulating signal reaching the surrounding cells that could initiate migration, proliferation, and differentiation into the defect site. Rizzi, et al. demonstrated that physical linkage of BMP-2 to a PEG matrix resulted in suboptimal bone formation in a rat calvarial defect model [199]. Matrix-bound growth factors can only transmit signals to nearby cells, whereas soluble growth factors are able to freely diffuse and act on the surrounding cells via paracrine signaling [174]. On the other hand, if the growth factor diffuses from the defect too rapidly, there will be insufficient sustainment of the osteoinductive signal to induce a significant biological response. This rapid diffusion has been observed in the current clinical treatments, which has been overcome with large, unsafe doses. These conflicting conditions introduce very significant challenges when designing an optimal spatiotemporal growth factor delivery system [100, 108]. Lutolf, et al. developed an

inducible system that enabled either rapid solubilization of BMP-2 or using an MMP-sensitive PEG gel system [200]. They demonstrated that the lack of a soluble BMP-2 signal resulted in less bone formation in a cranial defect and the MMP-sensitive implants released BMP-2 in relation to cell invasion into the gel resulting in higher amounts of bone formation [200].

Delivery of pre-complexed BMP-2/heparin in the collagen matrix presented in this work performed the best *in vivo*. The heparin helped protect the diffuse BMP-2 molecule from degradation, thereby maintaining the BMP-2 structure and subsequent bioactivity in the surrounding tissue [96, 117]. Design considerations for BMP-2 delivery systems not only need to address the temporal requirements, but also must ensure that the released BMP-2 remains biologically active [201]. The pre-complexing of BMP-2 and heparin resulted in significantly greater bone formation than both non-BMP-2 control groups, and was the only group not significantly different from intact bone properties. While this pre-complexed group was not significantly greater than the other BMP-2 groups, the delivery of BMP-2 in collagen and collagen/heparin matrices resulted in significantly lower mechanical properties than intact bone. These results indicate that further design of a BMP-2/heparin co-delivery system may prove to be a potential graft substitute therapy.

5.6 Conclusions

The work presented in this Chapter focused on evaluating the affinity-based BMP-2 delivery system previously developed in Specific Aim II (Chapter 4) in a challenging *in vivo* bone repair model. We observed that the delivery of pre-bound BMP-2 and heparin in a collagen matrix induced bone regeneration with mechanical

properties closest to those of native bone, while delivery of BMP-2 in collagen or collagen/heparin matrices had similar volumes of regenerated mineralized tissue but had significantly lower mechanical strengths than intact bone. We observed that the heparinized delivery system performed differently *in vitro* and *in vivo*, suggesting that *in vivo* experiments remain necessary to fully evaluate potential tissue engineering therapies. The results observed in this chapter indicate that the co-delivery of both BMP-2 and heparin may be beneficial for bone tissue engineering.

CHAPTER 6

CONCLUSIONS AND FUTURE DIRECTIONS

6.1 Summary

Tissue-engineered products that utilize growth factors to induce tissue regeneration and repair have demonstrated significant potential because of the highly specific activity of growth factors to induce cell differentiation, migration, proliferation, and matrix production. Such tissue engineering approaches involve the delivery of the growth factors within a carrier biomaterial. These carriers are included to provide a structure for tissue regeneration to occur on, as well as retain the growth factor at the implant site. However, current carriers are limited by their poor affinity for growth factors leading to rapid diffusion from the construct. Upon release from the carrier, protein therapies are further limited by poor protein stability. These limiting factors result in the use of high doses, and frequent injections. To address these limitations, delivery systems that are able to optimally control the rate and location of growth factor release are being investigated.

The goal of this work was to develop and evaluate the efficacy of BMP-2 delivery systems to improve bone regeneration. We examined two approaches for delivery of BMP-2 in this work. First, we determined the efficacy of a self-assembling lipid microtube system for the sustained delivery of BMP-2 (Specific Aim I, Chapter 3). We determined that sustained delivery of BMP-2 from the lipid microtube system was able to enhance osteogenic differentiation compared to control microtubes, however did not demonstrate a significant advantage over a bolus BMP-2 dose *in vitro*. Second, we

examined the use of an affinity-based system to sequester BMP-2 at the implant site and retain bioactivity by incorporating heparin within a collagen matrix (Specific Aim II, Chapter 4). Incorporation of heparin in the collagen matrix improved BMP-2 retention and bioactivity, thus enhancing cell-mediated mineralization *in vitro*. Lastly, the affinity-based BMP-2 delivery system was evaluated in a challenging *in vivo* bone repair model (Specific Aim III, Chapter 5). Delivery of pre-complexed BMP-2 and heparin in a collagen matrix induced bone regeneration with mechanical properties not significantly different from those of intact bone, whereas delivery of BMP-2 in collagen or collagen/heparin matrices had significantly lower mechanical properties than intact bone.

6.2 Sustained delivery of BMP-2 in lipid microtubes

In Specific Aim I we characterized the sustained release of BMP-2 from lipid microtubes and showed that the BMP-2 released from the microtubes remained biologically active. Therefore, we hypothesized that the lipid microtubes would improve BMP-2 mediated mineralization compared to a bolus dose and be a potential BMP-2 delivery system for bone tissue engineering.

Sustained delivery of BMP-2 from the microtubes demonstrated increased osteogenic differentiation compared to control microtubes, indicating the release of bioactive BMP-2. However, when compared to a bolus BMP-2 dose, this sustained release approach did not provide a significant advantage for osteogenic differentiation compared *in vitro*. Other studies have shown that the kinetics of BMP-2 exposure is a major factor for mineralization [16, 157-159]. Some have also hypothesized that a system with a biphasic release profile consisting of a burst release to recruit osteoprogenitor cells, followed by sustained release of growth factor to induce

differentiation of those recruited cells will be the most effective therapy [16, 100, 158]. Bostrom, et al. showed that there is a large increase in endogenous BMP and BMP receptor expression in the fracture callus immediately after fracture, inducing new woven bone formation within 1-2 weeks [33]. As the woven bone is remodeled into lamellar bone, the expression of BMPs decreases [33]. Endogenous expression can be stimulated by BMPs secreted by other cells or by exogenously added BMPs [202]. Therefore, exogenous addition of a higher concentration of BMP-2 followed by a lower, steady release of BMP-2 dose may enhance the native BMP expression profile, thereby potentiating bone repair. Future studies may possibly focus on combining the sustained release of BMP-2 from microtubes with an initial burst release component to determine a more efficacious release for mineralization. This could be achieved by delivering the BMP-loaded microtubes in a hydrogel carrier with unencapsulated BMP-2 suspended in the hydrogel. The two modes of BMP-2 delivery within the same system may provide a biphasic release profile.

The *in vitro* assays used in this thesis to examine the microtube performance were limited to two-dimensional cell assays. It has been demonstrated previously that cells respond very differently in two-dimensional and three-dimensional culture systems [203]. Since tissue engineering mainly requires three-dimensional constructs, potential therapies need to be validated in those conditions. We considered experimental designs to test this microtube delivery system in a 3D cell assay, and examined methods to deliver these microtubes in a 3D construct. Due to the small size of the microtubes, a hydrogel with low porosity is necessary for suspension in a 3D structure. Therefore, the microtubes were suspended in an RGD-alginate gel to achieve the necessary 3D structure for *in vivo*

implantation. We chose the RGD-alginate because it has been used previously for bone defect repair with BMP-2 [82, 189, 190]. However, cell culture within these gels is difficult and often results in significant cell death due to a lack of nutrient transport through the small pores of the hydrogel [204]. Previous work has examined the bioactivity of growth factors in delivered in 3D hydrogel systems by co-culturing cells with the delivery system suspended in transwells [22, 205]. However, these assays only examine the response of 2D cell cultures to the soluble released BMP-2, and do not directly assess cell responses in a 3D system. Therefore, future work can focus on developing a more effective 3D *in vitro* assay system.

The *in vitro* responses to the bolus BMP-2 and sustained release of BMP-2 may not directly correspond to potential *in vivo* results. We examined the *in vivo* response to the lipid microtube delivery system using the RGD-alginate system to suspend in 3D PCL scaffolds (data not included in this thesis). We observed that concentrations in excess of 5 mg/ml lipid microtubes in the alginate resulted in poor gel formation. This constraint in microtube concentration was a limiting factor when attempting to load physiological doses of BMP-2 into the microtube-alginate system. In order to obtain a high enough concentration of BMP-2 within the low concentration of microtubes, the microtubes would need to be incubated in very highly concentrated BMP-2 solutions (greater than 300 μg/ml) for the loading process. The loading concentration in addition to the limit of microtubes in the alginate solution leads to a restriction on how much BMP-2 can be loaded into the microtube-alginate system, which we determined to be approximately 0.5 μg/construct, or 5 μg/ml. We then examined the *in vivo* subcutaneous delivery of 0.5 μg BMP-2 in the microtubes suspended in the alginate gel and saw that

there was not a significant amount of mineralization in the constructs after 8 weeks. The same dose of BMP-2 delivered in the alginate gel without the microtubes also did not exhibit a significant amount of mineral formation, indicating that this dose was insufficient for *in vivo* applications. Other studies using similar *in vivo* ectopic models have demonstrated that doses of at least 1-2 µg BMP-2/construct were required to induce mineralization [186, 206, 207].

BMP-2 is generally known to require much higher doses than other growth factors and cytokines [95]. Therefore, a higher concentration of BMP-2 in the microtubes may have proved to be more advantageous than the bolus dose. However, a major concern with current clinical treatments is the high dose and cost of BMP-2 [103]. Thus increasing the dose in the microtube system will result in similar concerns. Although this microtube sustained delivery approach for BMP-2 did not provide a significant advantage over a bolus dose, there may be use for this system in bone tissue engineering by incorporating other osteogenic factors. This includes growth factors such as bFGF, EGF, VEGF, or TGF-ß, which have been shown to have an effect on bone healing at lower doses [39, 51, 97, 110, 208]. TGF-ß has previously been delivered in the lipid microtube system at a dose of 20-25 ng for wound healing applications, therefore this delivery approach for TGF-ß may also be beneficial for bone tissue engineering [82, 137].

6.3 Delivery of BMP-2 in a collagen/heparin matrix

The work presented for Specific Aims II and III addressed the hypothesis that the collagen/heparin matrix would improve BMP-2 retention and bioactivity. We showed that BMP-2 quickly releases from collagen matrices, and diffuses much slower from

collagen/heparin matrices *in vitro*. In addition, BMP-2 delivered in collagen/heparin matrices improved BMP-2 mediated differentiation *in vitro*.

There are multiple possible mechanisms of BMP-2 release from an affinity-based system including: solubility of the carrier-bound molecule (i.e. heparin), solubility of the growth factor, and degradation of the carrier [111, 114, 201]. However, the mode of release remains unclear from the *in vitro* release kinetics and confocal analyses presented in Chapter 4. Previous work has used mathematical models to understand the release of growth factors from heparinized delivery systems [111, 114]. This model demonstrated that much of the heparin is released through matrix degradation, and not through passive diffusion of the molecules [111, 114]. They also showed that growth factor release rate was largely dependent on the affinity to heparin, with release rate increasing as the heparin affinity was decreased [111]. However, these studies assumed that the association and dissociation rate constants for growth factors with heparin were the same regardless of pre-complexation of heparin with the matrix component, and likewise the heparin binds to the matrix with the same kinetics regardless of pre-complexation with BMP-2. These assumptions simplify the mathematical model to make solutions possible, however are not realistic and may result in inaccurate results.

A possible approach to determine how the BMP-2 and heparin are released from this system is to fluorescently-label both the BMP-2 and heparin to observe the co-localization of the two fluorescently labeled molecules. In preliminary work, we labeled heparin with Alexa Fluor 488 using a protocol previously described by Osmond, et al. [29]. However, this fluorescent probe has similar excitation and emission wavelengths to the FITC probe used in Chapter 4 to observe BMP-2 in the matrices, therefore these two

fluorescent probes cannot be observed simultaneously to determine the co-localization of BMP-2 and heparin. To resolve this, another probe may be used for either BMP-2 or heparin at different excitation and emission wavelengths to concurrently observe the two molecules. However, an important consideration when determining which fluorescent probes to use is the auto-fluorescent properties of collagen at certain wavelengths. Therefore, both probes will need to be at different wavelengths from the auto-fluorescent wavelength of collagen (excitation 470-490 nm, emission 550 nm) [209].

We observed that heparin concentration in the collagen matrix had an effect on BMP-2 content using the confocal microscopy method. Another consideration for this delivery system is the collagen concentration. Higher concentrations of collagen may provide lower matrix porosity and slower degradation, resulting in slower diffusion of molecules from the matrix [198]. The spatial dimensions of BMP-2 are much smaller than the pores of the collagen matrix, therefore diffusion is not inhibited or delayed by the matrix dimensions and is mainly dependent on the interactions of BMP-2 with the matrix components. Work performed by Friess, et al. demonstrated that higher concentrations of collagen resulted in higher BMP-2 retention and improved mineralization [15].

6.4 In vivo evaluation of collagen/heparin delivery system

In Specific Aim III we evaluated the collagen/heparin delivery system in a challenging *in vivo* model. We demonstrated that although BMP-2 delivered in the collagen/heparin matrix outperformed all other groups in the *in vitro* assays, the results *in vivo* were not as promising. Interestingly, delivery of pre-complexed BMP-2/heparin in the collagen matrix performed the best in our *in vivo* model.

The different conclusions from *in vitro* and *in vivo* experiments may have been caused by the differing experimental design and conditions. First, the *in vitro* assays had cells directly seeded on the scaffolds; therefore the BMP-2 signal did not have to diffuse to the surrounding environment to induce cellular activity. *In vivo*, the growth factor delivered in the heparinized results in less diffusible signal to the surrounding cells that could potentiate migration, proliferation, and differentiation into the defect site. Kim et al., showed a similar effect *in vivo* where BMP-2 delivered to an ecoptic site via heparin-conjugated PLGA nanoparticles had a significantly greater effect on mineralization with simultaneous delivery of undifferentiated MSCs [115]. On the other hand, if the growth factor too readily diffuses out of the construct, there will be inadequate sustainment of the osteoinductive signal to achieve a significant biological response in the cells that migrate to the defect site, unless a large dose is delivered. Hubbell, et al. has investigated methods of delivering growth factors within matrices that prevent the diffusion of the growth factor but permits its release upon local cell-mediated activation of matrix-degrading enzymes [114, 199, 210]. *In vitro* confocal analysis performed in Specific Aim II demonstrated that the BMP-2/heparin in the collagen matrix did not have as high levels of retention as BMP-2 did in the collagen/heparin matrix, but had better retention than BMP-2 in the collagen matrix. This indicates that *in vivo*, the BMP-2/heparin complex was able to diffuse out of the collagen matrix, but not so quickly as to remove the osteoinductive signal immediately after implantation.

There may have also been the added benefit that the pre-complexed BMP-2/heparin was released from the collagen matrix as a complex, which helped to protect the diffuse BMP-2 molecule from degradation, thereby prolonging and enhancing the

BMP-2 activity *in vivo*. Whereas, the BMP-2 delivered in the collagen/heparin matrix could have been released as BMP-2 only or as a complex with BMP-2, in which case the free BMP-2 will be quickly degraded. However, these possibilities were unclear from *in vitro* release kinetics and confocal analyses. Future studies could focus on determining the release kinetics for this delivery system *in vivo*. Characterization of *in vivo* growth factor release kinetics has previously been achieved using radioiodinated BMP-2 [15, 18, 128, 158]. However, the short half-life of these radiolabels may be a limitation for longer term *in vivo* studies, such as the segmental defect model. These radiolabels also involve exposing animals to ionizing radiation, which may have a negative effect on healing processes [211]. Other research has focused on developing noninvasive optical imaging techniques to track release of growth factors *in vivo* [212, 213]. A novel method was developed by Diagaradjane, et al. to track EGF *in vivo* using near-infrared quantum dots (QD) [213]. This group conjugated amine-functionalized QD to the EGF and performed *in vivo* optical imaging using an IVIS imaging system (Caliper Life Sciences, Mountain View, CA, USA) [213]. Analysis of the BMP-2 release kinetics *in vivo* may help clarify the results seen in Chapter 5 and provide a more complete assessment of this tissue engineering approach.

Heparin has been shown to have a significant effect on BMP-2 stability, activity, and inhibition [96, 117]. Therefore, the pre-complexed BMP-2/heparin group *in vivo* may have had the advantage of enhancing the BMP-2 binding to its receptor and protecting it from degradation thereby increasing its osteoinductive activity. This benefit of co-delivering BMP-2 and heparin may be beneficial in other carriers that have shown success in bone repair applications, such as the RGD-alginate hydrogel carrier previously

used by Kolambkar, et al. [195]. Another possible application of this co-delivery approach in order to stabilize and improve BMP-2 activity, is to use synthetic heparin-like molecules that don't have the same side effects of heparin [214]. Antibody-binding systems have also been used to retain and stabilize growth factors at the defect site [113].

Collagen concentration is an important design parameter that can improve the performance of BMP-2 delivery and therefore should also be examined *in vivo* [5]. As previously stated, the *in vivo* environment is very different from the controlled *in vitro* environment. Therefore a higher concentration of collagen may be necessary for *in vivo* applications to ensure matrix integrity upon implantation and prevent immediate solubilization of matrix molecules. The structural integrity of collagen sponges have been a concern previously, without a viable solution thus far [11]. The basis of this delivery system depends on the integrity of the matrix over time. The heparinized matrix may have had more of an effect if the matrix was degraded slower *in vivo*, reducing the solubilization of heparin. Research done by Uludag, et al. demonstrated previously that different preparations of collagen sponges changed the *in vivo* BMP-2 release kinetics [18].

This delivery system is not limited to applications for BMP-2. Enhanced growth factor activity is possible with use of any heparin-binding growth factor, such as VEGF and bFGF [26, 175]. However, characterization of the co-delivery with heparin specific to the growth factor of interest will be necessary due to the differing affinities for heparin among growth factors. For example, VEGF is mainly soluble and only binds heparin with low affinity, while BMP-2 binds heparin with high affinity [60]. This could result in different potential activity of VEGF with the heparin system than with BMP-2.

Previous work has attempted to correlate mechanical properties to bone volume in order to develop a method of estimating stiffness and maximum torque from *in vivo* or *in vitro* micro-CT scans and found that strong correlations with max torque depended on meeting a certain minimum bone volume [190]. Other work performed by Reynolds, et al. developed a method to correlate micro-CT measurements with biomechanical properties in order to assess the performance of autografts and allografts [74, 77]. The work in this thesis was able to demonstrate correlations between mineral matrix characteristics measured with the micro-CT and mechanical properties. Although the overall bone volumes and connectivity densities were not largely different between groups, these correlations varied with each treatment, indicating differences in matrix organization, which contributes to the mechanical properties. Future work could focus on examining the relationships between the matrix organization and material properties during fracture healing in order to assess remodeling of regenerated tissue into mature bone. Histological stains have been used previously to assess matrix composition and organization to determine mature bone formation [61, 62]. FT-IR imaging and spectroscopy have also been utilized to analyze matrix composition [41]. However, these techniques are semi-quantitative, destructive, and do not allow for the direct comparisons of bone matrix organization to biomechanical properties within the same samples. Developing a non-invasive quantitative CT method to assess fracture healing may prove to be clinically beneficial to identify patients with poor restoration of mechanical properties and are at risk for re-fracture.

6.5 Conclusions

Tissue engineering approaches involving growth factors have demonstrated significant potential because of their highly specific activity and ability to induce a variety of cell functions that are vital to tissue repair. The work in this thesis was performed to address some of the limitations currently preventing optimal performance of protein therapies, including stability, duration of exposure, and localization at the treatment site. We evaluated two approaches for the delivery of BMP-2. First, we examined the sustained release of BMP-2 from a lipid microtube system and demonstrated that this delivery approach was not significantly advantageous compared to a bolus dose of BMP-2 *in vitro*. Next, we developed and evaluated an affinity-based BMP-2 delivery system employing the binding affinity of heparin. We demonstrated that this heparinized collagen system improved BMP-2 retention and bioactivity *in vitro*; therefore we decided to validate this system in a small animal model. The *in vivo* results demonstrated a benefit when BMP-2 and heparin were pre-complexed and delivered in the collagen matrix, resulting in bone formation with mechanical properties not significantly different from those of intact bone. These results indicate that co-delivery of BMP-2 and heparin potentiates bone repair. Therefore, further consideration of systems with co-delivery of BMP-2 and heparin may result in a potential graft substitute treatment for clinically challenging bone defects.

APPENDIX A

FORMATION OF LIPID MICROTUBES

Purpose:

To form microtubes from $DC_{8,9}PC$ lipid for growth factor sustained delivery experiments. Procedure adapted from Meilander, et al. [120].

Materials:

1) 1,2-bis(tricosa-10,12-diyonyl)-sn-3-phosphocholine (powder, $DC_{8,9}PC$, Avanti Polar Lipids, Alabaster, AL, USA)
2) Trehalose cryoprotectant (Sigma, St. Louis, MO, USA)
3) 100% ethanol
4) sterile deionized water
5) 15ml conical tubes
6) Microprocessor-controlled refrigerated water bath (Isotemp Refrigerated Circulator, Fisher Scientific, Waltham, MA, USA)

Procedure:

1) Preheat water bath to 55°C
2) In separate 15 ml conical tubes, warm 7 ml of 100% ethanol and 3 ml sterile water to 55°C
3) Dissolve 10 mg lipid in the 7 ml of warm ethanol
4) Slowly add the water to the lipid/ethanol solution and discard the empty water tube
5) Place the lipid solution in the warm water bath
6) Use the following program to slowly cool the lipid solution in the water bath (total running time of 48 hours)

Table A.1 Cooling program for lipid microtube formation

Step	Start Temp (°C)	End Temp (°C)	Interval time (hours)
1	55	53	5
2	53	23	20
3	23	21	6
4	21	33	2
5	33	32	2
6	32	25	6
7*	25	20	7

*Program can be ended at any time during the last 7 hours (step 7)

7) Remove the 15 ml conical containing the lipid solution from the water bath
8) Incubate the lipid solution for two weeks at room temperature protected from light to allow the microtubes to completely form
9) Add 50mM trehalose (189mg/10ml) to the lipid solution and mix gently. Incubate overnight at room temperature
10) Centrifuge the lipid microtubes for 10 min at 1500*g*, remove the supernatant
11) Resuspend the microtubes in 0.5 ml sterile water
12) Lyophilize the microtubes for several hours until dry
13) Load the microtubes by rehydrating the dried microtubes in the protein solution of interest (40µl per mg of lipid) and incubate overnight at 8°C.
14) Centrifuge the protein-loaded lipid microtubes for 10 min at 1500*g* and remove the supernatant
15) Wash the microtubes with 0.5 ml sterile water twice, centrifuging and removing the supernatant after each wash

APPENDIX B

SELECTION OF MEDIA COMPONENTS FOR BMP-2 MEDIATED DIFFERENTIATION IN hMSCs

Purpose:

To determine the components of the cell culture media supplements in order to observe BMP-2 mediated differentiation of hMSCs. This includes determining the effect of dexamethasone and thyroxine on BMP-2 mediated differentiation.

Materials and Methods:

Cells were expanded and differentiated as described in Chapter 3. Media supplements are listed in **Table B.1**. RNA was isolated from cell layers and analyzed with quantitative real-time RT-PCR as described in Chapter 3.

Table B.1 Experimental groups to determine media supplements for analysis of BMP-2 mediated differentiation

Groups	Dex (nM) / Thyroxine (ng/ml)	BMP-2 (ng/ml)
1	--	--
2	--	100
3	1 / 50	--
4	1 / 50	100

Data are presented is the mean ± standard error of the mean (SEM). Statistical comparisons using Prism 5 software (GraphPad Software, Inc., San Diego, CA, USA) were based on an ANOVA and Tukey's *post hoc* analysis for pairwise comparison of three or more groups within each time point. P-value < 0.05 was considered statistically significant.

Results:

The addition of dexamethasone & thyroxine seemed to have a saturation effect on the cells, causing the groups without BMP-2 to express high levels of osteogenic genes(**Figure B.1)**. This resulted in no significant differences occurring between groups with or without BMP-2 when dexamethasone and thyroxine were included in the differentiation media. However, when dexamethasone and thyroxine were excluded from the media there were significant differences in gene expression between groups with or without BMP-2.

Conclusions:

Reducing the levels of media supplements that may encourage osteogenic differentiation allows for clearer evaluation of BMP-2 mediated differentiation. BMP-2 alone has been shown to have a greater effect on differentiation over dexamethasone [125]. In this experiment the addition of dexamethasone and thyroxine appeared to mask the differentiation effects of BMP-2.

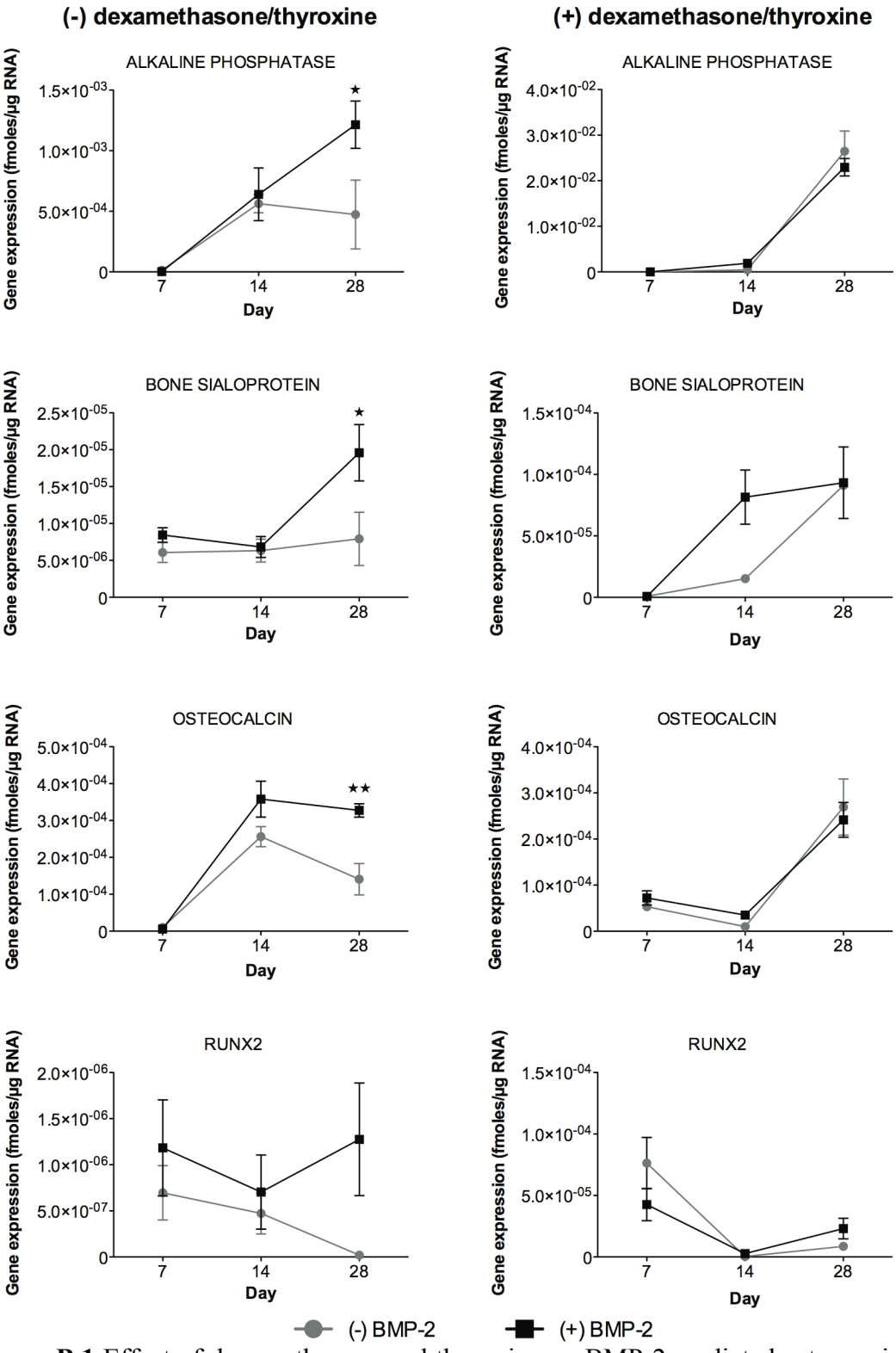

Figure B.1 Effect of dexamethasone and thyroxine on BMP-2 mediated osteogenic gene expression was assessed by real time RT-PCR analysis of osteoblastic markers including alkaline phosphatase (ALP), bone sialoprotein (BSP), osteocalcin (OCN), and Runx2. ★ $p<0.05$ and ★★ $p<0.01$ compared to (-) BMP-2.

APPENDIX C

BMP-2 DOSE RESPONSE OF OSTEOGENIC DIFFERENTIATION IN hMSCs

Purpose:

The purpose of this study was to determine the effects of dose and kinetics of BMP-2 exposure on osteogenic differentiation of hMSCs *in vitro*. First, determine the minimum dose of BMP-2 to induce osteogenic differentiation of hMSCs *in vitro*. Second, determine the effect of different durations of BMP-2 exposure on hMSC differentiation *in vitro*.

Materials and Methods:

Cells were expanded and differentiated as described in Chapter 3. RNA was isolated from cell layers and analyzed with quantitative real-time RT-PCR as described in Chapter 3.

Results:

In order to understand the differences seen between bolus delivery of BMP-2 and sustained release of BMP-2 in Chapter 3, the dose of BMP-2 was varied in cell culture media and the response was measured using RT-PCR. The dose requirement was examined by exposing hMSCs to different concentrations of BMP-2 for the entire duration of the 28 days in culture. The data indicate that osteogenic differentiation of hMSCs requires delivery of a minimum dose of 25 ng/ml BMP-2 (**Figure C.1**). The lowest dose (1 ng/ml) only increased Runx2 expression after 28 days, however remained lower than the other BMP-2 groups.

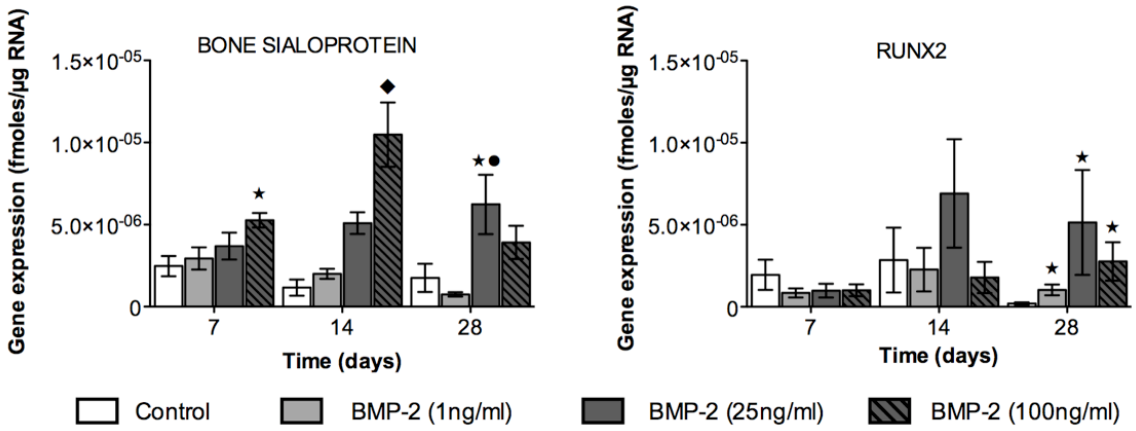

Figure C.1 BMP-2 dose response of osteogenic gene expression assessed by real time RT-PCR analysis of osteoblastic markers bone sialoprotein and Runx2. $p<0.05$: ★ compared to control, • compared to BMP-2 (1 ng/ml), ◆ compared to all groups.

Conclusions:

In this study we showed that a dose greater than 25 ng/ml is required to induce a significant osteogenic response in hMSCs in vitro. Other *in vitro* assays have demonstrated that BMP-2 only induces a significant cell response at doses above 10-25 ng/ml [91, 215, 216]. The lipid microtube system presented in Chapter 3 releases in incremental doses smaller than 25 ng/ml. Therefore, the sustained release of low dose BMP-2 may not be beneficial for bone tissue engineering. Previous work has shown that BMP-2 activity *in vivo* may be more beneficial with a larger initial dose rather than small, continuous doses [16, 100].

APPENDIX D

OPTIMIZATION OF CONFOCAL MICROSCOPE PARAMETERS FOR THE QUANTIFICATION OF FITC-LABELED BMP-2

Purpose:

Tissue engineering requires careful and deliberate selections of materials and biological agents to induce the desired effect. This choice and optimization of materials highly depends on sensitive and repeatable quantitative methods to measure the performance. Imaging techniques have a tremendous potential to help develop and improve tissue engineering strategies. Therefore, it is imperative to develop accurate and rapid imaging methods to understand the overall performance of tissue engineering approaches. Confocal miscrocopy and other characterization techniques have been used previously to determine protein content on two-dimensional, fixed samples [185, 217]. However, most tissue engineering constructs are three-dimensional and will require assessment in all spatial dimensions. This study focused on developing a simple and rapid protocol using confocal laser scanning microscopy (CLSM) for quantifying and analyzing protein content in 3D constructs.

Procedure:

Table D.1 Confocal microscope image capture parameters

Scan Mode	Plane, multi track, 8 bit
Stack Size	512 x 512, 912.4 μm x 921.4 μm
Pixel Time	1.6 μs
Objective	A-Plan 10x/0.25 PH1
Wavelength	488 nm
Pinhole	226 μm

Results:

FITC-labeled BMP-2 was placed on microscope slides with glass coverslips (size 1) at increasing concentrations and imaged on a CLSM. The images were analyzed using the LSM 510 image software (Zeiss, Inc., Thornwood, NY). The first method used to determine levels of background signal at increasing concentrations of fluorescent protein, was to quantify the total fluorescent area at different image threshold levels (**Figure D.2A**). At threshold levels below 30 the total area was nearly equivalent to the total area of the image slice (~1 mm^2, areas corresponding to thresholds below 20 were excluded from Figure D.2A). This indicates that the fluorescent signal intensity is well above a threshold of 30.

Another method of determining background levels in CLSM images is to quantify the coefficient of variance (CV), also known as the signal-to-noise ratio (**Figure D.3**). This value is defined as the ratio of the standard deviation (σ) to the mean fluorescent intensity (μ) of a population of pixels [218]. The CV is only defined for non-zero means and generally only for populations with positive values. In general, a lower CV (<1) corresponds to a system with low background signals and good resolution. Therefore, an image threshold level that results in lower CV values is optimal.

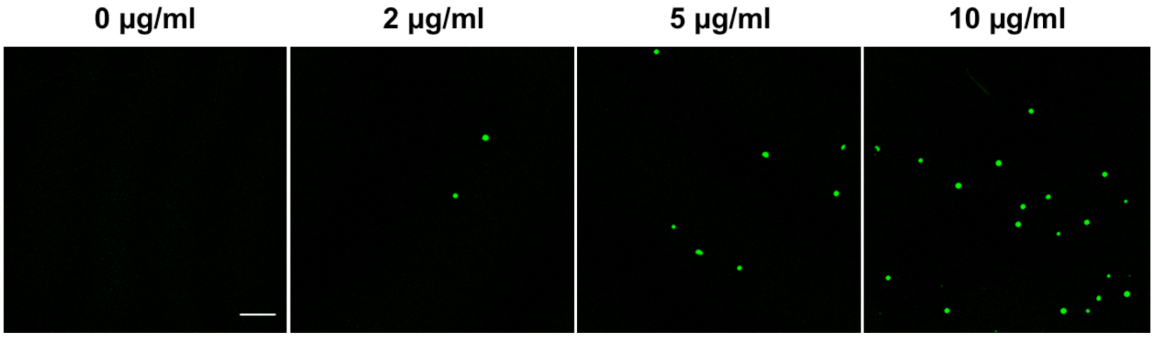

Figure D.1 Confocal microscope image of FITC-labeled BMP-2 standards. Scale bar = 100µm

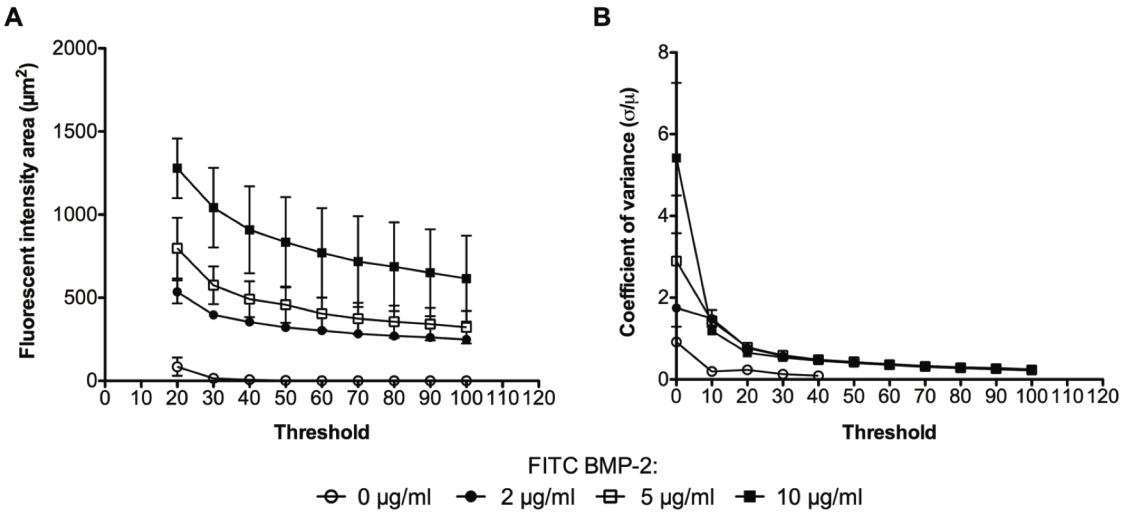

Figure D.2 Quantification of FITC-labeled BMP-2 standards using confocal microscopy **(A)** Fluorescent area (μm^2) at different fluorescent thresholds (values at thresholds less than 20 were excluded from the graph); **(B)** Quantification of the coefficient of variance (σ/μ) at different fluorescent thresholds; (n=3).

A threshold level of 50 was chosen to reduce the overall amount of background signal, while also ensuring no actual fluorescent signal was excluded. The fluorescent intensity area at threshold 50 was linearly correlated to the concentration of FITC-labeled protein (R^2 = 0.9604, **Figure D.3**). Lower threshold values resulted in weaker correlations (i.e. at threshold 10, R^2 = 0.2592). A line was fit to the correlating fluorescent intensity and FITC concentration data to be used in future studies to approximate the amount of BMP-2 in 3D scaffolds from CLSM images.

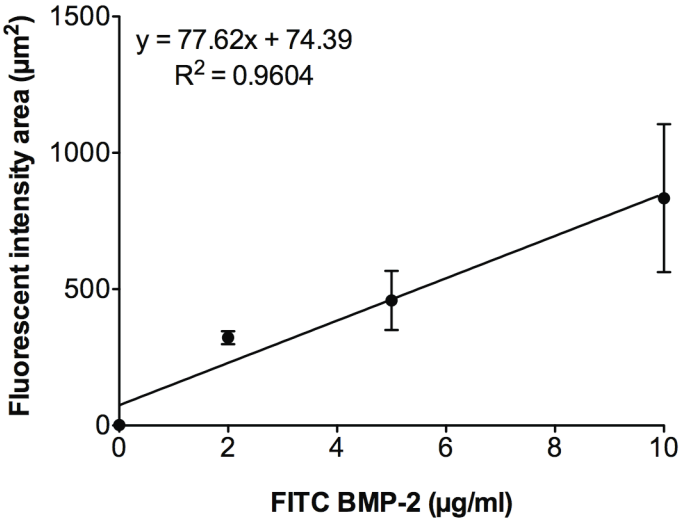

Figure D.3 Standard curve correlating FITC-labeled BMP-2 concentration (µg/ml) to fluorescent area (μm^2) at a threshold of 50 (n=3).

Conclusions:

The purpose of this experiment was to develop a protocol for the quantification of fluorescent signals from FITC-labeled BMP-2 using confocal laser scanning microscopy [219]. It was determined that a threshold value of 50 reduced the amount of background noise, while also not excluding the actual FITC signals. Lower threshold levels resulted in large amounts of background signal included in the calculations, and higher threshold levels resulted in much of the FITC-labeled protein excluded from the calculations. These methods utilize tools commonly available on confocal microscopes and can be applied to different types of fluorescently labeled proteins [220].

REFERENCES

1. Borrelli, J., W.D. Prickett, and W.M. Ricci, *Treatment of nonunions and osseous defects with bone graft and calcium sulfate.* Clin Orthop Relat Res, 2003(411): p. 245-54.

2. Carano, R.A. and E.H. Filvaroff, *Angiogenesis and bone repair.* Drug Discov Today, 2003. **8**(21): p. 980-9.

3. Hollinger, J.O., H. Uludag, and S.R. Winn, *Sustained release emphasizing recombinant human bone morphogenetic protein-2.* Adv Drug Deliv Rev, 1998. **31**(3): p. 303-318.

4. Soucacos, P.N., E.O. Johnson, and G. Babis, *An update on recent advances in bone regeneration.* Injury, 2008. **39 Suppl 2**: p. S1-4.

5. Geiger, M., R.H. Li, and W. Friess, *Collagen sponges for bone regeneration with rhBMP-2.* Adv Drug Deliv Rev, 2003. **55**(12): p. 1613-29.

6. Boden, S.D., *The ABCs of BMPs.* Orthop Nurs, 2005. **24**(1): p. 49-52.

7. Drosse, I., et al., *Tissue engineering for bone defect healing: an update on a multi-component approach.* Injury, 2008. **39 Suppl 2**: p. S9-20.

8. Boontheekul, T. and D.J. Mooney, *Protein-based signaling systems in tissue engineering.* Curr Opin Biotechnol, 2003. **14**(5): p. 559-65.

9. Lee, S.J., *Cytokine delivery and tissue engineering.* Yonsei Med J, 2000.

10. Tabata, Y., *Tissue regeneration based on growth factor release.* Tissue Eng, 2003. **9 Suppl 1**: p. S5-15.

11. Ohba, S., F. Yano, and U. Chung, *Tissue Engineering of Bone and Cartilage.* IBMS BoneKEy, 2009. **6**(11): p. 405-419.

12. Lysaght, M., A. Jaklenec, and E. Deweerd, *Great Expectations: Private Sector Activity in Tissue Engineering, Regenerative Medicine, and Stem Cell Therapeutics.* Tissue Engineering Part A, 2008. **14**(2): p. 305-315.

13. Trommelmans, L., J. Selling, and K. Dierickx, *Ethical reflections on clinical trials with human tissue engineered products.* Journal of medical ethics, 2008. **34**(9): p. e1.

14. Lysaght, M.J. and J. Reyes, *The growth of tissue engineering.* Tissue Eng, 2001. **7**(5): p. 485-93.

15. Friess, W., et al., *Characterization of absorbable collagen sponges as rhBMP-2 carriers.* Int J Pharm, 1999. **187**(1): p. 91-9.

16. Uludag, H., et al., *Implantation of recombinant human bone morphogenetic proteins with biomaterial carriers: A correlation between protein pharmacokinetics and osteoinduction in the rat ectopic model.* J Biomed Mater Res, 2000. **50**(2): p. 227-38.

17. Lin, H., et al., *The effect of crosslinking heparin to demineralized bone matrix on mechanical strength and specific binding to human bone morphogenetic protein-2.* Biomaterials, 2008. **29**(9): p. 1189-1197.

18. Uludag, H., et al., *Delivery systems for BMPs: factors contributing to protein retention at an application site.* J Bone Joint Surg, 2001. **83-A Suppl 1**(Pt 2): p. S128-35.

19. Patel, Z.S., et al., *Biodegradable gelatin microparticles as delivery systems for the controlled release of bone morphogenetic protein-2.* Acta biomaterialia, 2008.

20. von Walter, M., et al., *Biomimetic modification of the TiO(2)/glass composite Ecopore with heparinized collagen and the osteoinductive factor BMP-2.* Acta Biomater, 2008. **4**(4): p. 997-1004.

21. Visser, R., et al., *The effect of an rhBMP-2 absorbable collagen sponge-targeted system on bone formation in vivo.* Biomaterials, 2009. **30**(11): p. 2032-2037.

22. Kempen, D., et al., *Retention of in vitro and in vivo BMP-2 bioactivities in sustained delivery vehicles for bone tissue engineering.* Biomaterials, 2008. **29**(22): p. 3245-3252.

23. Panyam, J. and V. Labhasetwar, *Biodegradable nanoparticles for drug and gene delivery to cells and tissue.* Adv Drug Deliv Rev, 2003. **55**(3): p. 329-47.

24. Yi, F., H. Wu, and G.L. Jia, *Formulation and characterization of poly (d, l-lactide-co-glycolide) nanoparticle containing ....* Journal of Clinical Pharmacy & Therapeutics, 2006.

25. Chen, F.M., et al., *Release of bioactive BMP from dextran-derived microspheres: a novel delivery concept.* International journal of pharmaceutics, 2006. **307**(1): p. 23-32.

26. Shen, Y.H., M.S. Shoichet, and M. Radisic, *Vascular endothelial growth factor immobilized in collagen scaffold promotes penetration and proliferation of endothelial cells.* Acta Biomater, 2008. **4**(3): p. 477-89.

27. Wissink, M.J., et al., *Improved endothelialization of vascular grafts by local release of growth factor from heparinized collagen matrices.* Journal of Controlled Release, 2000. **64**(1-3): p. 103-14.

28. DeLong, S.A., J.J. Moon, and J.L. West, *Covalently immobilized gradients of bFGF on hydrogel scaffolds for directed cell migration.* Biomaterials, 2005. **26**(16): p. 3227-34.

29. Osmond, R.I., et al., *Protein-heparin interactions measured by BIAcore 2000 are affected by the method of heparin immobilization.* Anal Biochem, 2002. **310**(2): p. 199-207.

30. Robling, A., A. Castillo, and C. Turner, *BIOMECHANICAL AND MOLECULAR REGULATION OF BONE REMODELING.* Annu. Rev. Biomed. Eng., 2006. **8**(1): p. 455-498.

31. Allori, A.C., A.M. Sailon, and S.M. Warren, *Biological Basis of Bone Formation, Remodeling, and Repair—Part II: Extracellular Matrix.* Tissue Engineering Part B: Reviews, 2008. **14**(3): p. 275-283.

32. Hopwood, B., et al., *Microarray gene expression profiling of osteoarthritic bone suggests altered bone remodelling, WNT and transforming growth factor-beta/bone morphogenic protein signalling.* Arthritis Res Ther, 2007. **9**(5): p. R100.

33. Bostrom, M.P., *Expression of bone morphogenetic proteins in fracture healing.* Clin Orthop Relat Res, 1998(355 Suppl): p. S116-23.

34. Einhorn, T.A., *Enhancement of fracture-healing.* The Journal of Bone and Joint Surgery, 1995. **77**(6): p. 940-56.

35. Sciadini, M.F., et al., *Growth factor modulation of distraction osteogenesis in a segmental defect model.* Clin Orthop Relat Res, 2000(381): p. 266-77.

36. Boerckel, J.D., et al., *In vivo model for evaluating the effects of mechanical stimulation on tissue-engineered bone repair.* Journal of biomechanical engineering, 2009. **131**(8): p. 084502.

37. Nagaraja, S., T.L. Couse, and R.E. Guldberg, *Trabecular bone microdamage and microstructural stresses under uniaxial compression.* Journal of biomechanics, 2005. **38**(4): p. 707-16.

38. Long, M.W., *Osteogenesis and bone-marrow-derived cells.* Blood Cells Mol Dis, 2001. **27**(3): p. 677-90.

39. Allori, A.C., A.M. Sailon, and S.M. Warren, *Biological basis of bone formation, remodeling, and repair-part I: biochemical signaling molecules.* Tissue engineering Part B, Reviews, 2008. **14**(3): p. 259-73.

40. Allori, A.C., et al., *Biological Basis of Bone Formation, Remodeling, and Repair—Part III: Biomechanical Forces.* Tissue Engineering Part B: Reviews, 2008. **14**(3): p. 285-293.

41. Boskey, A. and N. Pleshko Camacho, *FT-IR imaging of native and tissue-engineered bone and cartilage.* Biomaterials, 2007. **28**(15): p. 2465-78.

42. Hunziker, E., et al., *Translation from research to applications.* Tissue Eng, 2006. **12**(12): p. 3341-64.

43. Hernandez, C.J., et al., *Trabecular microfracture and the influence of pyridinium and non-enzymatic glycation-mediated collagen cross-links.* Bone, 2005. **37**(6): p. 825-32.

44. Cheng, H., et al., *Osteogenic activity of the fourteen types of human bone morphogenetic proteins (BMPs).* The Journal of Bone and Joint Surgery, 2003. **85-A**(8): p. 1544-52.

45. Gerstenfeld, L.C., et al., *Fracture healing as a post-natal developmental process: molecular, spatial, and temporal aspects of its regulation.* J Cell Biochem, 2003. **88**(5): p. 873-84.

46. Shirley, D., et al., *Systemic recruitment of osteoblastic cells in fracture healing.* J Orthop Res, 2005. **23**(5): p. 1013-21.

47. Bostrom, M.P. and N.P. Camacho, *Potential role of bone morphogenetic proteins in fracture healing.* Clin Orthop Relat Res, 1998(355 Suppl): p. S274-82.

48. Kugimiya, F., et al., *Involvement of endogenous bone morphogenetic protein (BMP) 2 and BMP6 in bone formation.* J Biol Chem, 2005. **280**(42): p. 35704-12.

49. Gerstenfeld, L.C., et al., *Chondrocytes provide morphogenic signals that selectively induce osteogenic differentiation of mesenchymal stem cells.* J Bone Miner Res, 2002. **17**(2): p. 221-30.

50. Gerber, H. and N. Ferrara, *Angiogenesis and Bone Growth.* Trends in Cardiovascular Medicine, 2000. **10**: p. 223-228.

51. Street, J., et al., *Vascular endothelial growth factor stimulates bone repair by promoting angiogenesis and bone turnover.* Proc Natl Acad Sci USA, 2002. **99**(15): p. 9656-61.

52. Carvalho, R.S., et al., *The role of angiogenesis in a murine tibial model of distraction osteogenesis.* Bone, 2004. **34**(5): p. 849-61.

53. Hausman, M.R., M.B. Schaffler, and R.J. Majeska, *Prevention of fracture healing in rats by an inhibitor of angiogenesis.* Bone, 2001. **29**(6): p. 560-4.

54. Huang, Y.C., et al., *Combined angiogenic and osteogenic factor delivery enhances bone marrow stromal cell-driven bone regeneration.* J Bone Miner Res, 2005. **20**(5): p. 848-57.

55. Deckers, M.M., et al., *Bone morphogenetic proteins stimulate angiogenesis through osteoblast-derived vascular endothelial growth factor A.* Endocrinology, 2002. **143**(4): p. 1545-53.

56. Ferrara, N., *Vascular endothelial growth factor: basic science and clinical progress.* Endocr Rev, 2004. **25**(4): p. 581-611.

57. Isner, J.M., *Vascular endothelial growth factor: gene therapy and therapeutic angiogenesis.* Am J Cardiol, 1998. **82**(10A): p. 63S-64S.

58. Kleinheinz, J., et al., *VEGF-activated angiogenesis during bone regeneration.* J Oral Maxillofac Surg, 2005. **63**(9): p. 1310-6.

59. Carmeliet, P., *Mechanisms of angiogenesis and arteriogenesis.* Nat Med, 2000. **6**(4): p. 389-95.

60. Soker, S., M. Machado, and A. Atala, *Systems for therapeutic angiogenesis in tissue engineering.* World journal of urology, 2000. **18**(1): p. 10-8.

61. Le, A.X., et al., *Molecular aspects of healing in stabilized and non-stabilized fractures.* J Orthop Res, 2001. **19**(1): p. 78-84.

62. Palomares, K.T., et al., *Mechanical stimulation alters tissue differentiation and molecular expression during bone healing.* J Orthop Res, 2009. **27**(9): p. 1123-32.

63. Epari, D.R., et al., *Instability prolongs the chondral phase during bone healing in sheep.* Bone, 2006. **38**(6): p. 864-70.

64. Tsiridis, E., N. Upadhyay, and P. Giannoudis, *Molecular aspects of fracture healing: which are the important molecules?* Injury, 2007. **38 Suppl 1**: p. S11-25.

65. Matsubara, T., et al., *BMP2 regulates Osterix through Msx2 and Runx2 during osteoblast differentiation.* J Biol Chem, 2008. **283**(43): p. 29119-25.

66. Lee, K.S., et al., *Runx2 is a common target of transforming growth factor beta1 and bone morphogenetic protein 2, and cooperation between Runx2 and Smad5 induces osteoblast-specific gene expression in the pluripotent mesenchymal precursor cell line C2C12.* Mol Cell Biol, 2000. **20**(23): p. 8783-92.

67. Nakashima, K., et al., *The novel zinc finger-containing transcription factor osterix is required for osteoblast differentiation and bone formation.* Cell, 2002. **108**(1): p. 17-29.

68. Komori, T., et al., *Targeted disruption of Cbfa1 results in a complete lack of bone formation owing to maturational arrest of osteoblasts.* Cell, 1997. **89**(5): p. 755-64.

69. Tsuji, K., et al., *BMP2 activity, although dispensable for bone formation, is required for the initiation of fracture healing.* Nat Genet, 2006. **38**(12): p. 1424-9.

70. Schmidmaier, G. and B. Wildemann, *The Role of BMPs in Current Orthopedic Practice.* IBMS BoneKEy, 2009. **6**(7): p. 244-253.

71. Suzuki, A., et al., *A biodegradable delivery system for antibiotics and recombinant human bone morphogenetic protein-2: A potential treatment for infected bone defects.* J Orthop Res, 2006. **24**(3): p. 327-32.

72. Govender, S., et al., *Recombinant human bone morphogenetic protein-2 for treatment of open tibial fractures: a prospective, controlled, randomized study of four hundred and fifty patients.* The Journal of Bone and Joint Surgery, 2002. **84-A**(12): p. 2123-34.

73. Burwell, R.G., *STUDIES IN THE TRANSPLANTATION OF BONE VII. The Fresh Composite Homograft-Autograft of Cancellous ....* Journal of Bone & Joint Surgery, 1964.

74. Xie, C., et al., *Structural bone allograft combined with genetically engineered mesenchymal stem cells as a novel platform for bone tissue engineering.* Tissue Eng, 2007. **13**(3): p. 435-45.

75. Salgado, A.J., O.P. Coutinho, and R.L. Reis, *Bone tissue engineering: state of the art and future trends.* Macromolecular bioscience, 2004. **4**(8): p. 743-65.

76. Tilley, S., et al., *Taking tissue-engineering principles into theater: augmentation of impacted allograft with human bone marrow stromal cells.* Regenerative medicine, 2006. **1**(5): p. 685-92.

77. Reynolds, D.G., et al., *muCT-based measurement of cortical bone graft-to-host union.* J Bone Miner Res, 2009. **24**(5): p. 899-907.

78. Stock, U.A. and J.P. Vacanti, *Tissue engineering: current state and prospects.* Annu Rev Med, 2001. **52**: p. 443-51.

79. Burkus, J.K., J.D. Dorchak, and D.L. Sanders, *Radiographic assessment of interbody fusion using recombinant human bone morphogenetic protein type 2.* Spine, 2003. **28**(4): p. 372-7.

80. Warnke, P.H., et al., *Man as living bioreactor: fate of an exogenously prepared customized tissue-engineered mandible.* Biomaterials, 2006. **27**(17): p. 3163-7.

81. Singh, K., et al., *Use of recombinant human bone morphogenetic protein-2 as an adjunct in posterolateral lumbar spine fusion: a prospective CT-scan analysis at one and two years.* Journal of spinal disorders & techniques, 2006. **19**(6): p. 416-23.

82. Oest, M.E., et al., *Quantitative assessment of scaffold and growth factor-mediated repair of critically sized bone defects.* J Orthop Res, 2007. **25**(7): p. 941-50.

83. Lieberman, J.R., A. Daluiski, and T.A. Einhorn, *The Role of Growth Factors in the Repair of Bone Biology and Clinical Applications.* The Journal of Bone and Joint Surgery, 2002.

84. Riley, E.H., et al., *Bone morphogenetic protein-2: biology and applications.* Clin Orthop Relat Res, 1996.

85. Wozney, J.M., *Bone morphogenetic proteins.* Prog Growth Factor Res, 1989. **1**(4): p. 267-80.

86. Kloen, P., et al., *BMP signaling components are expressed in human fracture callus.* Bone, 2003. **33**(3): p. 362-71.

87. Sotobori, T., et al., *Bone morphogenetic protein-2 promotes the haptotactic migration of murine osteoblastic and osteosarcoma cells by enhancing incorporation of integrin beta1 into lipid rafts.* Exp Cell Res, 2006. **312**(19): p. 3927-38.

88. Lai, T., et al., *Osteoblasts-derived BMP-2 enhances the motility of prostate cancer cells via activation of integrins.* Prostate, 2008. **68**(12): p. 1341-1353.

89. Seib, F.P., et al., *Endogenous bone morphogenetic proteins in human bone marrow-derived multipotent mesenchymal stromal cells.* Eur J Cell Biol, 2009. **88**(5): p. 257-71.

90. Bishop, G.B. and T.A. Einhorn, *Current and future clinical applications of bone morphogenetic proteins in orthopaedic trauma surgery.* International orthopaedics, 2007. **31**(6): p. 721-7.

91. Yano, K., et al., *Osteoinductive capacity and heat stability of recombinant human bone morphogenetic protein-2 produced by Escherichia coli and dimerized by biochemical processing.* J Bone Miner Metab, 2009. **27**(3): p. 355-63.

92. Gueorguieva, L., et al., *Discontinuous and continuous separation of the monomeric and dimeric forms of human bone morphogenetic protein-2 from renaturation batches.* J Chromatogr A, 2006. **1135**(2): p. 142-50.

93. Kawabata, M., T. Imamura, and K. Miyazono, *Signal transduction by bone morphogenetic proteins.* Cytokine Growth Factor Rev, 1998.

94. Reddi, A., *Morphogenetic messages are in the extracellular matrix: biotechnology from bench to bedside.* Biochem Soc Trans, 2000.

95. Ruppert, R., E. Hoffmann, and W. Sebald, *Human bone morphogenetic protein 2 contains a heparin-binding site which modifies its biological activity.* Eur J Biochem, 1996. **237**(1): p. 295-302.

96. Zhao, B., et al., *Heparin potentiates the in vivo ectopic bone formation induced by bone morphogenetic protein-2.* J Biol Chem, 2006. **281**(32): p. 23246-53.

97. Groeneveld, E.H. and E.H. Burger, *Bone morphogenetic proteins in human bone regeneration.* Eur J Endocrinol, 2000. **142**(1): p. 9-21.

98. Medtronic-SofamorDanek. *FDA Recommends Approval*. 2002; Available from: http://sofamordanek.com/about-press-fda.html.

99. Swiontkowski, M.F., et al., *Recombinant human bone morphogenetic protein-2 in open tibial fractures. A subgroup analysis of data combined from two prospective randomized studies.* The Journal of Bone and Joint Surgery, 2006. **88**(6): p. 1258-65.

100. Li, R.H. and J.M. Wozney, *Delivering on the promise of bone morphogenetic proteins.* Trends Biotechnol, 2001. **19**(7): p. 255-65.

101. Han, D., et al., *Optimal delivery systems for bone morphogenetic proteins in orthopedic applications should model initial tissue repair structures by using a heparin-incorporated fibrin-fibronectin matrix.* Med Hypotheses, 2008. **71**(3): p. 374-8.

102. King, G.N., *The importance of drug delivery to optimize the effects of bone morphogenetic proteins during periodontal regeneration.* Current pharmaceutical biotechnology, 2001. **2**(2): p. 131-42.

103. Cahill, K.S., et al., *Prevalence, complications, and hospital charges associated with use of bone-morphogenetic proteins in spinal fusion procedures.* JAMA, 2009. **302**(1): p. 58-66.

104. Armstrong, D., Burton, T.M., *Medtronic Product Linked to Surgery Problems*, in *Wall Street Journal*. 2008, Dow Jones & Company, Inc.: New York City.

105. Gersbach, C.A., R.E. Guldberg, and A.J. García, *In vitro and in vivo osteoblastic differentiation of BMP-2- and Runx2-engineered skeletal myoblasts.* J Cell Biochem, 2007. **100**(5): p. 1324-36.

106. Hosseinkhani, H., et al., *Enhanced ectopic bone formation using a combination of plasmid DNA impregnation into 3-D scaffold and bioreactor perfusion culture.* Biomaterials, 2006. **27**(8): p. 1387-98.

107. Alsberg, E., et al., *Regulating bone formation via controlled scaffold degradation.* J Dent Res, 2003. **82**(11): p. 903-8.

108. Guldberg, R.E., *Spatiotemporal delivery strategies for promoting musculoskeletal tissue regeneration.* J Bone Miner Res, 2009. **24**(9): p. 1507-11.

109. Stolnik, S. and K. Shakesheff, *Formulations for delivery of therapeutic proteins.* Biotechnol Lett, 2009. **31**(1): p. 1-11.

110. Fan, V.H., et al., *Tethered Epidermal Growth Factor Provides a Survival Advantage to Mesenchymal Stem Cells.* Stem Cells, 2007.

111. Maxwell, D.J., et al., *Development of rationally designed affinity-based drug delivery systems.* Acta biomaterialia, 2005. **1**(1): p. 101-13.

112. Benoit, D.S. and K.S. Anseth, *Heparin functionalized PEG gels that modulate protein adsorption for hMSC adhesion and differentiation.* Acta biomaterialia, 2005. **1**(4): p. 461-70.

113. Zhao, Y., et al., *The osteogenic effect of bone morphogenetic protein-2 on the collagen scaffold conjugated with antibodies.* Journal of controlled release : official journal of the Controlled Release Society, 2009.

114. Sakiyama-Elbert, S.E. and J.A. Hubbell, *Development of fibrin derivatives for controlled release of heparin-binding growth factors.* Journal of controlled release : official journal of the Controlled Release Society, 2000. **65**(3): p. 389-402.

115. Kim, S.E., et al., *Enhancement of ectopic bone formation by bone morphogenetic protein-2 delivery using heparin-conjugated PLGA nanoparticles with transplantation of bone marrow-derived mesenchymal stem cells.* J Biomed Sci, 2008. **15**(6): p. 771-7.

116. Lutolf, M.P. and J.A. Hubbell, *Synthetic biomaterials as instructive extracellular microenvironments for morphogenesis in tissue engineering.* Nat Biotechnol, 2005. **23**(1): p. 47-55.

117. Takada, T., et al., *Sulfated polysaccharides enhance the biological activities of bone morphogenetic proteins.* J Biol Chem, 2003. **278**(44): p. 43229-35.

118. Chew, S.Y., et al., *Sustained release of proteins from electrospun biodegradable fibers.* Biomacromolecules, 2005. **6**(4): p. 2017-24.

119. Wan, A.C., et al., *Encapsulation of biologics in self-assembled fibers as biostructural units for tissue engineering.* Journal of Biomedical Materials Research Part A, 2004. **71**(4): p. 586-95.

120. Meilander, N.J., et al., *Lipid-based microtubular drug delivery vehicles.* Journal of Controlled Release, 2001. **71**(1): p. 141-52.

121. Leach, J.K., et al., *Coating of VEGF-releasing scaffolds with bioactive glass for angiogenesis and bone regeneration.* Biomaterials, 2006. **27**(17): p. 3249-55.

122. Mitragotri, S. and J. Lahann, *Physical approaches to biomaterial design.* Nature Materials, 2009. **8**(1): p. 15-23.

123. Khang, D., et al., *Nanotechnology for regenerative medicine.* Biomedical microdevices, 2008.

124. Oh, S., et al., *Stem cell fate dictated solely by altered nanotube dimension.* Proc Natl Acad Sci USA, 2009. **106**(7): p. 2130-5.

125. Boyan, B.D., et al., *Osteoblast-mediated mineral deposition in culture is dependent on surface microtopography.* Calcif Tissue Int, 2002. **71**(6): p. 519-29.

126. Hamilton, D.W., K.S. Wong, and D.M. Brunette, *Microfabricated discontinuous-edge surface topographies influence osteoblast adhesion, migration, cytoskeletal organization, and proliferation and enhance matrix and mineral deposition in vitro.* Calcif Tissue Int, 2006. **78**(5): p. 314-25.

127. Ohura, K., et al., *Healing of segmental bone defects in rats induced by a beta-TCP-MCPM cement combined with rhBMP-2.* J Biomed Mater Res, 1999. **44**(2): p. 168-75.

128. Bodde, E.W.H., et al., *The kinetic and biological activity of different loaded rhBMP-2 calcium phosphate cement implants in rats.* Journal of Biomedical Materials Research Part A, 2008. **87**(3): p. 780-91.

129. Fu, Y.C., et al., *Optimized bone regeneration based on sustained release from three-dimensional fibrous PLGA/HAp composite scaffolds loaded with BMP-2.* Biotechnol Bioeng, 2007.

130. Chen, R.R. and D.J. Mooney, *Polymeric growth factor delivery strategies for tissue engineering.* Pharm Res, 2003. **20**(8): p. 1103-12.

131. Issa, J.P., et al., *Sustained release carriers used to delivery bone morphogenetic proteins in the bone healing process.* Anatomia, histologia, embryologia, 2008. **37**(3): p. 181-7.

132. Woo, B.H., et al., *Enhancement of bone growth by sustained delivery of recombinant human bone morphogenetic protein-2 in a polymeric matrix.* Pharm Res, 2001. **18**(12): p. 1747-53.

133. Jeon, O., et al., *Long-term delivery enhances in vivo osteogenic efficacy of bone morphogenetic protein-2 compared to short-term delivery.* Biochem Biophys Res Commun, 2008. **369**(2): p. 774-80.

134. Boden, S.D., *The ABCs of BMPs.* Orthopaedic nursing / National Association of Orthopaedic Nurses, 2005. **24**(1): p. 49-52; quiz 53-4.

135. Sakou, T., *Bone morphogenetic proteins: from basic studies to clinical approaches.* Bone, 1998. **22**(6): p. 591-603.

136. Jain, A., et al., *In situ gelling hydrogels for conformal repair of spinal cord defects, and local delivery of BDNF after spinal cord injury.* Biomaterials, 2006. **27**(3): p. 497-504.

137. Spargo, B.J., et al., *Controlled release of transforming growth factor-beta from lipid-based microcylinders.* J Microencapsul, 1995.

138. Yager, P. and P.E. Schoen, *Formation of Tubules by a Polymerizable Surfactant.* Molecular Crystals and Liquid Crystals, 1984.

139. Chappell, J.S. and P. Yager, *Electrolyte effects on bilayer tubule formation by a diacetylenic phospholipid.* Biophys J, 1991. **60**(4): p. 952-65.

140. *Avanti Polar Lipids, Inc.* 2009; Available from: www.avantilipids.com.

141. Xiao, Y., et al., *Development and transplantation of a mineralized matrix formed by osteoblasts in vitro for bone regeneration.* Cell transplantation, 2004. **13**(1): p. 15-25.

142. Phillips, J.E., R.E. Guldberg, and A.J. García, *Dermal fibroblasts genetically modified to express Runx2/Cbfa1 as a mineralizing cell source for bone tissue engineering.* Tissue Eng, 2007. **13**(8): p. 2029-40.

143. Phillips, J.E., et al., *Mineralization capacity of Runx2/Cbfa1-genetically engineered fibroblasts is scaffold dependent.* Biomaterials, 2006. **27**(32): p. 5535-45.

144. Zambaux, M.F., et al., *Influence of experimental parameters on the characteristics of poly(lactic acid) nanoparticles prepared by a double emulsion method.* Journal of Controlled Release, 1998. **50**(1-3): p. 31-40.

145. Chen, X. and C.P. Ooi, *Hydrolytic degradation and drug release properties of ganciclovir-loaded biodegradable microspheres.* Acta biomaterialia, 2008.

146. Birnbaum, D. and L. Brannon-Pepas, *Drug Delivery Systems in Cancer Therapy.* 2003: p. 390.

147. Cohen, H., et al., *Sustained delivery and expression of DNA encapsulated in polymeric nanoparticles.* Gene Ther, 2000. **7**(22): p. 1896-905.

148. Dong, Y. and S.S. Feng, *Poly(D,L-lactide-co-glycolide) (PLGA) nanoparticles prepared by high pressure homogenization for paclitaxel chemotherapy.* International journal of pharmaceutics, 2007. **342**(1-2): p. 208-14.

149. Faisant, N., et al., *Effects of the type of release medium on drug release from PLGA-based microparticles: experiment and theory.* International journal of pharmaceutics, 2006. **314**(2): p. 189-97.

150. Davda, J. and V. Labhasetwar, *Characterization of nanoparticle uptake by endothelial cells.* Int J Pharm, 2002. **233**(1-2): p. 51-9.

151. Qaddoumi, M.G., et al., *The characteristics and mechanisms of uptake of PLGA nanoparticles in rabbit conjunctival epithelial cell layers.* Pharm Res, 2004. **21**(4): p. 641-8.

152. Reddi, A.H., *Bone and cartilage differentiation.* Curr Opin Genet Dev, 1994. **4**(5): p. 737-44.

153. Carlson, P.A., M.H. Gelb, and P. Yager, *Zero-order interfacial enzymatic degradation of phospholipid tubules.* Biophys J, 1997. **73**(1): p. 230-8.

154. Meilander, N.J., et al., *Sustained release of plasmid DNA using lipid microtubules and agarose hydrogel.* Journal of Controlled Release, 2003. **88**(2): p. 321-31.

155. Mikos, A., et al., *Host response to tissue engineered devices.* Adv Drug Deliv Rev, 1998. **33**(1-2): p. 111-139.

156. Johnson, M., et al., *Sustained release of BMP-2 in a lipid-based microtube vehicle.* Acta Biomater, 2008.

157. Puleo, D.A., *Dependence of mesenchymal cell responses on duration of exposure to bone morphogenetic protein-2 in vitro.* J Cell Physiol, 1997. **173**(1): p. 93-101.

158. Uludag, H., et al., *Characterization of rhBMP-2 pharmacokinetics implanted with biomaterial carriers in the rat ectopic model.* J Biomed Mater Res, 1999. **46**(2): p. 193-202.

159. Maeda, H., A. Sano, and K. Fujioka, *Controlled release of rhBMP-2 from collagen minipellet and the relationship between release profile and ectopic bone formation.* Int J Pharm, 2004. **275**(1-2): p. 109-22.

160. Maeda, H., A. Sano, and K. Fujioka, *Profile of rhBMP-2 release from collagen minipellet and induction of ectopic bone formation.* Drug Development and Industrial Pharmacy, 2004. **30**(5): p. 473-80.

161. Ohta, H., et al., *The effects of heat on the biological activity of recombinant human bone morphogenetic protein-2.* J Bone Miner Metab, 2005. **23**(6): p. 420-5.

162. Sampath, T.K., N. Muthukumaran, and A.H. Reddi, *Isolation of osteogenin, an extracellular matrix-associated, bone-inductive protein, by heparin affinity chromatography.* Proc Natl Acad Sci USA, 1987. **84**(20): p. 7109-13.

163. Luong-Van, E., et al., *Controlled release of heparin from poly(epsilon-caprolactone) electrospun fibers.* Biomaterials, 2006. **27**(9): p. 2042-50.

164. Rider, C.C., *Heparin/heparan sulphate binding in the TGF-beta cytokine superfamily.* Biochem Soc Trans, 2006. **34**(Pt 3): p. 458-60.

165. Woodruff, M.A., et al., *Sustained release and osteogenic potential of heparan sulfate-doped fibrin glue scaffolds within a rat cranial model.* J Mol Histol, 2007. **38**(5): p. 425-33.

166. Street, J.T., et al., *Thromboprophylaxis using a low molecular weight heparin delays fracture repair.* Clin Orthop Relat Res, 2000(381): p. 278-89.

167. Hak, D., R. Stewart, and S. Hazelwood, *Effect of low molecular weight heparin on fracture healing in a stabilized rat femur fracture model.* Journal of Orthopaedic Research, 2006. **24**(4).

168. Nelson-Piercy, C., *Heparin-induced osteoporosis.* Scand J Rheumatol Suppl, 1998. **107**: p. 68-71.

169. Weitz, J.I., *Low-molecular-weight heparins.* N Engl J Med, 1997. **337**(10): p. 688-98.

170. Ohkawara, B., et al., *Action range of BMP is defined by its N-terminal basic amino acid core.* Curr Biol, 2002. **12**(3): p. 205-9.

171. Scheufler, C., W. Sebald, and M. Hülsmeyer, *Crystal structure of human bone morphogenetic protein-2 at 2.7 A resolution.* J Mol Biol, 1999. **287**(1): p. 103-15.

172. Prestrelski, S.J., G.M. Fox, and T. Arakawa, *Binding of heparin to basic fibroblast growth factor induces a conformational change.* Arch Biochem Biophys, 1992. **293**(2): p. 314-9.

173. Edlund, U., S. Dånmark, and A.C. Albertsson, *A strategy for the covalent functionalization of resorbable polymers with heparin and osteoinductive growth factor.* Biomacromolecules, 2008. **9**(3): p. 901-5.

174. Liu, H.-W., et al., *Targeted delivery system for juxtacrine signaling growth factor based on rhBMP-2-mediated carrier-protein conjugation.* Bone, 2006. **39**(4): p. 825-36.

175. Somers, P., et al., *Sustained release and activation of the growth factor basic fibroblast growth factor from loaded scaffolds in heart valve tissue engineering.* Growth Factors, 2008. **26**(5): p. 293-9.

176. Chum, Z.Z., et al., *Porcine bone marrow stromal cell differentiation on heparin-adsorbed poly(e-caprolactone)–tricalcium phosphate–collagen scaffolds.* Acta biomaterialia, 2009: p. 1-11.

177. Porter, B.D., et al., *Noninvasive image analysis of 3D construct mineralization in a perfusion bioreactor.* Biomaterials, 2007. **28**(15): p. 2525-33.

178. Peister, A., et al., *Amniotic fluid stem cells produce robust mineral deposits on biodegradable scaffolds.* Tissue Engineering Part A, 2009. **15**(10): p. 3129-38.

179. Cartmell, S., et al., *Quantitative microcomputed tomography analysis of mineralization within three-dimensional scaffolds in vitro.* Journal of Biomedical Materials Research Part A, 2004. **69**(1): p. 97-104.

180. Jiao, X., et al., *Heparan sulfate proteoglycans (HSPGs) modulate BMP2 osteogenic bioactivity in C2C12 cells.* J Biol Chem, 2007. **282**(2): p. 1080-6.

181. Hausser, H.-J. and R.E. Brenner, *Low doses and high doses of heparin have different effects on osteoblast-like Saos-2 cells in vitro.* J Cell Biochem, 2004. **91**(5): p. 1062-73.

182. Kanzaki, S., et al., *Heparin inhibits BMP-2 osteogenic bioactivity by binding to both BMP-2 and BMP receptor.* J Cell Physiol, 2008. **216**(3): p. 844-50.

183. Kuhl, P.R. and L.G. Griffith-Cima, *Tethered epidermal growth factor as a paradigm for growth factor-induced stimulation from the solid phase.* Nat Med, 1996. **2**(9): p. 1022-7.

184. Fan, V.H., et al., *Tethered epidermal growth factor provides a survival advantage to mesenchymal stem cells.* Stem Cells, 2007. **25**(5): p. 1241-51.

185. Togashi, D.M., A.G. Ryder, and G. Heiss, *Quantifying adsorbed protein on surfaces using confocal fluorescence microscopy.* Colloids Surf B Biointerfaces, 2009.

186. Jeon, O., et al., *Enhancement of ectopic bone formation by bone morphogenetic protein-2 released from a heparin-conjugated poly(L-lactic-co-glycolic acid) scaffold.* Biomaterials, 2007. **28**(17): p. 2763-71.

187. Chu, T.M., et al., *Segmental bone regeneration using a load-bearing biodegradable carrier of bone morphogenetic protein-2.* Biomaterials, 2007. **28**(3): p. 459-67.

188. Sciadini, M.F. and K.D. Johnson, *Evaluation of recombinant human bone morphogenetic protein-2 as a bone-graft substitute in a canine segmental defect model.* J Orthop Res, 2000. **18**(2): p. 289-302.

189. Kolambkar, Y. (2009). *Electrospun Nanofiber Meshes for the Repair of Bone Defects* (Doctoral Dissertation). Georgia Institute of Technology, Atlanta, GA.

190. Oest, M. (2007). *Dual Osteogenic and Angiogenic Growth Factor Delivery as a Treatment for Segmental Bone Defects* (Doctoral Dissertation). Georgia Institute of Technology, Atlanta, GA.

191. Case, N.D., et al., *Bone formation on tissue-engineered cartilage constructs in vivo: effects of chondrocyte viability and mechanical loading.* Tissue Eng, 2003. **9**(4): p. 587-96.

192. Rai, B., et al., *Combination of platelet-rich plasma with polycaprolactone-tricalcium phosphate scaffolds for segmental bone defect repair.* Journal of Biomedical Materials Research Part A, 2007. **81**(4): p. 888-99.

193. Turner, C.H. and D.B. Burr, *Basic biomechanical measurements of bone: a tutorial.* Bone, 1993. **14**(4): p. 595-608.

194. Box, G. and D. Cox, *An analysis of transformations.* Journal of the Royal Statistical Society. Series B (Methodological), 1964. **26**(2): p. 211-252.

195. Kolambkar, Y.M., Dupont, K.M., Mooney, D.J., Hutmacher, D.W., Guldberg, R.E. *Effect of Nanofiber Mesh Design on BMP-mediated Segmental Bone Defect Repair*. in *55th Annual Meeting of the Orthopaedic Research Society*. 2009. Las Vegas, NV.

196. Yasko, A.W., et al., *The healing of segmental bone defects, induced by recombinant human bone morphogenetic protein (rhBMP-2). A radiographic, histological, and biomechanical study in rats.* The Journal of Bone and Joint Surgery, 1992. **74**(5): p. 659-70.

197. Odgaard, A. and H.J. Gundersen, *Quantification of connectivity in cancellous bone, with special emphasis on 3-D reconstructions.* Bone, 1993. **14**(2): p. 173-82.

198. Friess, W., *Collagen--biomaterial for drug delivery.* European journal of pharmaceutics and biopharmaceutics, 1998. **45**(2): p. 113-36.

199. Rizzi, S.C., et al., *Recombinant protein-co-PEG networks as cell-adhesive and proteolytically degradable hydrogel matrixes. Part II: biofunctional characteristics.* Biomacromolecules, 2006. **7**(11): p. 3019-29.

200. Lutolf, M.P., et al., *Repair of bone defects using synthetic mimetics of collagenous extracellular matrices.* Nat Biotechnol, 2003. **21**(5): p. 513-8.

201. Winn, S.R., H. Uludag, and J.O. Hollinger, *Carrier systems for bone morphogenetic proteins.* Clin Orthop Relat Res, 1999(367 Suppl): p. S95-106.

202. Yang, L.J. and Y. Jin, *Immunohistochemical observations on bone morphogenetic protein in normal and abnormal conditions.* Clin Orthop Relat Res, 1990(257): p. 249-56.

203. Huang, W., et al., *BMP-2 exerts differential effects on differentiation of rabbit bone marrow stromal cells grown in two-dimensional and three-dimensional systems and is required for in vitro bone formation in a PLGA scaffold.* Exp Cell Res, 2004. **299**(2): p. 325-34.

204. Coleman, R. (2007). *Development of a Small Animal Model to Study Tissue Engineering Strategies for Growth Plate Defects* (Doctoral Dissertation). Georgia Institute of Technology, Atlanta, GA.

205. Mauney, J.R., et al., *In vitro and in vivo evaluation of differentially demineralized cancellous bone scaffolds combined with human bone marrow stromal cells for tissue engineering.* Biomaterials, 2005. **26**(16): p. 3173-85.

206. Hosseinkhani, H., et al., *Bone regeneration through controlled release of bone morphogenetic protein-2 from 3-D tissue engineered nano-scaffold.* Journal of Controlled Release, 2007. **117**(3): p. 380-6.

207. Kato, M., et al., *Optimized use of a biodegradable polymer as a carrier material for the local delivery of recombinant human bone morphogenetic protein-2 (rhBMP-2).* Biomaterials, 2006. **27**(9): p. 2035-41.

208. Kratchmarova, I., et al., *Mechanism of divergent growth factor effects in mesenchymal stem cell differentiation.* Science, 2005. **308**(5727): p. 1472-7.

209. Gareau, D.S., et al., *Confocal fluorescence spectroscopy of subcutaneous cartilage expressing green fluorescent protein versus cutaneous collagen autofluorescence.* Journal of biomedical optics, 2004. **9**(2): p. 254-8.

210. Sakiyama-Elbert, S.E., A. Panitch, and J.A. Hubbell, *Development of growth factor fusion proteins for cell-triggered drug delivery.* FASEB J, 2001. **15**(7): p. 1300-2.

211. Dudziak, M.E., et al., *The effects of ionizing radiation on osteoblast-like cells in vitro.* Plast Reconstr Surg, 2000. **106**(5): p. 1049-61.

212. Jacobson, G.B., et al., *Sustained release of drugs dispersed in polymer nanoparticles.* Angew Chem Int Ed Engl, 2008. **47**(41): p. 7880-2.

213. Diagaradjane, P., et al., *Imaging epidermal growth factor receptor expression in vivo: pharmacokinetic and biodistribution characterization of a bioconjugated quantum dot nanoprobe.* Clin Cancer Res, 2008. **14**(3): p. 731-41.

214. Degat, M.C., et al., *Enhancement of the biological activity of BMP-2 by synthetic dextran derivatives.* Journal of Biomedical Materials Research Part A, 2008.

215. Yamaguchi, A., et al., *Recombinant human bone morphogenetic protein-2 stimulates osteoblastic maturation and inhibits myogenic differentiation in vitro.* J Cell Biol, 1991. **113**(3): p. 681-7.

216. Thies, R.S., et al., *Recombinant human bone morphogenetic protein-2 induces osteoblastic differentiation in W-20-17 stromal cells.* Endocrinology, 1992. **130**(3): p. 1318-24.

217. Cheng, F., L.J. Gamble, and D.G. Castner, *XPS, TOF-SIMS, NEXAFS, and SPR characterization of nitrilotriacetic acid-terminated self-assembled monolayers for controllable immobilization of proteins.* Anal Chem, 2008. **80**(7): p. 2564-73.

218. Zucker, R.M. and O.T. Price, *Statistical evaluation of confocal microscopy images.* Cytometry, 2001. **44**(4): p. 295-308.

219. Smith, C.L., *Basic confocal microscopy.* Current protocols in molecular biology / edited by Frederick M Ausubel [et al], 2008. **Chapter 14**: p. Unit 14.11.

220. Glasbey, C.A. and G.W. Horgan, *Image analysis for the biological sciences*. Statistics in Practice, ed. V. Barnett. 1995: John Wiley & Sons.